DECENTRALIZED OPERATION AND CONTROL OF INTEGRATED TRANSACTIVE AND PHYSICAL GRIDS

A Dissertation
Presented to
The Academic Faculty

by

Rohit Atul Jinsiwale

In Partial Fulfillment
of the Requirements for the Degree
Doctor of Philosophy in the
School of Electrical and Computer Engineering

Georgia Institute of Technology
May 2021

DECENTRALIZED OPERATION AND CONTROL OF INTEGRATED TRANSACTIVE AND PHYSICAL GRIDS

Approved by:

Dr. Deepak Divan, Advisor
School of Electrical and
Computer Engineering
Georgia Institute of Technology

Dr. Maryam Saeedifard
School of Electrical and Computer
Engineering
Georgia Institute of Technology

Dr. Santiago Grijalva
School of Electrical and
Computer Engineering
Georgia Institute of Technology

Dr. Marilyn Brown
School of Public Policy
Georgia Institute of Technology

Dr. Daniel Molzahn
School of Electrical and
Computer Engineering
Georgia Institute of Technology

Date Approved: December 8th, 2020

To my late grandfather Shridhar Jinsiwale,

who always believed in me and nurtured my talents

ACKNOWLEDGEMENTS

This journey towards my PhD would not have been possible without support, encouragement and help from many people. I would like to express my heartfelt gratitude to everyone involved.

First, I would like to thank my advisor, Dr. Deepak Divan. I could not have achieved this without your patience, continued guidance and inputs. In addition to my academic enrichment, I have learnt valuable problem-solving skills as well as a new outlook towards approaching tough problems. I am deeply grateful for your support during my PhD journey and will likely seek your guidance on many matters henceforth.

I also want to express my gratitude towards my parents – Atul and Swati Jinsiwale for instilling me with values and aspirations that still drive me to this day. It is their continued support and encouragement that made this journey possible. I would also like to thank my fiancée Sarah Menz, for being patient, understanding and comforting me when I faced difficulties and problems in both academic and personal matters.

I would like to extend my gratitude towards Dr. Daniel Molzahn, Dr. Santiago Grijalva, Dr. Maryam Saeedifard and Dr. Marilyn Brown for serving on my dissertation committee and providing feedback and inputs. I appreciate that you took the time and effort to look over my thesis and helped shape this document.

I would like to thank the entire Center for Distributed Energy (CDE) family for all the stimulating discussions, help and support. The work presented in this document could not have been possible without valuable inputs from Dr. Rajendra Prasad Kandula and

Frank Lambert. I would also like to thank Yunkyung Chang-Hoffman and Brandon Royal for helping me execute some aspects of this work and making the logistics feel like a breeze. I would like to personally thank Mickael Mauger, Shreyas Kulkarni, Kavya Ashok and Eric Myers. I couldn't have asked for a better set of friends. This journey wouldn't have been possible without your camaraderie and I will sorely miss our breakroom conversations.

I would also like to thank Umang Deora, Shantanu Kotkar, Sravan Talluri, Abhishek Naik, Anirudh Ramanujapuram, Nitish Sihag, Karthik Swaminathan, Prasoon Suchandra and Umesh Unnikrishnan for being there during all the hard and good times. I will cherish all the memories I shared with you for the rest of my life.

I have been fortunate enough to make a lot of friends in this journey. I would like to thank Mohammad Miranbeigi, Nishant Bilakanti, Anirudh Marellapudi, Priya Thekkumparambath Mana, Xiangyu Han, Zheng An, Decheng Yan, Liran Zheng, Karthik Kandasamy, Kartavya Agarwal, Sathish Jayaraman and Orestis Vasios for their help and encouragement.

TABLE OF CONTENTS

ACKNOWLEDGEMENTS **IV**

LIST OF TABLES **XII**

LIST OF FIGURES **XIII**

LIST OF SYMBOLS AND ABBREVIATIONS **XVIII**

KEY DEFINITIONS **XXI**

SUMMARY **XXIII**

CHAPTER 1. INTRODUCTION **1**

1.1 Unprecedented Adoption of Volatile Renewable Energy Sources **2**

1.2 Lack of Scalability for Multi-owner and Massively Multi-agent Systems **5**

1.3 Resiliency and Cost of Control **7**

1.4 Research Scope **10**

1.5 Outline of Chapters **12**

CHAPTER 2. STATE OF THE ART GRID CONTROL ARCHITECTURE **13**

2.1 Grid Control Architecture -Status Quo **13**

2.1.1 Overview of grid control layers 14

2.1.2 Fragility of today's grid architecture 17

2.2 State-of-the-art Congestion Relief and Voltage Support Mechanisms **21**

2.2.1 Centralized Control over Power Flows 23

2.2.2 Distributed Power Flow Control Solutions 27

2.2.2.1 Distributed Power Flow Controllers - Principle 27
2.2.2.2 Phase Shifting Transformers (PSTs) 29
2.2.2.3 Fully rated High-Voltage Direct Current (HVDC) Links 30
2.2.2.4 Unified Power Flow Controller (UPFC) 32
2.2.2.5 Distributed Series Impedance (DSI) 33
2.2.3 Voltage Control Solutions 34
2.2.3.1 On-Load Tap Changers (OLTCs) 34
2.2.3.2 Mechanically Switched Capacitor Banks 36
2.2.3.3 Thyristor Controlled Reactors (TCRs) and Switched Capacitors (TSC) 37
2.2.4 Constraints with controlling low-voltage meshed grids 37
2.2.5 Control of Physical Grid Parameters - Discussion 38
2.3 Existing transactive control mechanisms to leverage flexibility 39
2.3.1 Incentive-based Mechanisms 40
2.3.1.1 Time-of-Use (TOU) Pricing 41
2.3.1.2 Critical Peak Pricing (CPP) 42
2.3.1.3 Peak-Time Rebate (PTR) 42
2.3.1.4 Challenges with Incentive-based Mechanisms 43
2.3.2 Real-time Pricing (RTP) 43
2.4 Required Attributes and Functionality from Future Grid Architectures 46
CHAPTER 3. DECENTRALIZED MANAGEMENT OF PHYSICAL GRID PARAMETERS 49
3.1 Hybrid Transformers - Concept 50
3.2 Comparison with other grid control techniques 53

3.2.1 Qualitative Comparison 53

3.2.2 Economic Comparison 55

3.3 Dynamic control over grid parameters 57

3.3.1 Simulation Setup 57

3.3.2 Power Flow Control 58

3.3.3 Congestion control and DER management 60

3.3.4 Enhanced voltage management with high PV penetration 61

3.4 Impact on Grid Resiliency 63

3.5 Sensitivity of System Flows and the effect of Hybrid Transformers 67

3.5.1 Power Transfer Distribution Factors (PTDFs) 67

3.5.2 Flow Sensitivity to Hybrid Transformers 71

3.5.3 Power Flow Sensitivity with hybrid transformers- Simulation Study 72

3.6 Discussion and Contributions 75

CHAPTER 4. DECENTRALIZED TRANSACTIVE CONTROL ARCHITECTURE 78

4.1 Grid frequency as a global signal 79

4.2 Decentralized Marketplace based on grid frequency 81

4.3 Market participation mechanism for Sources using Universal Market Nodes (UMNs) 86

4.3.1 Conventional Merit Order Curves and Dispatch 87

4.3.2 Source control using the price-frequency rule to achieve decentralized economic dispatch 88

4.3.3 Source Control to achieve better transient performance while augmenting existing market processes in regulated environments 92

4.4 Distributed Demand Response through robust edge intelligence 98

4.4.1 Edge intelligence constraints and nuances 98

4.4.2 Local Optimization Framework for UMNs 100

4.4.2.1 Priority Levels and Varying Benefit Levels 101

4.4.2.2 Consumer discomfort and load rescheduling 102

4.4.2.3 Uncertain Prices in the Receding Horizon and 'Grid-friendly' Behavior 103

4.4.2.4 Implementation of Edge Intelligence 109

4.4.2.5 Simulation Test Case for Consumer UMN 110

4.5 Need for Physical Grid Control in Transactive Frameworks 114

4.6 Role of Hybrid Transformers in a Decentralized Transactive Framework 115

4.6.1 Estimation of system flows 116

4.6.1.1 Assumption of base case loading in control areas 118

4.6.1.2 Estimation of worst-case system flows based on error 118

4.7 Discussion and Contributions 120

CHAPTER 5. SIMULATION PLATFORM FOR MASSIVELY DISTRIBUTED MULTI-AGENT SYSTEMS 123

5.1 Simulation platform for long-term studies involving frequency dynamics 123

5.1.1 Power System Equation Types and Characteristics 124

5.1.2 QSS simulator with frequency dynamics 125

5.2 Multi-agent System Simulation Scheme 128

5.3 Contributions 131

CHAPTER 6. DECENTRALIZED INTEGRATED TRANSACTIVE AND PHYSICAL ARCHITECTURE 132

6.1 Multi-Agent Test Bed 132

6.1.1 Source UMN Agents 133

6.1.2 Consumer UMN Agents 135

6.1.3 Hybrid Transformer UMN Agents 138

6.2 Simulation Study 138

CHAPTER 7. CONCLUSIONS, CONTRIBUTIONS AND FUTURE WORK 144

7.1 Conclusions 144

7.2 Contributions 146

7.2.1 Analysis of hybrid transformers as an effective grid control tool 146

7.2.2 Novel Decentralized Transactive Architecture 147

7.2.3 Simulation engine to analyse multi-agent decentralized architectures 147

7.3 Future Work 148

7.3.1 Quantification of Stability 148

7.3.2 Policy, Regulation and Role of the System Operator 148

7.3.3 Rules of Connection, penalties and load tripping 149

7.3.4 Role of Storage and Prosumers 149

7.4 Acknowledgement 150

APPENDIX A. RETROFITTABLE HYBRID TRANSFORMERS FOR LOW-VOLTAGE MESHED GRIDS 151

APPENDIX B. LIMITATIONS OF HYBRID TRANSFORMERS UNDER EXTREME SCENARIOS **160**

APPENDIX C. PUBLICATIONS **162**

REFERENCES **164**

VITA **177**

LIST OF TABLES

Table 1 Comparison of Dynamic Control Techniques – 60 MVA target system Cost Assumptions: Transformer cost: $30/kVA, UPFC series transformer cost: $60/kVA, Converter: 150/kVA…….. 55

Table 2 PTDFs and system flows for passive 5-bus system..... 73

Table 3 Hybrid Transformer Sensitivities..... 74

Table 4 Characteristics of the 1111 modelled agents 137

LIST OF FIGURES

Figure 1.1 (a) Decreasing LCOEs of renewable energy sources (b) Increase in adoption of PV based sources at the residential, commercial and utility scale 2

Figure 1.2 Wide variation between peak load and PV output patterns 3

Figure 1.3 (a) California 'Duck curve' [6] (b) Feeder Voltage volatility with high DER penetrations [7] 4

Figure 1.4 Microgrids as a measure for resilience improvement [11] 8

Figure 2.1 Existing grid operation and market control architecture 14

Figure 2.2 Existing control and coordination paradigm 17

Figure 2.3 Illustration of meshed grid structures at the (a) bulk power level (IEEE 30 bus system) (b) low voltage level [57,58] 22

Figure 2.4 Power flows over a two-bus system 27

Figure 2.5 Power flow variation over a two bus system with a power flow controller (*pfc*) 28

Figure 2.6 Phase shifting transformers [69] 29

Figure 2.7 HVDC (fully rated back-to-back) General Schematic 30

Figure 2.8 Unified Power Flow Controller (UPFC) 32

Figure 2.9 Distributed Series Impedance [79] 33

Figure 2.10 (a) OLTC Schematic (b) Commercial OLTC Product [84] 35

Figure 2.11 (a) Mechanically Switched Capacitor bank (b) Commercial Switched capacitor bank (Eaton) [86] 36

Figure 2.12 (a) TCR Schematic (b) TSC Schematic 37

Figure 2.13 TOU-D-PRIME Pricing Scheme (SCE) [102] 41
Figure 2.14 LMP Calculation Procedure 44
Figure 2.15 LMP Contour across the MISO territory 45
Figure 3.1 Hybrid Transformer Concept and Equivalent 50
Figure 3.2 Detailed Schematic of Hybrid Transformers 51
Figure 3.3 Dynamic Control over power flows, voltages and apparent impedances using Hybrid Transformers 52
Figure 3.4 Simulation Scheme to analyze the system level impacts of hybrid transformers 58
Figure 3.5 Modified IEEE 30 bus system with hybrid transformer (T6-10) 58
Figure 3.6 (a) Real power and (b) apparent power variation affected by hybrid transformer T6-10 59
Figure 3.7 (a) Line 15-18 getting congested due to presence of PV plant (b) PV output and spilled output due to congestion 60
Figure 3.8 Dynamic congestion control on line 15-18 61
Figure 3.9 (a) 13 bus system with 0.5 MW PV farm (b) Voltage management with an LTC 62
Figure 3.10 Comparison between voltage management using an LTC and a hybrid transformer 62
Figure 3.11 Concept of Modular Controllable Transformers (MCTs) 64
Figure 3.12 IEEE 30 bus system modelled with MCTs 65
Figure 3.13 Impedance control to match replaced unit 66

Figure 3.14 Power flow matched to base case using mismatched unit with added control 66
Figure 3.15 Link with hybrid transformer to add 1 MW above nominal flow 71
Figure 3.16 Equivalent to capture the effect of additional MW on other system flows ... 71
Figure 3.17 Base flows on passive 5 bus system 72
Figure 3.18 Power flows on 5-bus network (Hybrid transformer increasing flow by 1 MW) 73
Figure 3.19 Methodology to analyze effect of hybrid transformers on arbitrary systems 75
Figure 4.1 Droop curve and biasing mechanism 80
Figure 4.2 Real-time price vs frequency mapping 82
Figure 4.3 Decentralized transactive architecture based on global signals and edge intelligence 84
Figure 4.4 Production cost bids for two sample generators 87
Figure 4.5 Economic dispatch (merit order curve) for the two participating sources 87
Figure 4.6 Nonlinear locally synthesized droops 89
Figure 4.7 Two source test system with nonlinear droops 89
Figure 4.8 Detailed governor model with nonlinear droop 90
Figure 4.9 Power sharing corresponding to economic dispatch with nonlinear droops ... 91
Figure 4.10 Modified price-frequency mapping for operation around day-ahead setpoints 92
Figure 4.11 Sample load profile (15-minute intervals) 93
Figure 4.12 Economic dispatch set points for the given load curve 93
Figure 4.13 Desired deviation in price for deviation from dispatch 94

Figure 4.14 Nonlinear droop for one dispatch point 94
Figure 4.15 Nonlinear droops for all dispatch points (source 1) 95
Figure 4.16 Nonlinear droops for all dispatch points (source 2) 96
Figure 4.17 Economic power sharing between sources with nonlinear droops during disturbance on two dispatch points 97
Figure 4.18 Incorrect sharing between sources during load disturbance (5% droop) 97
Figure 4.19 Notation used to signify time intervals 104
Figure 4.20 Acceptable band of prices for a risk averse consumer 105
Figure 4.21 Acceptable band of prices for an opportunistic consumer 105
Figure 4.22 Implementation scheme for algorithm (26) on UMNs 109
Figure 4.23 Sample residential consumer profile with three priority categories 111
Figure 4.24 Modelled time varying benefits for priority 2 loads 111
Figure 4.25 Sample real-time price profile 112
Figure 4.26 UMN response to varying consumer discomfort 112
Figure 4.27 UMN real-time consumption for extravagant consumer 113
Figure 4.28 UMN real-time consumption for an opportunistic consumer 113
Figure 4.29 UMN drops consumption to priority 1 loads during high price contingency intervals 114
Figure 4.30 5-bus system with two areas 115
Figure 5.1 Simulation Scheme based on QSS approach 127
Figure 5.2 Multi-agent simulation scheme to analyze the effects of the proposed transactive and physical architecture 129
Figure 6.1 Multi-agent test bed 133

Figure 6.2 Price-frequency characteristic deployed on test bed 134
Figure 6.3 PV output pattern..... 134
Figure 6.4 Locally synthesized nonlinear droops with global characteristic and local preferences 135
Figure 6.5 Baseline load profiles for modelled consumers..... 136
Figure 6.6 Baseline load curve and expected PV output 136
Figure 6.7 Real-time price variation in response to changing frequency 138
Figure 6.8 Behavior of 1111 consumers in response to real-time prices..... 139
Figure 6.9 Consumption pattern for 454 agents (Profile 1) for (a) priority 1 (b) priority 2 and (c) priority 3 loads..... 140
Figure 6.10 Load flexibility leveraged using edge intelligence to achieve better consumption patterns in PV dominant systems 141
Figure 6.11 Controlled local power flow on 2-5 by hybrid transformer 141
Figure 6.12 Line flows controlled by hybrid transformer to avoid congestion 142
Figure 7.1 Decentralized Integrated Physical and Transactive Architecture..... 145

LIST OF SYMBOLS AND ABBREVIATIONS

LCOE	Levelized cost of energy
PMU	Phasor measurement unit
AMI	Advanced metering infrastructure
OPF	Optimal power flow
SCED	Security constrained economic dispatch
ISO	Independent system operator
DER	Distributed energy resources
GENCO	Generating company
TransCo	Transmission company
DisCo	Distribution company
LMP	Locational marginal pricing
DLMP	Distribution locational marginal pricing
HILF	High intensity low frequency
LPT	Large power transformer
EMS	Energy management system
DMS	Distribution management system
SCADA	Supervisory control and data acquisition
AGC	Automatic generation control
PTDF	Power transfer distribution factor
SCOPF	Security constrained optimal power flow
QCQP	Quadratically constrained quadratic program
SOCP	Second order cone program

SDP	Semi-definite programming
DC OPF	DC optimal power flow
PST	Phase shifting transformer
TSPST	Thyristor controlled phase shifting transformer
HVDC	High voltage direct current
FACTS	Flexible AC transmission system
VSC	Voltage source converter
FRBTB	Fractionally rated back-to-back
UPFC	Unified power flow controller
DSI	Distributed series impedance
OLTC	On-load tap changer
TCR	Thyristor controlled reactor
TSC	Thyristor switched capacitor
FERC	Federal energy regulatory commission
DR	Demand response
TOU	Time-of-use
CPP	Critical peak pricing
PTR	Peak-time rebate
RTP	Real-time pricing
NPC	Neutral point clamped
BIL	Basic insulation level
QSS	Quasi-static simulation
LVR	Line voltage regulator
SED	Spare equipment database
STEP	Spare transformer equipment program

MCT	Modular controllable transformers
HTFS	Hybrid transformer flow sensitivity
SIVOM	Stacked isolated voltage optimization module
ACE	Area control error
ABT	Availability based tariff
UMN	Universal market nodes
MPPT	Maximum power point tracking
GTG	Governor-turbine-generator
AVR	Automatic voltage regulator
DSO	Distribution system operator
CWT	Coaxial winding transformer

KEY DEFINITIONS

Grid Architecture	Realized modus operandi for managing a power grid structure based on control theory, communication systems as well as the physical characteristics of the system
Physical Grids	The most visible layer of the power grid consisting of lines, power transformers, generating units, loads and renewable energy sources
Transactive	A framework that governs the exchange of a commodity in a given architecture. For power grids the fundamental quantity being traded is energy. Any mechanism that facilitates such an exchange for a given monetary value can be deemed a transactive mechanism
Decentralized	An approach towards operating a complex system without performing analysis and real-time control at a central entity. Decentralized systems typically utilize edge intelligence to regulate complex multi-agent systems in a collective manner
Autonomous	Pertains to decision making. If a given intelligent device exercises control actions based on local information rather than interacting with a central entity it can be considered autonomous

Fractal	The term fractal is used to describe control architectures in this document. The term implies a control principle that remains entirely scalable even when the system size is arbitrarily changed.
Prosumer	An agent connected to the grid typically at the distribution level that possesses the ability to consume as well as deliver energy

SUMMARY

With exponentially decreasing prices of photovoltaics, the adoption of volatile and non-dispatchable sources into the grid has increased. While, these technologies provide avenues for grid independence and system resiliency improvements, the operation and control architecture in place, prevents the scalability of these approaches. Reliance on high speed communication and complex computations to handle these fast phenomena introduces points of failure and dramatically decreases the controllability and resiliency of the system. Fast volatility and line congestions across the network are challenging to control using this central control architecture that relies on full visibility, low-latency communications and complex centralized algorithms. Moreover, the adoption of these sources at the grid-edge has also ensured that the number of independent asset owners on the system has also been on the rise. It will be challenging to scale the existing market mechanisms to allow stable operation of such multi-agent and geographically dispersed systems. Yet, it is critical to manage supply-demand imbalances in real-time through market dynamics.

The objective of the proposed research is to develop a decentralized grid architecture to manage the physical and transactive aspects of power systems. The proposed research showcases fast localized grid control solutions in the form of hybrid transformers to manage physical phenomenon like congestion and voltage volatility. This ensures that all the additional flexibility can be leveraged from a traditionally passive network by making it more active using intelligent devices. Furthermore, a decentralized, communication-free and topology-agnostic real-time pricing mechanism is proposed to

enable collective stabilization even under wide variations in available generation. The architecture is designed to operate around global rules and globally available signals making it highly robust and resistant to communication failures. This framework allows all connected agents to participate in a real-time market platform and transact energy to ensure that supply-demand balances are maintained collectively. Thus, an architecture is presented where the transactive and physical grid constraints are handled in a decoupled fashion while being integrated through the physics of the network. The architecture provides a robust mechanism to operate highly volatile, multi-agent grid structures in a resilient fashion.

CHAPTER 1. INTRODUCTION

The power infrastructure has undergone significant changes over the last few decades. Over the years, the grid has transitioned from a ‘small, localized generator’ paradigm seen in the Pearl street era, to one that is characterized by large concentrated points of generation from where power is delivered over elaborate, long and highly meshed transmission networks. Lower levelized costs of energy (LCOEs) through bulk generation and the ability to leverage load diversity have led to this change. However, as these structures became more elaborate new challenges arose in the form of control and coordination requirements. The advent of improved sensing and communication platforms in the form of phasor measurement units (PMUs) and advanced metering infrastructure (AMI) made it possible to gain visibility and exercise some control over these structures using complex algorithms like Optimal Power Flow (OPF) and Security Constrained Economic Dispatch (SCED). Further with partial deregulation, an electricity market structure was established in some places to allow producers, utilities and Independent System Operators (ISOs) to manage grid transactions, making energy a tradable commodity in addition to it being a service.

However, this has resulted in a control and operation paradigm that relies on a top-down centralized approach, is extremely hierarchical and relies on complex computations in a few centralized locations along with dispatched generation to realize stable operation. The current infrastructure succeeds in managing grid operations with relatively limited market participants, slow dynamics, complex computations and low-latency communications However, there are certain key trends and disruptions that could be

challenging to address using existing grid management principles. These disruptions are already beginning to create points of stress from a flexibility, resiliency, reliability and scalability perspective. The disruptions strongly point to the need for a complete overhaul in the grid control and operation architecture and new perspective on what a grid as a service entails in the future. A discussion about some of the key disruptors as well as the accompanying set of challenges is presented next.

1.1 Unprecedented Adoption of Volatile Renewable Energy Sources

A key development of consequence is the exponential decline in costs of PV, wind and energy storage systems. This cost decline has ensured that the LCOEs of these technologies are lower, even at much smaller capacities as compared to the `centralized bulk generation' approach [1], [2]. Fig. 1.1(a) [1] illustrates this trend. With no requirements for coordinated fuel logistics, and the modular nature of these systems, these technologies have become viable candidates to meet clean energy mandates and energy independence goals. Consequently, a rapid uptake in the adoption of these

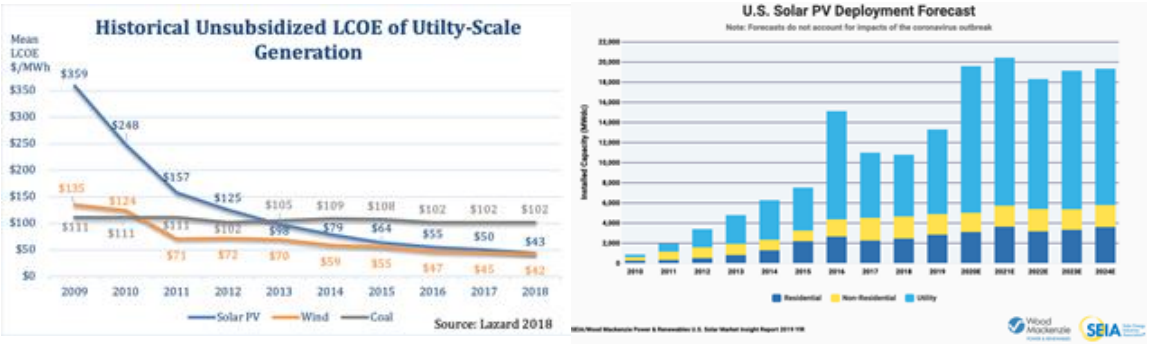

(a) (b)

Figure 1.1 (a) Decreasing LCOEs of renewable energy sources (b) Increase in adoption of PV based sources at the residential, commercial and utility scale

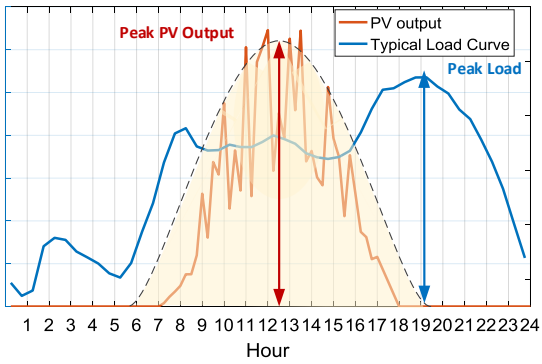

Figure 1.2 Wide variation between peak load and PV output patterns

Distributed Energy Resources (DERs) on a household level as well as at utility scale is being seen. Fig. 1.1 (b) [3] shows the exponential increase in PV deployment as the utility and residential level. Microgrids are being deployed with a PV dominant resource mix as a measure to attain energy independence and boost resilience. The grid of the future is poised to be one characterized by huge amounts of distributed generation [4]. However, the non-dispatchable nature of these DERs and the associated volatility makes operation of PV dominant grid structures extremely challenging.

An operation paradigm where 'generation-follows-load' is utilized to address load changes and disturbances in modern grid structures. System operators have employed an approach where PV penetration is treated as a disturbance. Operators often rely on corrective dispatch procedures to stabilize the system. This offsets the burden of balancing the supply and demand to the utility or ISO. Fig. 1.2 shows the time varying nature of PV outputs and typical load curves. With very few points of operation where the supply and demand balances are naturally met, operating PV dominant grids of the future is going to be extremely challenging. Storage could be deployed in such networks to balance supply-demand ratios. However, this could prove to be an expensive solution to deal with these issues. Relying on supply side flexibility alone to address these imbalances is going to be inadequate in these futures DER

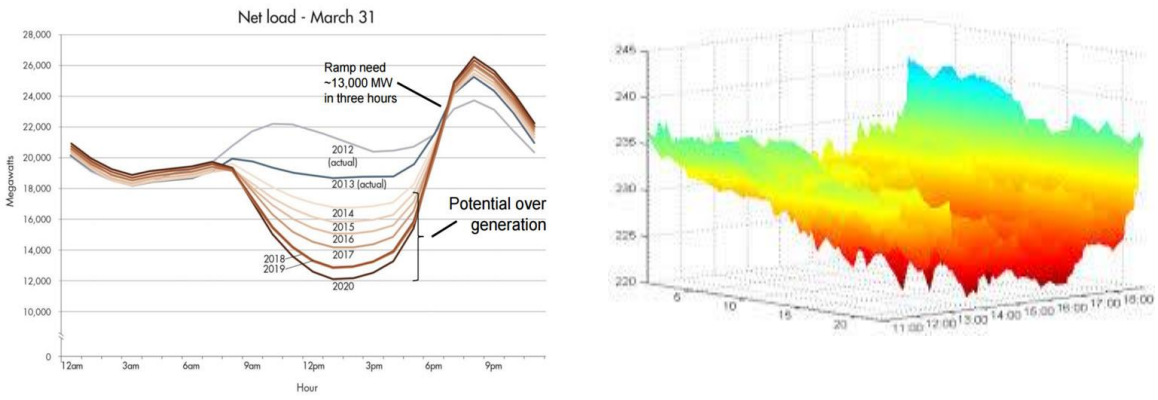

(a) **(b)**

Figure 1.3 (a) California 'Duck curve' [6] (b) Feeder Voltage volatility with high DER penetrations [7]

dominant grid structures. This shows that there need to be mechanisms that can fundamentally alter the way load is consumed to facilitate stable operation. Challenges associated with addressing supply-demand imbalances in grid structures with rapidly varying resource availability need to be addressed to enable stable operation future grids.

The 'Duck curve' seen in CAISO territory and shown in Fig.1.3 (a) is an example of grid balancing challenges in PV dominant environments [5]. DERs like PV also introduce voltage volatility on to the grid. Fig 1.3 (b) shows the observed volatility on a distribution feeder [6]. Legacy voltage control devices like OLTCs and capacitor banks only succeed in exerting discrete amounts of control. Moreover, these devices were never designed to operate with the frequency seen in volatile grid structures. Thus, addressing volatility on PV rich grids becomes another significant challenge.

Injections of massive amounts of power at the grid edge on meshed transmission, sub transmission and distribution networks also create line congestion issues and unexpected power flow patterns. Bidirectional power flows are becoming commonplace in distribution networks with high PV penetration and are quite challenging to address from a grid operator's perspective. Control over power flows and congestion relief across the system has traditionally

been exercised by using low-latency communications to retrieve states, recalculating power flow, optimizing control and altering generator dispatch patterns or through topology reconfiguration [7]. However, as generation centers move towards to the grid-edge, it becomes extremely challenging to derive optimal dispatch procedures. With millions of active agents on the system that may be geographically dispersed, the complexity of running centralized computations to decipher these new set points would be enormous. Further, with faster phenomenon being observed, the requirements of ultra-low latency communications to continuously exert said centralized control would drive up infrastructure costs and necessitate a major upgrade on existing systems. Finally, the need to ensure centralized grid operations in the event of communication failures or cyber attacks raises an extra layer of complexity that is rarely addressed.

1.2 Lack of Scalability for Multi-owner and Massively Multi-agent Systems

In traditional vertically integrated grid structures, a majority of the sources are owned by few participating entities in the form of Generating companies (GenCos) or ISOs ensuring that proper coordination from a physical power delivery perspective as well as from a transactive perspective can be managed centrally. Even managing the grid with these limited entities is significantly challenging; often requiring complex SCED procedures and low-latency communications to issue appropriate commands to participants.

With sources being privately owned, the number of asset owners at the grid edge have increased by a tremendous amount. Along with the increase in grid edge sources, the adoption of smart home devices has enabled prosumers to optimize and manage their consumption patterns. This has led to vastly different net consumption patterns compared

to those seen historically and has made real-time grid stabilization based on forecasts very challenging for grid operators. Performing central calculations to issue set points to these rapidly growing grid edge entities in a volatile setting is extremely challenging. These new independent agents often don't receive any signals from the grid operator to promote collective grid stabilization.

The transactive architecture in place is based on an auction-based approach. Locational Marginal Prices (LMPs) and Distribution LMPs (DLMPs) are popular transactive mechanisms to achieve real-time pricing but strongly rely on real-time knowledge of system topologies and real-time states [8]. These mechanisms work well with a limited number of players, a small set of asset owners and slower coordination mechanisms, but, are challenging to scale. The communication framework required to coordinate such an auction-based market structure with millions of active agents would be highly complex and prone to failure. Moreover, the existing architecture does not possess adequate mechanisms to enable collective stabilization of such volatile structures using demand-side participation methods.

Yet, in such PV rich grid structures where the system can rapidly swing between modes of resource abundance and resource scarcity, demand-side participation and demand flexibility are key requirements to sustain stable operation. Demand side mechanisms in place today rely on leveraging a very limited amount of flexibility to avoid overloads on limited time horizons. Some utilities and system operators have instituted programs to issue dynamic prices to end agents. However, none of these mechanisms effectively create a scalable marketplace for millions of agents that will become commonplace at the grid edge.

It is important to build a marketplace that allows supply-demand imbalances to be settled in real-time for these geographically dispersed, massively multi-agent systems. Moreover, the market structure needs to enable every agent to perform arbitrage and demand scheduling while ensuring that every agent is actively incentivized to support the grid and improve the net resiliency. This would be key to stabilizing supply-demand imbalances using both the supply and demand side flexibility in PV dominant grids.

1.3 Resiliency and Cost of Control

The issue of grid resiliency has been brought to the forefront in recent times and has served as a primary motivator for most grid enhancement programs. Resiliency is an important measure of the robustness of a grid control and operation architecture. Resiliency encompasses the reliability, resistance to failure, recovery time and flexibility of the system [9]. Both from a physical and transactive perspective, today's grid infrastructure has some resilience issues. Control over physical power flows over today's highly meshed systems is often centrally coordinated using complex algorithms to alter dispatch patterns. This framework relies on the ability to send low-latency control signals to all dispatchable sources to control flows as well as supply-demand imbalances. Similarly, the transactive layer relies on complete information of system topology and system states to determine nodal prices. An architecture that depends so heavily on the communication layer to sustain operation in real-time is prone to failure in the event of any communication infrastructure damage. With increasing High Intensity Low Frequency (HILF) events in the form of hurricanes, tornadoes, earthquakes and cyber-physical attacks on the system the fragility of the current architecture becomes apparent and a need for a more robust architecture is felt [10].

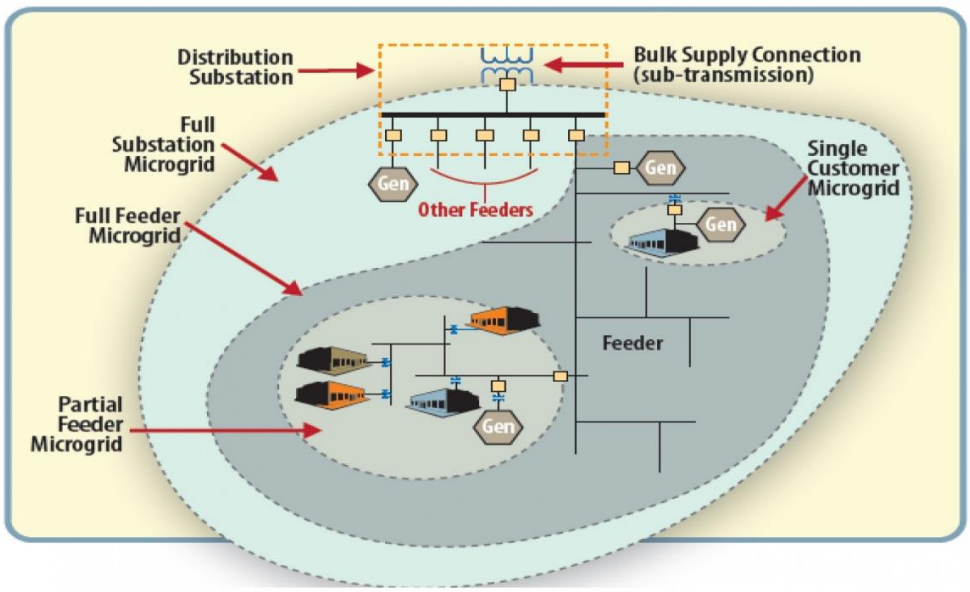

Figure 1.4 Microgrids as a measure for resilience improvement [11]

Resiliency also encompasses the ability of a system to fragment and continue operation in the event of any damage. This requires the control and operation architecture to be based on fractal rules of operation. DERs at the grid edge can, in principle, restore and supply broken fragments of the grid in case of a HILF event. In fact, the Department of Energy's (DOE's) recent push into the Resilient Energy Community (RECs) based approaches is an indication that this approach would provide tremendous value [11]. Fig. 1.4 shows an illustration of such a concept. However, the system architecture and control strategy do not support the possibility of operating portions of the grid without the presence of the main grid [12]. This is owing to the extreme dependence on centralized communication and control mechanisms prevalent in the grid today. As a result, the resiliency of the existing paradigm under failure modes is extremely low [13] with long recovery times post contingency. Power restoration in Puerto Rico took eleven months following the mass destruction caused by Hurricane Maria in 2017. With widespread,

catastrophic damage and impassable roads, repairs and logistics pose a big challenge [14]. Thus, an increased emphasis should be laid on improving the resiliency of systems against these events, in addition to hardening them against failure modes.

Another key consideration when evaluating the resiliency of the system is the recovery time associated with failure modes. A recent DOE report outlines the vulnerability of Large Power Transformers (LPTs) [15]. These devices are typically rated to handle upwards of 100MVA of power making them extremely critical to the power grid. With a significant portion of the LPT fleet reaching the end of their stipulated component life there have been growing concerns about the impacts of LPT failures. Recent instances of physical attacks on LPTs [16] and the slow recovery process associated with fixing or replacing these damaged units has created an increased awareness for this issue. LPTs designs are highly customized owing to specific field requirements. Owing to this, the design and manufacturing process is significantly different for each customer.

Transportation of these units is often extremely challenging owing to the large form factor. Moreover, the unit needs to be disassembled to enable transportation. Specialized railcars and road trucks are required to transport these devices. Differing permit regulations in each state make the process even more challenging. In addition to this a crew of personnel from different law enforcement agencies is required to co-ordinate safe transportation on roads. Once the LPT arrives on site, assembling the bushings, filling oil and bringing it online adds to the lead time. The whole process from the acceptance of the tender to commissioning takes about a year [15]. Long lead times coupled with transportation delays make procuring LPTs a lengthy process. Thus, in the event of any failure to these key components, the time to recovery for the system is extremely high. This

points to the need for embedding features and flexibility in the architecture to sustain operation during such events. By minimizing the mean time to failure, the resilience of the system can be dramatically improved.

However, it stands to reason that resiliency is to be achieved at a modest cost. While the most redundant solution to achieving maximum resiliency is simply duplicating components, this is often quite expensive. Thus, any potential solution needs to be able to showcase, all the above attributes at a cost that is acceptable. Moreover, the added control solution needs to be one that doesn't create more points of failure on the system.

1.4 Research Scope

For future DER dominant grid structures, certain requirements emerge out of this discussion. With multiple owners, mixed local objectives, fragility of operating architectures and fast disturbances to the system, it becomes necessary to implement a highly resilient, flexible and scalable architecture that can manage the transactive and physical attributes in a more integrated and decentralized fashion while being agnostic to technology migration, communication failures and topology. Physical phenomenon and constraints like congestion of power flow corridors and voltage volatility need to be addressed. Similarly, with millions of geographically dispersed active prosumers, a multi-agent system is created, with each asset owner wanting to transact power and meet their own local objectives.

Existing transactive and physical control solutions are centralized, rely on low-latency communications, often require detailed knowledge of network topologies and are often highly coupled. The computation and communication requirements associated with

scaling current technologies would prove to be a bottleneck in operating these grid structures. Thus, the future grid architecture will have to be one that can enable stable operation in real-time by adding flexibility to the passive physical grid while incorporating a decentralized marketplace to allow collective stabilization of power balance constraints for this multi-owner paradigm with minimal reliance on centralized coordination or communication.

Two distinct issues emerge from this discussion. The first one involves meeting physical constraints in real-time such as congestion and ensuring that voltage profiles are managed. The second issue involves achieving a scalable transactive framework for all sources and loads to address supply-demand balances in real-time – the real goal of an energy market. The solutions proposed in this research focus on utilizing simple rules and global signals across the system to minimize the dependence on central communication and coordination. A localized grid control solution in the form of hybrid transformers is presented in this research. The solution shows the ability to exert control over power flows and aids in voltage management while improving the net resiliency of the system. This allows enormous control over grid flows in otherwise passive meshed networks.

Furthermore, a decentralized communication-free and topology-agnostic real-time pricing mechanism is also presented to enable collective stabilization of supply demand balances. Moreover, by managing physical and power balance constraints in a decentralized fashion based on local parameters, the architecture could break apart into smaller fractals while relying on the marketplace to provide signals conveying energy constraints to sustain operation at varying levels of degradation.

The solutions and technologies aiding this realization are designed to minimize costs and allow this architecture to be deployed in environments where energy access is a priority. An architecture is proposed here where congestion and voltage issues are dealt with autonomously while letting individual agents transact the fundamental quantity - power, in a viable marketplace to extract maximum elasticity out of the system.

1.5 Outline of Chapters

A literature survey on the current state of the grid architecture is presented in Chapter 2. An overview of numerous control techniques to manage physical grid parameters like voltage levels and line congestion is presented. State of the art transactive mechanisms to leverage demand elasticity are also highlighted. The chapter highlights the vulnerability of state-of-the-art grid architectures and highlights the lack of scalability of existing control principles for future grids. A modular and cost-effective control solution to address physical grid constraints is presented in the form of Hybrid Transformers in Chapter 3. The efficacy of this solution is shown through numerous simulation studies. Chapter 4 presents a novel frequency dependent transactive architecture that allows supply-demand balances to be addressed in real-time without the need for central coordination or low-latency communication. The approach shows great value in managing PV dominant grid structures. A simulation platform is developed and presented in Chapter 5 to allow such multi-agent grid architectures with edge intelligence to be analyzed. Chapter 6 showcases the efficacy of these solutions in managing both the physical and transactive elements of the system in real-time, in an integrated fashion. Finally, the conclusions, contributions and future work are highlighted in Chapter 7.

CHAPTER 2. STATE OF THE ART GRID CONTROL ARCHITECTURE

This chapter provides an overview of the current grid architecture and control mechanisms. A review of the overall architecture in terms of different layers of control is presented first. Section 2.1 then focuses on aspects and challenges associated with controlling the physical layer of the grid architecture. This delves into issues associated with transmission capacity, management of power flows, congestion control as well as voltage management. A comprehensive review of physical grid control techniques is provided in Section 2.2. Similarly, existing measures to incentivize demand side flexibility are elaborated in Section 2.3. Following a review of the existing control techniques a discussion is presented that details attributes and requirements of future grid architectures in Section 2.4.

2.1 Grid Control Architecture -Status Quo

The grid control architecture seen today is a complex multi-layer one with each layer tackling a key aspect of operation. These layers also operate on various time scales depending on the requirements on the control mechanism. Primarily, it is possible to think of the grid architecture as falling into 3 main layers – device and system layer, control and measurement layer and the market layer. An overview of the layers and time scales of operation is shown in Fig. 2.1.

2.1.1 Overview of grid control layers

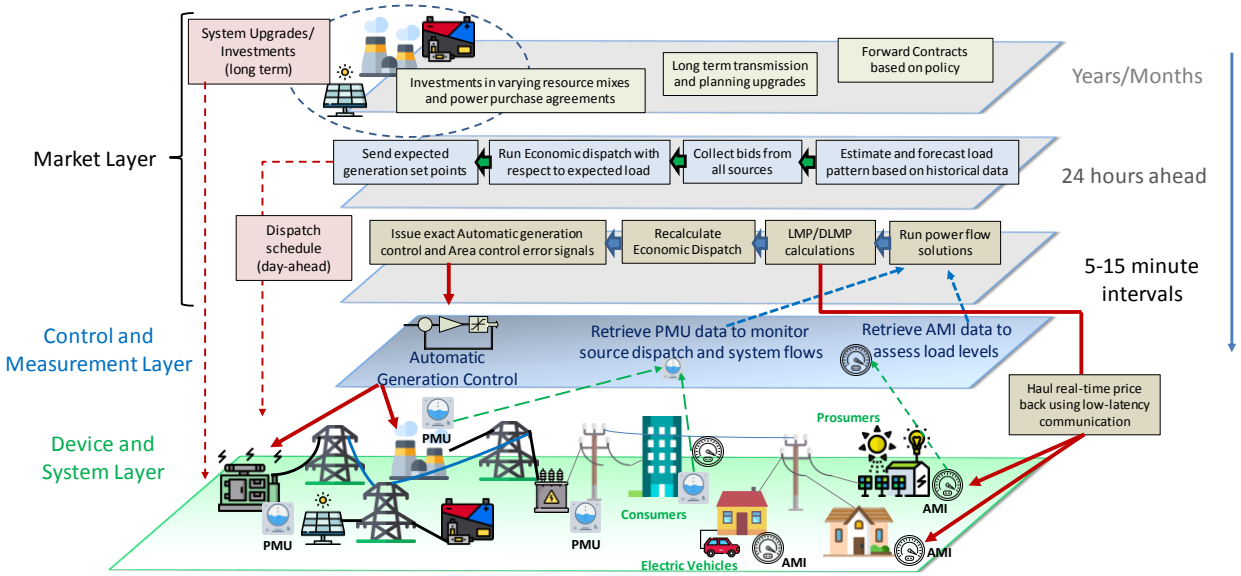

Figure 2.1 Existing grid operation and market control architecture

The primary layer and often the most visible one is the device and physical layer. This layer encompasses the physical power infrastructure including miles of transmission lines [17], points of voltage change in the form of transformers, generators and consumers. These devices are the ones responsible for energy delivery.

The advent of the digital age enabled an augmented layer in the form of control and measurement to be implemented. This layer consists of devices and control mechanisms to regulate the flow of power as well as capture valuable data about power flows and consumption patterns from the grid. Advanced Metering Infrastructure (AMI) was a key driver in deploying smart measurement devices at the grid edge to allow utilities and system operators visibility into individual consumer's load consumption pattern as well as achieve billing management remotely[18]. A wide range of applications such as data analytics about consumption patterns, network topology estimation and outage

management have been facilitated using this added visibility [19]–[22]. The power flows across the grid depend highly on magnitudes and phase angles of voltage vectors at different flow points. This information is critical to analyzing system flows and ensuring that the network continues to operate smoothly without running into line congestion issues. The advent of phasor measurement units (PMUs) was instrumental in providing points of visibility across the network to enable centralized estimation of system flows [23], [24]. These units are GPS synchronized to allow extraction of phase angle differences across a bulk network.

Energy management systems (EMS) were developed as a platform for power flow management and grid estimation based off of PMUs. Utilizing detailed system models and measurements from PMUs and AMI meters, supervisory control and data acquisition (SCADA) systems are able to embed EMS platforms and deliver numerous functionalities. SCADA systems run a complete power flow based on measurements (every 10-30 seconds), to provide an estimate of the system state to the operator [25]. This allow real-time monitoring of network conditions, provides a measure of grid stability, allows contingency scenarios to be calculated, and allows optimizations to be performed to coordinate dispatch points for sources [26]. Automatic generation control (AGC) is embedded into every generating unit to allow precise control over the power being delivered. Independent System Operators (ISOs) often take charge of using SCADA and EMS mechanisms to ensure that network is operating without congestion patterns and that supply-demand balances are being met in real-time [27]. This involves re-dispatching all participating sources in order to ensure smooth operation.

From a transactive perspective, the electric grid is a natural monopoly. The National Energy Policy Act of 1992 allowed for the creation of a wholesale marketplace for electricity through deregulation in some parts of the US [28]. Deregulation has ensured that numerous entities participate in this multi-layer electricity infrastructure. The objective of this reform was to promote competition and ensure that the market would be driven to a point where energy was being delivered at the cheapest price point to consumers. Today, an ecosystem of participants in the generating companies (GenCos), transmission companies (TransCos) and distribution companies (DisCos) all participate in an energy market. There are numerous time scales and planning horizons implemented. Each of these rely on tight coordination between all involved entities. Using a long-term forecast, some power purchase agreements and forward contracts may be set up [29], [30]. These are implemented to hedge against some uncertainty using bulk generation sources [31], [32]. Investment decisions involving future source mixes and long-term infrastructure placement are typically carried out several months or years ahead. On a daily basis, a dispatch procedure is settled based on a load forecast using a Security Constrained Economic Dispatch (SCED) or Security Constrained Optimal Power Flow (OPF) algorithm [33]–[36]. These procedures may be performed again on an hourly basis based on expected hourly deviations from day-ahead predictions. SCED and SCOPF algorithms use either load forecasts or actual measured load data from PMUs and AMI units, and real-time information about the current system topology, to compute system flows and optimize generation costs or system losses. EMS and SCADA systems embed SCED and SCOPF algorithms to allow periodic redispatch procedures (AGC) even on an intra-day basis.

The operation and control mechanisms in place today are primarily governed by the market layer. It is important to note that the core functionality of the grid under normal operating conditions, remains transportation of power without running into network constraints while ensuring that supply-demand balances are met using market principles. Thus, these complex, layered, grid management principles can be condensed and divided into two main layers -the physical layer that manages parameters like voltage and congestion, and the transactive layer that enables a marketplace for all independent asset owners. While, today's architecture is significant in functionality and efficiency, there are some key challenges.

2.1.2 Fragility of today's grid architecture

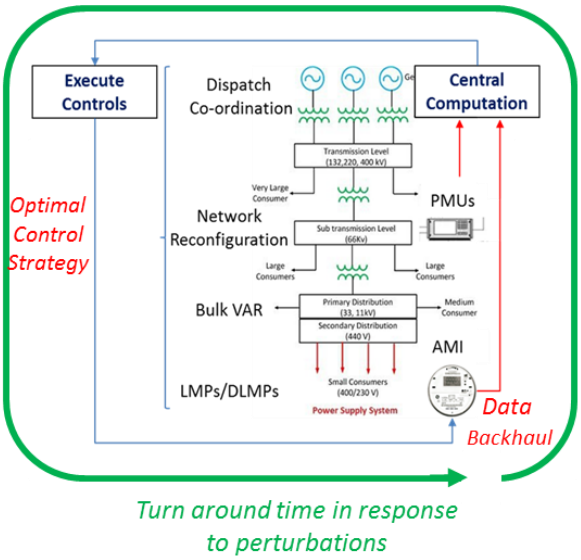

Figure 2.2 Existing control and coordination paradigm

It is apparent to see that the 'Achilles heel' of the modern grid operation paradigm is the dependence on continuous communication and centralized computations. Each of the layers mentioned in the previous discussion depend heavily on accurate knowledge of the current system topology and precise information about system states. System operators are

tasked with utilizing low-latency communications to periodically retrieve load patterns using AMI and PMU data, synchronize the readings, run complex SCED or SCOPF procedures and issue control signals (AGC or network reconfiguration) to stabilize the system. Fig. 2.2 illustrates this control principle. Loss of measurements from certain locations could severely hamper the entire control architecture. Konstantinou et.al have shown the effects of GPS spoofing cyber-attacks and the resulting destabilization of the system in question [37]. The 2015 Ukraine blackout is an example of such a coordinated cyber-attack [38]. Even in cases without malicious intent, loss of GPS signals in PMU units or damage to communication systems can severely hamper wide area monitoring system in place today [39].

Dispatch has traditionally worked well with the `top-down architecture' with limited participants and predictable load patterns. With generation centers moving towards to the grid-edge, and growing numbers of asset owners, it becomes extremely challenging to derive optimal dispatch procedures for all participating agents. The volatility introduced by non-dispatchable DERs like PV further complicates this issue. In contrast to the traditional dispatch procedures where the capacity limits are known, the available capacity fluctuates significantly in PV rich areas - sometimes in the millisecond time frame. Often, an independent asset owner may choose to not participate in the power pool making estimation of available capacity from the grid edge even more challenging. The central computation-based approach where every grid state is retrieved before recalculating dispatch or controls fails to cope against fast phenomenon and the growing number of participants seen in today's systems. Moreover, the reliance on low-latency communication also introduces numerous points of failure and resiliency concerns. Yet it is inevitable that

future grid structures will largely be dominated by volatile PV-based sources. Microgrids are being deployed with volatile sources in developing economies. The cost of communication systems becomes an issue when deploying grids in such environments. Moreover, the challenges associated with managing supply-demand imbalances and volatility are accentuated in these settings. Centralized approaches would not be scalable in such settings.

System operators rely on accurate load forecasts to generate baseline dispatch procedures and alter them periodically. However, with DERs severely altering the way energy is consumed, it becomes challenging to forecast optimal procedures. AGC signals are issued at best in the 5-15-minute time frame to address congestion leaving the system vulnerable to fast phenomenon introduced by volatile sources [40]. The market layer is designed to optimize the cost of operation, but it completely fails to leverage any form of demand elasticity. Prosumers and consumers are abstracted form the dynamics and only exposed to flat-rate prices in most marketplaces. Yet, demand flexibility is key to stabilizing these highly volatile PV dominant grids of the future.

Numerous approaches have been proposed in literature to deal with certain aspects discussed above. To reduce the dependence on communication with centralized control locations, graph-theoretic stabilization mechanisms are being explored in literature. Vaccaro et.al have explored the use of consensus algorithms at the community level to achieve economic dispatch [41]. This architecture relies on communication of some key parameters between neighbors or peers in a system to achieve a common goal. Zhang et.al have proposed an architecture in [42] that relies on exchanging power mismatches between agents to achieve economic dispatch in a decentralized fashion. However, the architecture

is based on the election and presence of a leader node on the connected graph that becomes the root node for the consensus algorithm. The number of nodes that can be elected as leaders limit the reconfigurability of the architecture and the make the entire architecture prone to failure if any cyber-attack occurs on the designated leader node at any instance in time. Most of these approaches rely on knowledge of topology, incremental costs, plant capacities or other source and participant parameters. While some centralized communication and coordination can be avoided by using peer-to-peer or cloud-to-agent approaches, the entire architecture is crippled in the event of damage to any communication infrastructure. Moreover, in areas where the agents are geographically dispersed, the communication requirements of a peer-to-peer model are similar to those seen in centralized architectures.

Loia et.al have also proposed a decentralized voltage management approach which also relies on radio-based communication with adjacent agents and control devices [43]. The idea of using mechanisms in the market layer to aid grid stabilization have been explored in literature as well. Virtual power plants and their role in the energy market is considered in [44]. Decentralized trading architectures have been presented by Hijgenaar et.al in [45]. Some blockchain based adaptations to achieve a decentralized transactive marketplace have been shown in [46]–[48]. This approach assumes high speed communication with the cloud for all associated agents. Demand-side participation and decentralized market implementations have largely been ignored while focusing on reaching economic dispatch using source-side controls. Transactive energy platforms are being explored in literature to allow stabilization of supply-demand imbalances and volatility using collective supply and demand participation [49]–[51]. However, these

approaches again rely on either a graph-theoretic approach or centralized market clearing, compromising their resilience Approaches using HEMS systems to provide some demand response have been investigated in [52]–[54]. Thus, while key developments have been made to reduce the reliance on centralized computations and coordination, no holistic and robust solution is available to manage future grids.

An integrated structure to achieve autonomous decongestion while facilitating power trading between all associated agents has seldom been realized. To achieve resiliency improvements, the grid control principles need to be scalable, and agnostic to system size and topology while stabilizing the system in a decentralized fashion. Thus, a truly fractal approach is required towards designing control architectures for future grids where the system could break into smaller sub-grids but still operate using the same control principles [55]. The research presented in this document highlights a framework and a set of solutions to achieve decentralized control over transactive and physical grid aspects in a resilient fashion. The next subsection provides an overview of existing control techniques that are used to control system flows.

2.2 State-of-the-art Congestion Relief and Voltage Support Mechanisms

As the grid has evolved over the last few decades, reliability and redundancy have been severely enforced, to ensure a robust physical infrastructure. This has resulted in a highly meshed grid architecture. It has been shown that meshing power networks has significant advantages in terms of minimizing transmission losses [56]. While meshing has largely been prevalent on bulk systems, large urban centers are also implementing such

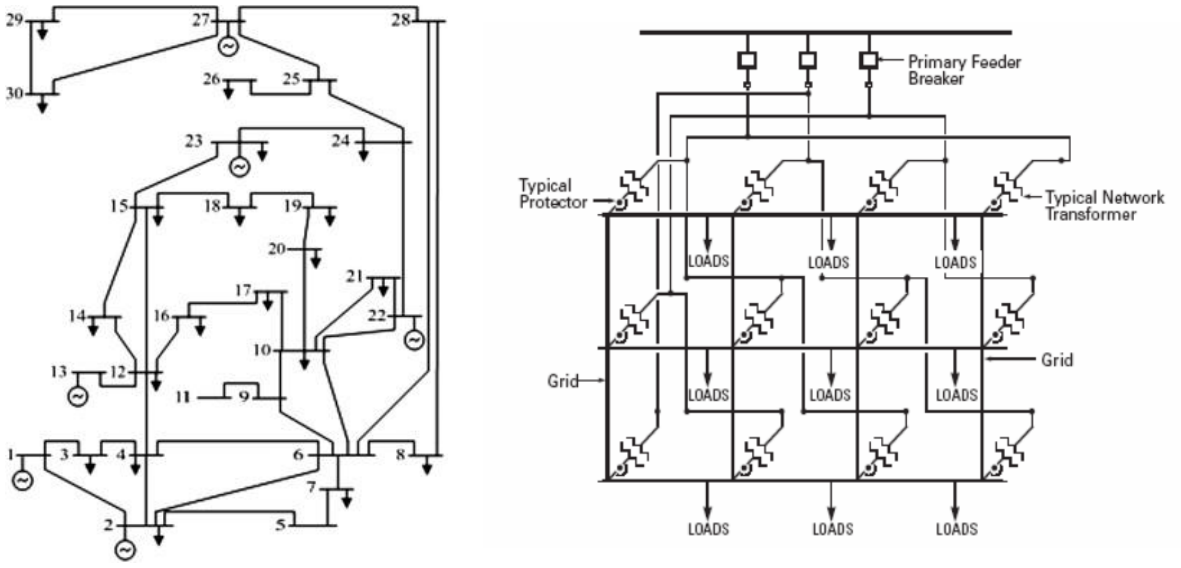

(a) **(b)**

Figure 2.3 Illustration of meshed grid structures at the (a) bulk power level (IEEE 30 bus system) (b) low voltage level [57,58]

architectures at the low voltage level to maximize reliability. Mega cities like New York, Los Angeles and a few cities in Germany have employed novel meshed low voltage architectures where multiple megawatts of power are transported at distribution voltages in underground networks. Fig. 2.3 (a) and 2.3(b) show a generalized overview of bulk meshed grids[57] as well as newer low voltage meshed grid structures [58].

However, control of power flows and voltage profiles across such networks is extremely challenging. Line congestion occurs when the state of the grid is characterized by one or more violations of the current carrying limits of transmission links. Unprecedented DER adoption at the grid-edge further accentuates this issue. Unexpected power flow patterns and line congestion patterns are seen as a result of this. Severe voltage volatility is also observed on feeders with heavy PV penetration. Dynamic grid control becomes a necessity in such environments. Congestion management and control over power flows has generally been exercised in two ways. The first involves a centralized

approach where sources are redispatched to alter power flows patterns or the topology of the network is altered to affect power flows. The second approach involves deploying distributed controllable solutions to affect power flows on certain corridors. An overview of both these control techniques along with their associated challenges is presented in this subsection. A review of commonly used voltage control solutions is presented as well.

2.2.1 Centralized Control over Power Flows

In vertically integrated structures, the generation units, transmission corridors and the distribution network were typically administered and managed by a single entity. Congestion would occur as a phenomenon on a sporadic basis and the operator would have to resort to altering generation dispatch pattern using AGC to change grid flows. One of the most powerful algorithms in terms of addressing this phenomenon has been the Optimal Power Flow (OPF) algorithm [36]. The problem typically consists of an objective function that is being minimized while enforcing certain constraints. The function being minimized could be the net generation cost or the cumulative transmission losses. Typically, in today's electricity markets with multiple participants and bidding entities, the generation cost is often the quantity being minimized. The constraints often embed the security requirements of the grid structure. These could include voltage regulation requirements as well as the line capacity constraints. OPF algorithms are finding their place in control centers as parts of their SCADA or EMS systems.

Since, congestion is a spatial and temporal phenomenon that arises in real-time, based on loading variations or contingencies, it needs to be addressed in a timely manner on an intra-day basis. In the pre-congestion time frame, dispatch points for all generating

units are a result of the respective generator bids as well as the market dispatch procedure. However, when a congestion pattern is observed on the state of the grid, a new OPF problem specifically targeted towards reaching an optimal grid state needs to be solved. This iterative algorithm first imports system states by retrieving them over low-latency communications and computes a base case power flow solution. Once, an estimate for the complete system state is obtained, an optimization routine is used to derive a feasible solution under given constraints. An example of a formulation [59] is summarized in (1).

Objective function:

$$Minimize\ \sum_{g}^{Ng} C_g(\Delta P_g)\Delta P_g \tag{1}$$

Subject to

$$\sum_{g}^{Nl}\left((GS)\Delta P_g\right) + F_k^0 \leq F_k^{max} \tag{1a}$$

$$P_g^{min} \leq P_g \leq P_g^{max} \tag{1b}$$

$$P_g - P_g^{min} = \Delta P_g^{min} \tag{1c}$$

$$\Delta P_g^{min} \leq \Delta P_g \leq \Delta P_g^{max} \tag{1d}$$

$$\Delta P_g^{max} = P_g^{max} - P_g \tag{1e}$$

Where,

ΔP_g - Required adjustment in real power outputs

$GS(\Delta P_g)$ – Line flow sensitivities to generation set points

C_g - Price bids from participating generators

F_k^0 - Base case power flow for branch k

F_k^{max} – Line loading limit for a given link

N_g - Number of participating sources

N_l - Number of active transmission links

$P_g^{min}\ and\ P_g^{max}$ – Limits on generator outputs

The formulation presented above can be embedded with higher complexity depending on other constraints that may need to be embedded. The problem highlighted in (1) can be solved using a linear programming approach. Generator sensitivities are typically embedded in the form of power transfer distribution factors (PTDFs) [60]. The OPF formulation then generates a feasible solution that contains real power adjustments that need to made to take the system back to a non-congested state. These signals are issued in the form of AGC signals to bias governor operations of generating units. This ensures that all units dispatch the required power set points at a 60Hz point on their droop curves. Further complexity can be added by accounting for a few contingency cases. Thus, a new class of algorithms in the form of security constrained optimal power flow (SCOPF) algorithms can be realized. Actual power flow equations are however, quadratic. This makes the OPF problem a quadratically constrained quadratic program (QCQP). The problem is generally nonconvex and NP-hard making it challenging to solve. Numerous approaches to solve OPF problems have been proposed in literature using the second order cone program (SOCP) [61] as well as other semidefinite program methodologies (SDP) [62]. A popular approximation used in most EMS and SCADA systems today is the DC optimal power flow (DC OPF) methodology [63]. This method relies on linearization of power equations to reduce the complexity of conventional OPF problems[64].

Topology reconfiguration is another solution that is used to change system flows. Reconfiguration of power networks relies on operating tie line switches and sectionalizers in a pattern that alters the net power flow across the system[65]. Reconfiguration has been used a measure to reduce losses on meshed distribution network. Reconfiguration for congestion management is known to be a nonlinear complex combinatorial optimization problem. These problems have been solved using Genetic algorithms and particle swarm optimization based solutions in literature [66], [67]. Much like the OPF based approach, reconfiguration also relies on establishing visibility using measurements from PMUs over low latency communications and performing complex optimizations centrally.

Both solutions involve complete knowledge of system topologies and low-latency communications to issue commands. Altering the dispatch patterns impacts the transactive layer of the system and adds a congestion cost component to the system. The centralized solutions presented in this section focus on utilizing a communication loop with a centralized entity to address congestion issues. With power flows becoming unpredictable owing to rapid deployment of PV and wind, rapid dynamic congestion management becomes extremely necessary. Moreover, OPF problems work well with limited participants in a market structure. The computational complexity requirements to accommodate millions of prosumers with their own constraints using today's centralized approaches will be astronomical. This ensures that the scalability of centralized congestion management solutions in future DER heavy grids is limited owing to the computational and communication requirements.

2.2.2 Distributed Power Flow Control Solutions

Centralized solutions presented in Section 2.2.1 assume that the network is entirely passive. This makes it necessary to change source setpoints to change power flows. These approaches involve using algorithmic frameworks to affect control at the generator level. However, a large number of hardware devices have been proposed in literature to make the passive network more flexible and active. These solutions ensure that grid flows can be altered in scenarios with congestion by reconfiguring physical characteristics of the meshed grid itself. These hardware solutions allow active control over meshed passive networks. Since, these solutions are located in sparse locations across meshed structures, they will be referred to as distributed solutions in this document. Some of the methods as well as their attributes will be summarized in this subsection. An overview of the principle behind distributed power flow controllers will be presented first followed by some technologies that enable the same.

2.2.2.1 Distributed Power Flow Controllers - Principle

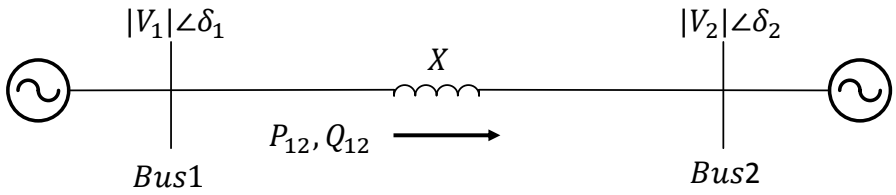

Figure 2.4 Power flows over a two-bus system

The power flow across any given corridor is a function of the voltage magnitudes across the link, the phase angles as well as the impedance of the corridor itself. Consider a two-bus system shown in Fig. 2.4. The power flow across the link is governed by equations (2) and (3). Here, $|V_1|$ and $|V_2|$ are the magnitudes of the voltage phasor at both ends of the

line and δ_1 and δ_2 are their respective phase angles. X represents the impedance of the transmission corridor.

$$P_{12} = \frac{|V_1||V_2|}{X}\sin(\delta_1 - \delta_2) \tag{2}$$

$$Q_{12} = \frac{(|V_1|^2 - |V_1||V_2|\cos(\delta_1 - \delta_2))}{X} \tag{3}$$

The equations show that the amount of power flow across any given link can be controlled by affecting changes on the phase angle between the sending and receiving end of the link or the apparent impedance itself. Any device that can achieve these attributes would show promise in addressing congestion patterns in a distributed fashion. Fig. 2.5 shows such a power flow control device that can add a voltage at a certain magnitude in series with the sending end voltage. Fig. 2.5 also shows the resultant phasor diagram for such a system. Here V_{pfc} represents the additional voltage phasor that is injected by the series power flow control device. As a consequence, the resultant sending voltage is $|V_1'|\angle\delta_1{}'$. Thus, with an added power flow control device on the like, the active power flow equation becomes that shown in equation (4).

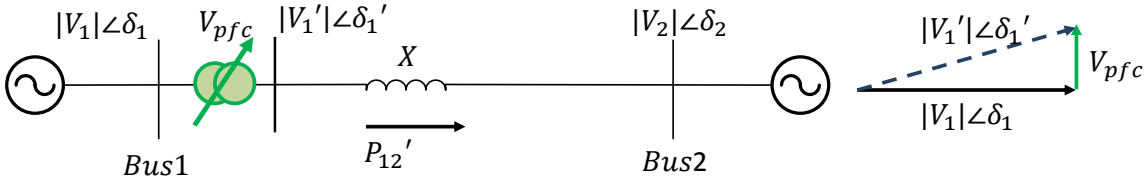

Figure 2.5 Power flow variation over a two bus system with a power flow controller (*pfc*)

$$P_{12}{}' = \frac{|V_1'||V_2|\sin(\delta_1{}' - \delta_2)}{X} \tag{4}$$

Most distributed power flow control devices use this principle. Some of these power flow control devices are presented next.

2.2.2.2 Phase Shifting Transformers (PSTs)

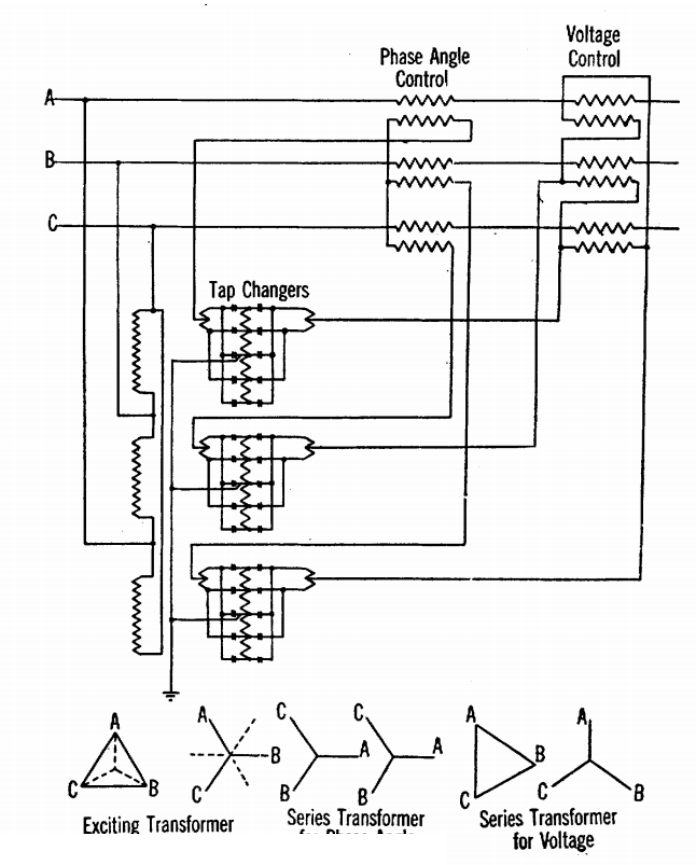

Figure 2.6 Phase shifting transformers [69]

Phase shifting transformers (PSTs) have been used traditionally as a power flow control device in meshed grids. These devices were designed to accommodate changes in power flows that were observed on a seasonal basis[68]. PSTs are mechanical devices that utilize a series of winding and taps to synthesize a fractional out-of-phase voltage that can be injected to change power flows. The out-of-phase component and its magnitudes are a result of the inherent phase shifts between delta and wye winding connections on a transformer as well as the taps on them. Fig. 2.6 shows a schematic of a typical PST [69].

While, these devices do add some flexibility their response times are not adequate for real-time control. The tap settings are controlled mechanically, and they often degrade through continuous operation. This ensures that PSTs are inadequate to address fast congestion phenomenon on future DER-heavy grids. The presence of limited tap settings significantly complicates the real-time optimization algorithms. Thus, slow dynamics and degradation due to rapid switching ensures that these solutions have limited effect of addressing congestion issues in future DER heavy grids. Thyristor controlled phase shifting transformers (TSPSTs) have been developed to ensure faster response times [70]. However, problems associated with thyristor control and fault management in series injection windings have ensured that these technologies are not being widely adopted in the current power infrastructure [71].

2.2.2.3 Fully rated High-Voltage Direct Current (HVDC) Links

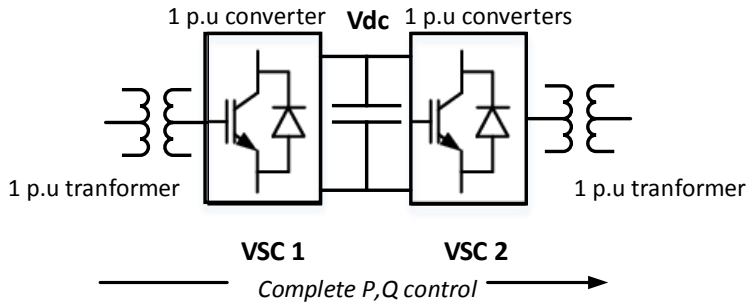

Figure 2.7 HVDC (fully rated back-to-back) General Schematic

Power electronics-based approaches have shown great merit for dynamic grid control. Flexible AC Transmission systems (FACTS)-based solutions like HVDC were originally utilized to transfer power over large distances. In addition to the efficiency of transmission, these links also enable controllable power flows. HVDC links involve two

fully rated converter units that enable transmission of power over a DC link. HVDC in itself does have its own set of challenges. Investment requirements for converter stations, poor power factors, reactive power compensation requirements and harmonic management issues make these solutions challenging to implement [72], [73]. While HVDC does make transporting power over large lengths possible, the controllability over any given link can be achieved by any fully rated back-to-back (FRBTB) link. Fully rated implies that all components are rated at 1 p.u which is the rating for the desired link.

HVDC-light is one such realization where a controllable link is created by using two sets of voltage source converters (VSCs) in a FRBTB configuration with a DC link in between [74]. Fig. 2.7 shows a generalized schematic of an HVDC FRBTB implementation. The BTB units are accompanied by two coupling transformers on either side of the link. Since the link is asynchronous, a completely controllable corridor can be realized to alter active and reactive power flows in a bidirectional fashion. Today, HVDC-light has been implemented in numerous locations in Sweden, China, Denmark, Australia and North America [75].

However, from an economic perspective an HVDC FRBTB implementation involves building a completely new corridor. This involves long execution times and high investment costs. Elaborate planning studies need to be conducted to size the link and its attributes correctly. Another key factor to analyze with these solutions is resiliency. When considering the HVDC FRBTB implementation, failure of any one component hampers the operation of the entire unit. Since, the link involves two coupling transformers, two fully rated VSC converters and a DC link capacitor, the probability of failure is quite high. Damage to any one component, would cripple the entire link in addition to losing any added

controllability achieved. Fully rated approaches are also more expensive as all components need to be rated to handle nominal and fault currents for the entire link.

2.2.2.4 Unified Power Flow Controller (UPFC)

UPFCs are another FACTS-based approach towards adding controllability to system flows. Rather, than embed a fully asynchronous link with FRBTB converters, the UPFC approach embeds the fractional control approach elaborated in Section 2.2.2.1. Fig. 2.8 shows a

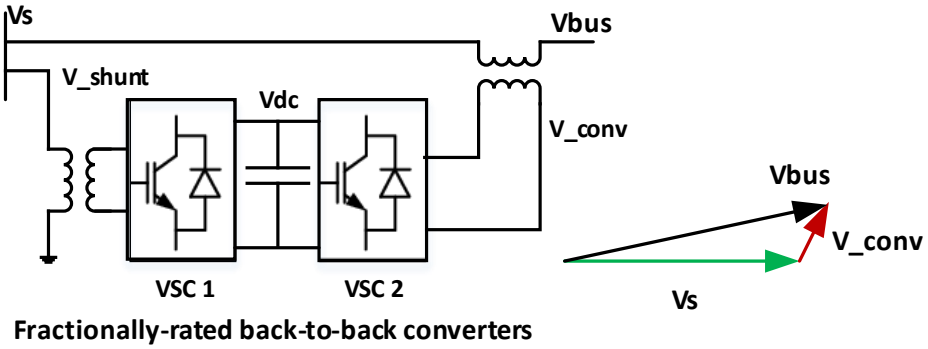

Figure 2.8 Unified Power Flow Controller (UPFC)

generalized schematic of the approach. The configuration involves a back-to-back (BTB) converter set that takes a fractional voltage from the line side and synthesizes a fractional voltage of controllable magnitude and phase [76]. This synthesized fractional voltage is injected in series with the line voltage thereby allowing power flow control based on the principles discussed in Section 2.2.2.1. The shunt transformer allows the voltage to be stepped down for the line-side converter unit whose sole purpose is to regulate the DC link voltage and regulate VARs. The series converter unit then synthesizes the fractional voltage which is injected in series by utilizing the series transformer. Since, the entire approach is based off the fractional injection approach, the sizing requirements as well as converter and device ratings can be reduced significantly. Compared to the FRBTB

approach discussed earlier, UPFCs are much cheaper for the same level of control. In addition to active and reactive power flow control, UPFCs can also improve voltage profiles by injecting an in-phase series voltage component. The first UPFC installation in the U.S was carried out in Kentucky in 1998 [77].

Since, the entire UPFC topology can be bypassed, failure modes associated with the BTB unit do not cripple the entire link. However, the series transformer does have to fully rated for current since it is a series component. Series transformers in UPFC systems need to be rated to handle full fault currents making them prohibitively expensive [78]. Further, failure modes associated with the series transformer can cripple the entire link along with the loss of controllability. Additional complexity and costs have limited the adoption of UPFCs into today's systems.

2.2.2.5 Distributed Series Impedance (DSI)

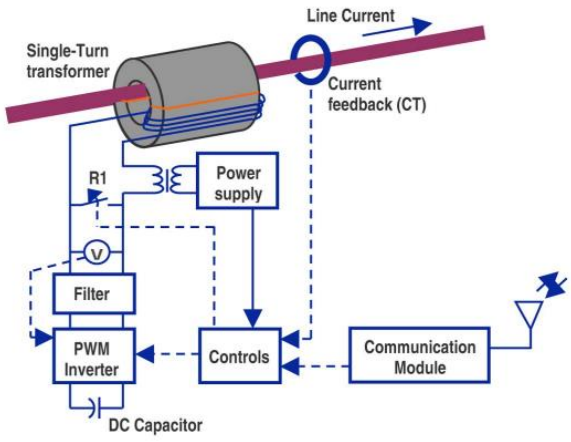

Figure 2.9 Distributed Series Impedance [79]

While adding fractional series voltage components on the line can add controllability, so can altering the apparent impedance. As discussed in Section 2.2.2.1, the impedance

term plays a key role in determining the power flow across a link. DSI modules aim to augment existing corridors with switching impedance changes to achieve the same. Fig. 2.9 shows an example of a DSI implementation [79]. The setup consists of a single turn series transformer, an inductor and a capacitor. The inductor can be switched on the line using the thyristor control circuit. This allows the impedance characteristics of the line to be controlled dynamically. Moreover, the number of modules can be scaled to increase or decrease controllability on any given corridor. Smart Wires has a DSI product that has shown tremendous potential in terms of delaying transmission expansion, aiding better utilization of existing assets and providing congestion relief [80].

2.2.3 Voltage Control Solutions

One of the key challenges with heavy DER penetration is managing local voltage profiles. Problems associated with over voltages on feeders with heavy PV based DERs are visible today [81], [82]. A range of voltage control solutions have been proposed to address the same. An overview of some legacy as well as advanced solutions will be presented next.

2.2.3.1 On-Load Tap Changers (OLTCs)

OLTCs are a legacy technology to achieve control local voltage profiles. Much like the PSTs, OLTCs are designed to accommodate slow variations in voltage owing to seasonal voltage changes. Fig. 2.10(a) shows a schematic of an OLTC [83]. Fig. 2.10(b) shows an image of a commercial OLTC [84]. The technology is based on discrete taps that

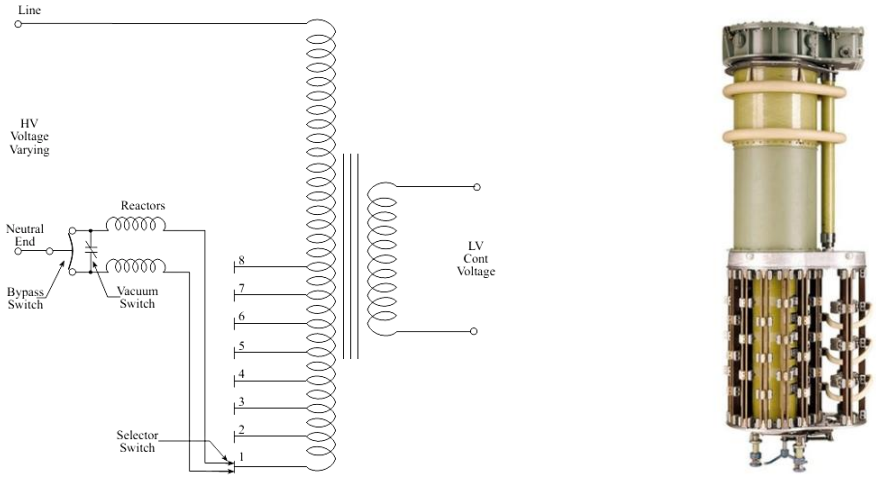

(a) **(b)**

Figure 2.10 (a) OLTC Schematic (b) Commercial OLTC Product [84]

are created on the secondary or primary winding of a conventional transformer to alter the turns ratio by switching between different combinations. The switching action is typically done mechanically.

The technology is limited in terms of speed owing to the mechanical motions it must go through. Rapid volatility seen in DER heavy grids would have to be addressed by rapidly switching these devices. However, the mechanical nature limits their real-time usability. OLTCs in today's grids are having to switch far more than they were designed for [85]. Moreover, the delays in switching actions often imply that the phenomenon to be addressed has often passed before the switching action is completed.

2.2.3.2 Mechanically Switched Capacitor Banks

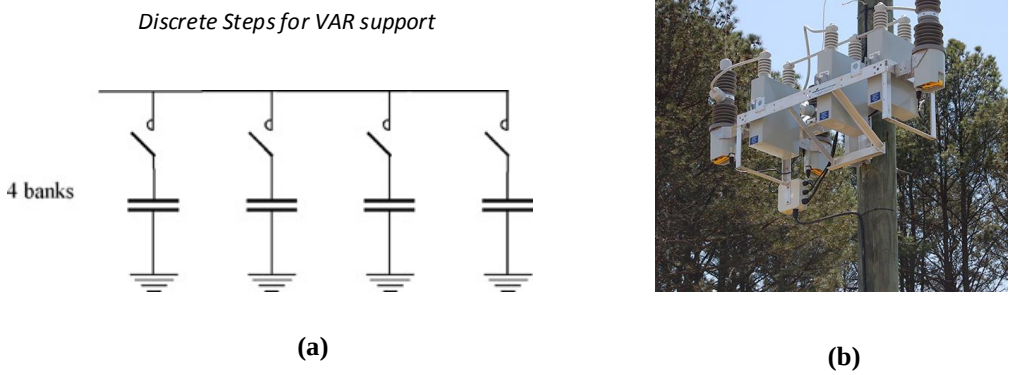

(a) **(b)**

Figure 2.11 (a) Mechanically Switched Capacitor bank (b) Commercial Switched capacitor bank (Eaton) [86]

Another approach towards providing voltage support involves using capacitor banks. By switching in a set of capacitors into the system depending on the local voltage reactive power support can be provided. Control set points for these devices may also be issued by a centralized DMS entity using a volt-var optimization algorithm. This aids in improving the local voltage profile. Fig. 2.11 (a) shows a schematic of a capacitor bank with 4 steps. This allows discrete amounts of reactive power to be introduced on the system. Fig. 2.11 (b) shows a commercial capacitor bank [86]. These devices are widely adopted in today's distribution grids.

However, much like the OLTCs, switched capacitor banks are mechanically controlled limiting their response time. Further, the discrete steps limit the amount of regulation that can be added. Decaying ring wave transients and inrush phenomenon associated with the switching actions make these devices seem less robust [87].

2.2.3.3 Thyristor Controlled Reactors (TCRs) and Switched Capacitors (TSC)

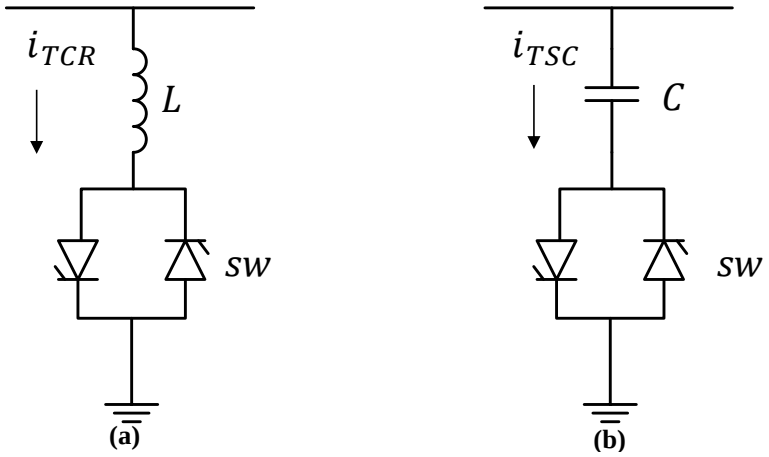

Figure 2.12 (a) TCR Schematic (b) TSC Schematic

FACTS based approaches have shown promise in addressing some of the issues associated with capacitor banks. TSCs and TCRs consist of a capacitor and reactor connected in shunt through a pair of thyristors. By controlling the thyristor firing angle, the effective capacitance or reactance inserted into the system can be controlled [88], [89]. Fig. 2.12 (a) and (b) show general schematics for TCRs and TSCs respectively.

TCRs and TSCs provide discrete control and allow the reactive power inserted to be finely controlled. However, these approaches have been known to introduce undesirable harmonics. Methods involving delta connection of modules as well as symmetric control over thyristors have been proposed in literature to address some harmonic issues.

2.2.4 Constraints with controlling low-voltage meshed grids

FACTS-based solutions have shown some promise as power flow controllers on the bulk power level. However, when dealing with low voltage meshed grids in urban centers some key considerations ensure that FACTS based solutions do not address voltage and

asset loading problems. The low impedance of the network along with the high degrees of coupling observed between transformers poses significant problems. Geospatial loading variations on low voltage meshes significantly alter the voltage profiles, relative asset loading and reactive power flows. Shunt capacitors and FACTS-based VAR support has been studied extensively for radial networks [90], [91] However, bulk VAR support often results in reactive power loops on such networks. Thus, the desired volt-var solutions need to be more distributed to affect voltage profiles locally and efficiently. Small amounts of control exercised in multiple locations have more value than centralized bulk VAR deployment. Another key consideration is the high amounts of current (> 50kA) observed on these low voltage meshes. Thus, any control device would have to be able to sustain these fault current levels. In addition, there are numerous environmental constraints that are desirable. Low voltage meshed networks in urban centers are typically underground with a network of cables and transformers lying in underground mains. Thus, any solution deployed would have to sustain operation in such tight spaces and exhibit high water resistance. This ensures that FACTS based solutions cannot be deployed under these constraints. Thus, cheaper, more resilient control solutions that can be retrofitted at points of interest in the grid are required.

2.2.5 Control of Physical Grid Parameters - Discussion

Legacy physical grid control approaches have been shaped around the assumption that control over system flows can only be achieved by altering source dispatch points. It is clear that this approach cannot scale to future grids where fast dynamics, increased volatility and grid edge sources will be commonplace. As DER penetration levels on the system rise, it becomes necessary to add solutions that can make the passive grid more

active. FACTS based solutions have enabled faster response times and increased controllability over grid phenomenon. However, most of these approaches show poor resiliency owing to certain failure modes. Further, most of these solutions are significantly expensive and involve massive infrastructure upgrades and dedicated links.

Thus, an ideal grid control solution would be one that adds significant control at numerous points without adding tremendous cost in terms of implementation. The solution would have to be retrofittable. Further, the solution would have to be designed in a way where failure modes don't cripple existing links. Moreover, the solution would have to embed the attributes of all the devices summarized in this section. Hybrid Transformers are presented as a resilient and cost-effective grid control solution in this document.

2.3 Existing transactive control mechanisms to leverage flexibility

The non-dispatchable nature of DERs and their fluctuating availability make operation and control aspects of DER heavy grid structures challenging. Grid operators often use dispatchable sources to cover fluctuations in DER availability. As the resource mix moves towards one that is dominated by PV, relying on a slack bus becomes infeasible. Moreover, as millions of consumers turn into generation asset owners, it becomes necessary to create a formal incentive structure to ensure that global supply-demand balances are met. With wide variations in supply-demand balances, incentivizing demand flexibility is key to stabilizing and managing future grids. Moreover, by reflecting the state of the system to the users in real-time, end nodes could be incentivized to fulfil local objectives while globally stabilizing the system.

Dynamic pricing as an instrument to leverage demand flexibility has been extensively investigated to manage supply-demand imbalances.[92], [93] Federal Energy Regulatory Commission (FERC) defines demand response (DR) as "Changes in electric usage by end-use customers from their normal consumption patterns in response to changes in the price of electricity over time, or to incentive payments designed to induce lower electricity use at times of high wholesale market prices or when system reliability is jeopardized" [94]. Long term demand response programs aim at designing structures, to shift power consumptions over long periods of time, allowing significant changes in investments into resource mixes and portfolios [95]. Demand response programs aid in assessing long-term planning needs for generation, transmission and distribution levels [96]–[98].

The advent of intelligent end devices [99] and smart home energy management systems has allowed DR to be leveraged more effectively. Demand response programs to aid intra-day phenomenon have been created and exercised by numerous system operators. As the FERC definition states, most demand response frameworks are designed around creating incentives or exposing connected agents to real-time prices [100]. An overview of some schemes is presented next.

2.3.1 Incentive-based Mechanisms

With the advent of the AMI infrastructure, grid operators gained visibility into consumption dynamics. Grid operators realized that sporadic system overloads could be reduced by creating time-based incentive structures for consumers. These rate or tariff

structures are quite prevalent and are exercised by numerous utilities to reduce stress on their grid structures.

2.3.1.1 Time-of-Use (TOU) Pricing

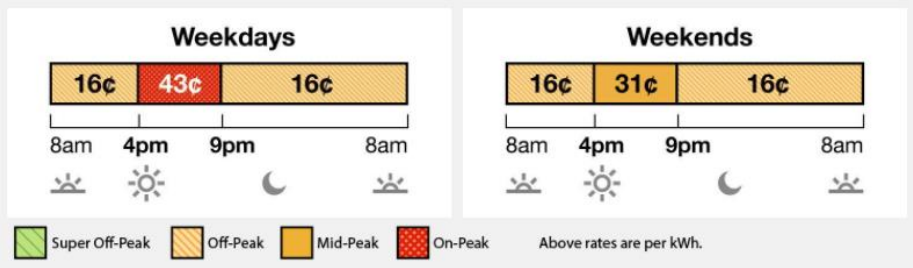

Figure 2.13 TOU-D-PRIME Pricing Scheme (SCE) [102]

TOU pricing has been adopted by a large number of utilities across the world. The scheme involves designing a rate structure where the price of energy varies over different times across the day [101]. A utility operator could look at historical trends and analyze periods where the cost of generation has been traditionally high or periods where there is an incentive to reduce system stresses by incentivizing demand reduction. This could mean that TOU pricing schemes could incentivize different consumption patterns across a season or even on an intra-day basis. Southern California Edison (SCE) has instituted a TOU pricing framework as that seen in Fig. 2.13 as part of their 'TOU-D-PRIME' scheme [102]. TOU schemes allow utilities to ensure that demand levels are maintained at manageable levels. A key point to note here is that TOU schemes do not require bidirectional communication. Since this is a tariff structure, the user is informed of the rate plan and billed accordingly.

2.3.1.2 Critical Peak Pricing (CPP)

Utilities and system operators may anticipate heavily loaded intervals owing to weather phenomenon or other factors. CPP involves sending updated prices for these intervals to incentivize reduction in consumption. This pricing structure is very similar to the TOU structure where multiple prices are established depending on the expected load profiles and dispatch procedures [103]. The key difference with CPP is that it is typically implemented for a limited number of times annually. For instance, Xcel energy utilizes a CPP program where consumers may be subjected to peak prices upto 15 times a year., for a maximum of 4 hours and between noon and 8 PM [104]. The main takeaway is that both these methods involve a planning decision to pre-declare these prices for a significant amount of time. These prices are set in a way to ensure that generation and transmission costs are covered. Moreover, a one-way communication link suffices for CPP.

2.3.1.3 Peak-Time Rebate (PTR)

Another implementation of a price-based demand response algorithm would be a peak-time rebate mechanism [105]. This structure relies on offering incentives to users to drop their collective consumption. This is exactly opposite to the CPP structure. The rebate is awarded by calculating the reduction in consumption as compared to the baseline load curve. However, this involves analyzing and creating a base line load curve which can be challenging [106]. Another key point of consideration is that the user pays the same rate for higher consumption while only a reduction is awarded. This structure is created to offer price protection to consumers while educating a consumer to provide support to the grid.

2.3.1.4 Challenges with Incentive-based Mechanisms

The incentive-based schemes described above have shown limited impact in terms of leveraging demand flexibility. Some of the more favorable structures proposed above involve some form of load estimation procedures. This is quite challenging as it involves characterizing each consumer's baseline load consumption and their elasticity to decide an appropriate incentive. Another drawback of this scheme is that there is no penalty system in place for higher than expected consumption. More direct methods involve direct load control or revolving blackouts. These schemes are invasive and result in consumer dissatisfaction. The implication of this is that the system administrator needs to carefully design these price points to hedge the actual generation price volatility. It is apparent that by updating prices more frequently, a lower hedging premium needs to be maintained as the market dynamics can be reflected more effectively in terms of prices.

2.3.2 Real-time Pricing (RTP)

From a system operator's perspective, spot market pricing mechanisms are designed to hedge the uncertainty and generation price volatility in real-time. It is immediately apparent that by updating price more frequently to reflect the true cost, a lower hedging premium can be maintained while operating with lower risk. Real-time pricing (RTP) mechanisms aim to achieve just that by leveraging maximum elasticity from all connected agents [107].

In 1988, Schweppe et.al proposed a framework based on spot pricing of electricity which is considered to be the foundation for all modern nodal pricing mechanisms [108]. The framework focused on realizing an energy marketplace where the commodity (energy)

was being bought and sold in a manner where the prices reflected the time and geospatial aspects of power delivery. This method was proposed to maximize benefits for the producers and the consumers. This framework has been adopted into the nodal price frameworks seen today.

Locational Marginal Prices (LMPs) and Distribution Locational Marginal Prices (DLMPs) are used to convey real-time prices in most implementations. LMP has worked great at the transmission level in terms of capturing congestion and geospatial marginal costs of production [8]. The system relies on data from PMUs and AMI meters [109]. The energy component of the price is decided using the marginal prices of all participating sources. The congestion component involves running power flows based on the apparent load to calculate the congestion patterns to calculate flows across the system

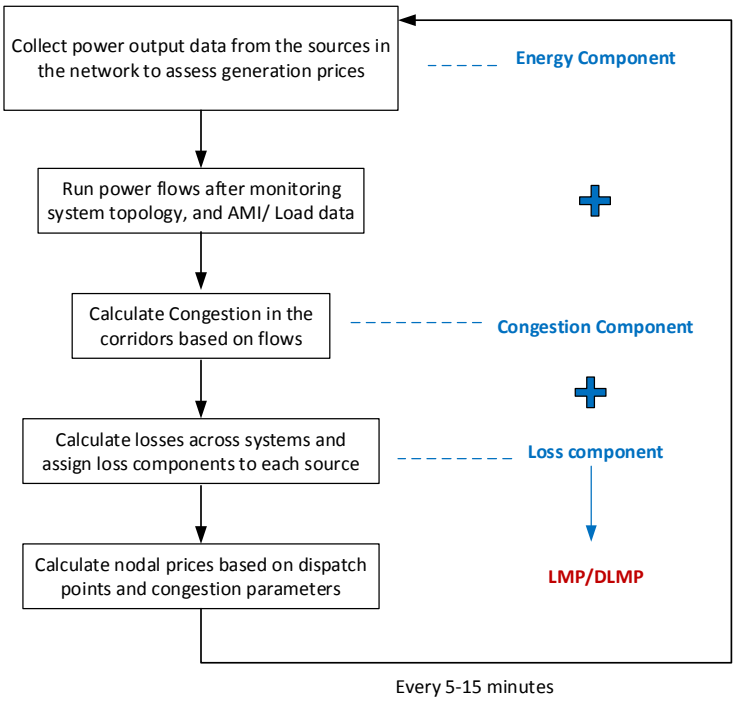

Figure 2.14 LMP Calculation Procedure

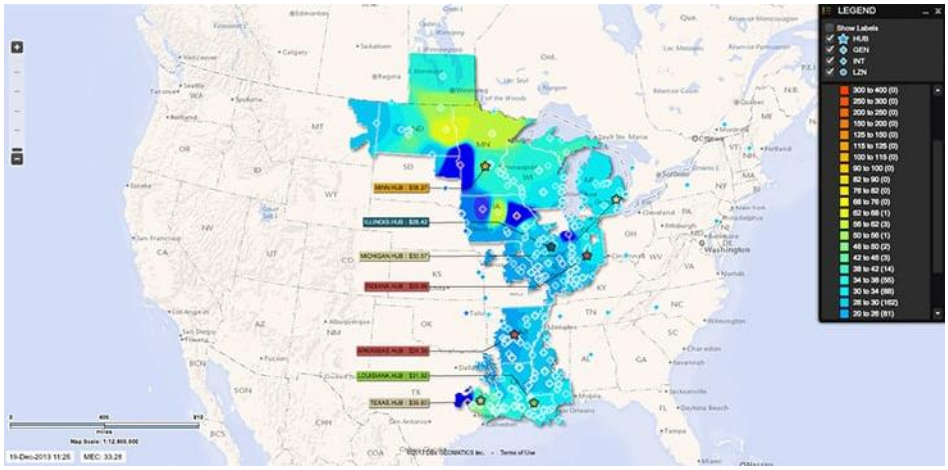

Figure 2.15 LMP Contour across the MISO territory

every 5-15 minutes. Further, by calculating losses and factoring the cost of those, a loss component of price can be estimated. A nodal price for each location can be provided in the form of an LMP metric. Fig. 2.14 illustrates the LMP calculation procedure. Fig. 2.15 shows a map of the nodal prices across the MISO operating region. LMPs are calculated by using the same OPF procedure described in Section 2.2.1. The lagrangian variable is an indication of the variation of prices across different geospatial points and captures the effect of congestion [110]. This system is an efficient means of calculating the locational price when all dispatch points, loading levels and topologies are known on a real- time basis. DLMP is an emulation of this process on a distribution level.

Calculating a price becomes a process of retrieving states, performing computations and communicating the rate back to all consumers. Owing to this process, most real-time pricing algorithms update the prices on a 15-minute basis while some ISOs have been seen to update them every 5 minutes [111]. Complex computations and communication bottlenecks will only become more of an impediment in future grids with multiple asset

owners and faster dynamics. These mechanisms require accurate knowledge of system topology and feeder configuration. Additionally, these are largely based on incremental costs of generation observed while ignoring transient phenomenon like ramp-rate violations.

Lack of accurate information about distribution network topologies, impedances and status of control devices makes deriving DLMPs challenging. With PV becoming increasingly prevalent, fast and dynamic phenomenon need to be captured effectively and encoded into these pricing dynamics. This will allow collective stabilization using supply and demand elasticity. From a resilience perspective, the LMP and DLMP mechanisms fail in the event of damage to the communication infrastructure or when volatile phenomenon that are faster than DLMP tracking cycles occur. It is essential to note that when such events occur, running a scalable and topology-independent market structure can ensure that smaller microgrids can continue to operate and supply critical loads. The discussion shows that RTP is an efficient way of running electricity markets to leverage supply and demand side elasticity. However, there is a need for a decentralized and autonomous implementation for RTP. Moreover, there is a need to couple the device operational layer and the market layer in a more integrated fashion.

2.4 Required Attributes and Functionality from Future Grid Architectures

Certain requirements emerge out of the previous discussions for future grid architectures. With faster phenomenon being observed on the grid, the scalability of the operation paradigm will be limited. Managing congestion patterns, addressing volatility and maintaining supply-demand balances will be extremely challenging as generating

structures move to the grid edge and maintaining visibility over low-latency communications becomes challenging. Centralized control principles often assume that the resource availability is far higher than the possible demand and that a slack bus can absorb disturbances and deviations. The application of such a centralized control paradigm to managing such grid structures will be challenging. However, it is worth evaluating the utility of a grid structure in itself. The function of the physical grid is to deliver energy without violating physical constraints. Meanwhile, energy balance is managed through the transactive processes to ensure that energy is bought and sold as a commodity.

Thus, the future grid architecture will have to be one that can enable stable operation in real-time by adding flexibility to the passive physical grid while incorporating a decentralized marketplace to allow collective stabilization of power balance constraints for this multi-owner paradigm with minimal reliance on centralized coordination or communication. Moreover, by managing physical and power balance constraints in a decentralized fashion based on local parameters, the architecture could break apart into smaller fractals while relying on the marketplace to provide signals conveying energy constraints to sustain operation at varying levels of degradation. This is of special importance during High Intensity Low Frequency (HILF) events such as natural disasters, cyber and physical attacks where the fragility of the current operation mechanisms is exposed.

It becomes necessary to implement a highly resilient, flexible and scalable architecture that can manage the transactive and physical attributes in a more integrated and decentralized fashion while being agnostic to communication failures and topology. It is key to design efficient market structures that incentivize usage in a way that matches

resource availability better, while operating at the most economical operation point. Moreover, reliance on a global control signal that reflects the physics of the network is essential to ensure independence from coordinated control. It is important to ensure that operation is still economic or close to the optimal point of operation while achieving all these objectives.

It is also important to ensure that any augmentation that adds control to grid structures does not cripple the network when it fails. While, failure modes are inevitable, an architecture needs to be realized that can sustain sub-optimal operation while limiting the effect of the failure. Another key component is the cost of the added solutions. The solution needs to be cost-effective to allow widespread implementation and adoption.

An architecture is proposed here where congestion and voltage issues are dealt with autonomously while letting individual agents transact the fundamental quantity -power, in a viable marketplace to extract maximum elasticity out of the system. This research presents hybrid transformers as an effective means to manage physical grid constraints. A powerful transactive framework is presented next to manage supply-demand imbalances in PV-dominant grid settings. Finally, an integration of the novel integrated physical and transactive architecture is presented.

CHAPTER 3. DECENTRALIZED MANAGEMENT OF PHYSICAL GRID PARAMETERS

The meshed grid architecture –critical for reliability, is difficult to control dynamically in terms of power flows and voltages Unprecedented, rapid and sustained growth of distributed energy resources (DERs) on the power grid further accentuates this problem by introducing fast volatility on the system, severely undermining the centralized control scheme. This results in congestion, curtailment of DER sources, and an inability to utilize the full capacity of the transmission system. The physical grid has traditionally been managed using slow source-side controls or slow phase shifting transformers. These solutions are robust but often too slow to handle volatility. FACTS-based controllers, do allow fast control over grid parameters but are expensive, require a full link to be built and cripple the entire link in the event of component failure.

This chapter proposes the use of hybrid transformers to achieve significant control over traditionally passive networks. The proposed approach relies on using fractionally rated power electronic topologies to exercise large amounts of control on the target system. The approach manages to embody all the favorable attributes of the approaches discussed in Chapter 2. In addition, the approach demonstrates an increase in net resiliency and helps speed up recovery times in the event of a contingency. The core objective of this technology is to add tremendous flexibility to the passive grid to leverage the infrastructure in the best way possible while allowing the grid to become a true enabler of energy transactions.

3.1 Hybrid Transformers - Concept

It has become necessary for localized, dynamic and decentralized controls and intelligence to be embedded in grid components. Power transformers present optimal locations to add cost-effective control solutions owing to their abundance in the grid. The high X/R ratio of these units makes it feasible to exercise high amounts of control on both the medium and high voltage sections of the grid. Moreover, the geospatial locations of these transformers in existing grids make them ideal candidates to improve system resiliency, derive more capacity utilization out of existing grid assets, achieve better recovery from contingencies and optimize system parameters such as voltage and power flows.

Rather than building dedicated links for control, hybrid transformers leverage existing transformer locations to realize points of grid control. Fig. 3.1 shows the hybrid transformer concept as proposed by Divan et.al [112]. The hybrid transformer approach relies on a fractionally rated converter, typically in the range of 5-10% of the application's power, integrated to a conventional power transformer with a tertiary low-voltage winding

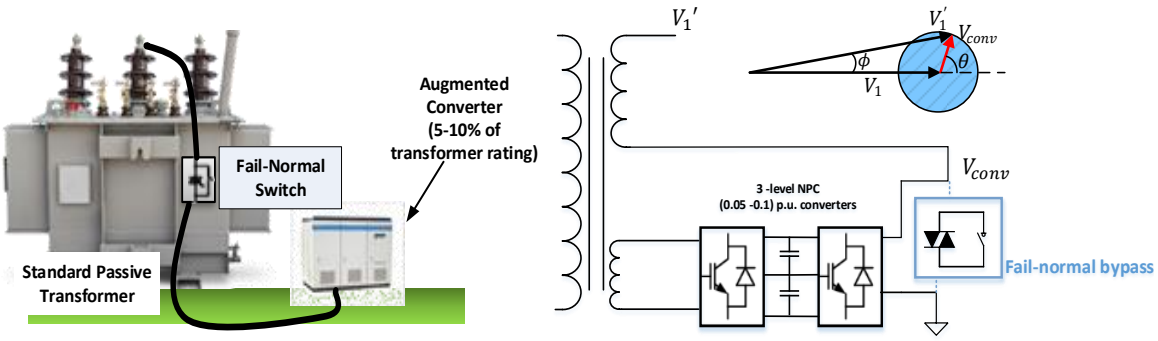

Figure 3.1 Hybrid Transformer Concept and Equivalent

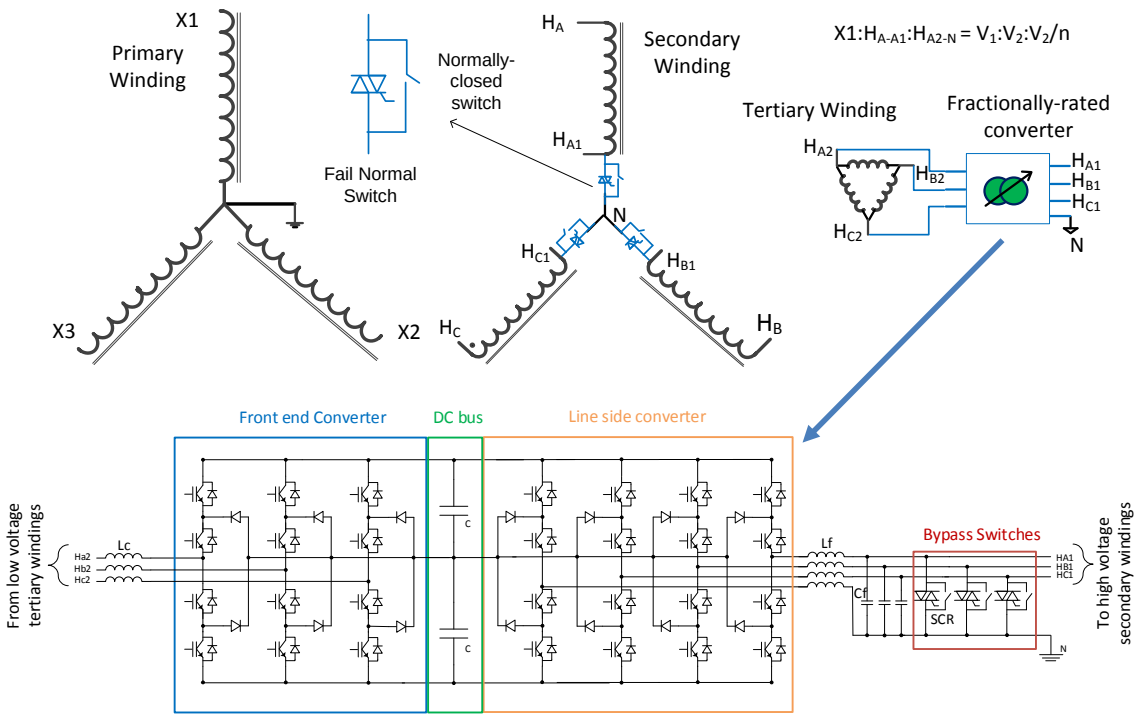

Figure 3.2 Detailed Schematic of Hybrid Transformers

in addition to the standard high voltage windings. Thus, with minimal modifications to a standard power transformer, controllability over power flows can be attained. Previous versions of this technology – the Grounded compact dynamic phase angle regulator (G-CDPAR) and the grounded controllable network transformer (G-CNT) have showcased the efficacy of this approach experimentally and in field deployments [113], [114].

Fig. 3.2 shows the detailed schematic for the hybrid transformer implementation. The primary and secondary transformer windings are the standard high voltage windings and are connected to the line. A delta or wye configuration of the primary winding is possible to accommodate the application requirements while the secondary winding is in open-wye configuration to interface with the power converter. Finally, the tertiary low voltage winding is in delta configuration and sources or sinks power depending on the operating

point of the unit. The power converter is a standard three-level back-to-back (BTB) neutral-point clamped (NPC) converter, rated for 5-10% of the nominal voltage, and offering an additional leg on the line side to interface with the system neutral and operate under unbalanced line conditions. In this configuration, the converter dynamically injects a fractional voltage of controllable magnitude and phase angle, in series with the line voltage to achieve the desired control action in a precise and granular fashion. The fractionally rated converter is significantly cheaper than fully rated approaches and is much easier to cool. As shown in Fig. 3.2, three "fail-normal" switches are connected across the output of the converter to bypass and protect the power converter in case of line fault and retain basic transformer functionality upon converter failure. Thus, the system-level reliability of the hybrid transformer approach is close to that of traditional power transformers. The operation principle has been elaborated in Section 2.2.2.1. Control over power flows, voltages and apparent impedances can be exercised as shown in Fig. 3.3 by altering the phase angle of the injected voltage.

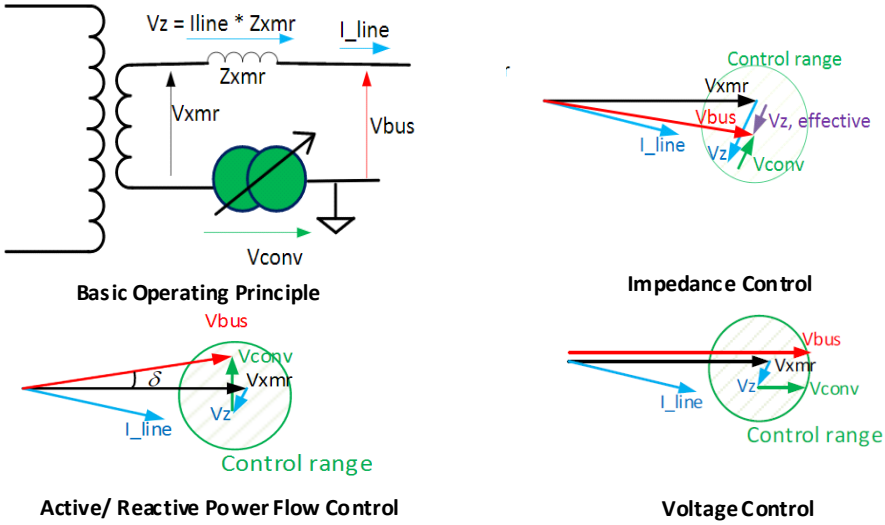

Figure 3.3 Dynamic Control over power flows, voltages and apparent impedances using Hybrid Transformers

Both the power converter and the power transformer are based on standard and proven technologies, widely available in the voltage and power range of interest to reach the transmission level, therefore ensuring the scalability of the proposed approach. The fractional rating of the power converter, both in terms of voltage and power, makes the solution cost-effective across the entire application spectrum. Finally, the power converter operates close to the ground level, therefore shifting the challenging Basic Insulation Level (BIL) requirements, as high as 350 kV for a 115 kV system [115], to the standard power transformer design. This eliminates a major constraint that has been plaguing the voltage scaling of solutions based on floating power electronics and reduces the overall cost of the proposed solution. Thus, a resilient, fast and granular grid control solution can be achieved at much lower costs. Moreover, hybrid transformers enable fast disruptions to be handled through local controls while not affecting the economics associated with dispatch or market procedures. A qualitative and economic comparison with traditional FACTS based approaches is presented next.

3.2 Comparison with other grid control techniques

Power electronics-based approaches for dynamic grid control like UPFC and HVDC-light have been summarized in Section 2.2.2. A comparison is made here between the proposed hybrid transformer approach and these technologies.

3.2.1 Qualitative Comparison

Fully rated technologies like HVDC-light involve setting up a dedicated link to achieve a controllable corridor. This involves a fully rated BTB unit and two coupling transformers. The UPFC unit also involves two transformers and a fractionally rated (BTB)

unit. It is immediately apparent that the hybrid transformer approach relies on lower number of components. Adding control using UPFC or HVDC-light based solutions relies on complex modifications at the control locations. On the contrary, the hybrid transformer approach can be factored into the planning stage by building power transformers with the required taps and connections, enabling the ability to augment them with a converter in the future to add dynamic grid control. This is meaningful since the manufacturing cost of the power transformer does not change significantly from a regular replacement unit while providing the ability to add control as and when required. Moreover, location at a typical voltage change point is meaningful because control can be exerted between these two regions of the grid.

Slow electromechanical functionality can be replaced with the hybrid transformer approach allowing fast granular control. Another important aspect is the failure modes seen on traditional FACTS solutions. When considering HVDC-light, failure of any one component hampers the operation of the entire unit. This is the same with failure modes associated with the series transformers of UPFC solutions. From a fault current management perspective, the series transformer in UPFC systems needs to be rated to handle full line currents which makes them prohibitively complex and expensive. On the other hand, the hybrid transformer approach is equipped with a 'fail-normal' function. This means that in the event of any failure on the augmented converter, the BTB converter output will be by-passed. This means that the transformer asset would continue to operate as a passive element while only losing the added control.

3.2.2 Economic Comparison

The hybrid transformers approach requires fewer components than the HVDC-light and UPFC-based approaches. A preliminary analysis was done to quantify the cost-effectiveness of this approach. Some cost assumptions for the same are stated below. While the cost points fluctuate significantly depending on the application, for different components, the analysis holds true in almost all cases. The base case presented here is that of a passive transformer. Since the passive transformer would be the one component that would have to exist at the change in voltage level in the grid, the cost of this component is considered as the base line. Approaches like UPFC, HVDC-light and the hybrid transformer approach are compared here. A 60 MVA target system is considered for the purpose of comparison.

The comparison points for both the qualitative and economic aspects are presented in Table I. The UPFC and hybrid transformer approaches implement series voltage injection, with varying phase and magnitude, to exercise control. It is assumed that both these approaches inject +/10% voltage in series, allowing +/- 10% control over voltage

Approach	Hardware Cost	Substation Cost	Control	Losses	Cooling	Fail-Normal	Fault Current
Passive Transformer (60 MVA)	~$1.8 Mill	1x	No	~2%	Air	N/A	Yes
UPFC (including 60 MVA LPT and 6 MVA converter)	~$4.14 Mill	4x	Yes	~2.4%	Deionized water	Yes	Yes
BTB with DC link (60 MVA transformer and converter)	~$21.6 Mill	10x	Yes	~6%	Deionized water	No	No
Hybrid Transformers (60 MVA transformer, 6 MVA converter)	~$3.3 Mill	1.2x	Yes	~2.2%	Air	Yes	Yes

Table 1 Comparison of Dynamic Control Techniques – 60 MVA target system
Cost Assumptions: Transformer cost: $30/kVA, UPFC series transformer cost: $60/kVA, Converter: 150/kVA

magnitudes and full bidirectional control over real and reactive power flowing on the line. HVDC-light is also assumed to have full control over the real and reactive power over the link. However, every component is fully rated with this approach. Transformer costs are estimated to be at $30/kVA. An exception to this is the series transformer in the UPFC system. Fault management requirements on the series transformer push the estimated cost point to $60/kVA for the same. Converters in all these approaches are assumed to be 3-level BTB units with an estimated cost point of $150/kVA. UPFCs and fully rated BTB based converters use deionized water to cool the systems. In contrast to this, the hybrid transformer approach uses air cooling making the cooling systems less complex and cheaper. As previously mentioned, the hybrid transformer-based approach is built with a 'fail-normal' functionality rendering operation of the asset as a passive device possible in the event of a failure. While, UPFCs can exhibit the same, the operation could be hampered owing to issues with the series transformer. Fully rated BTB based approaches like HVDC-light typically handle fault currents poorly.

Table I clearly shows that hybrid transformer-based approaches provide a low-cost way of implementing dynamic control on the grid, particularly when the cost of the substation, cooling system and losses are included. It also provides the possibility of designing the power transformer as a passive device that can be retrofitted in the future with a converter to add control, allowing a deferred investment plan. This is an appealing economic incentive for grid planners and operators. The augmented control allows control over apparent impedances of the link eliminating, the need for building custom transformer units with customized impedances. Standardization of transformer units for different power

levels makes the cost of transformer manufacturing lower. The economic value added from attributes like active, reactive power flow control, voltage control, congestion control and resiliency improvement make the hybrid transformer approach the prime contender among these numerous control approaches.

3.3 Dynamic control over grid parameters

Deploying hybrid transformers at different points of control can allow precise control over voltages and power flows. This can help address a variety of issues associated with PV dominant grid structures such as voltage volatility and congestion. This subsection shows the value that can be gained by utilizing this functionality. In order to validate the controllability of the hybrid transformer approach, a few simulation studies were conducted.

3.3.1 Simulation Setup

This section presents some simulation cases to showcase the additional flexibility that can be realized from hybrid transformers. The hybrid transformer can be modelled as a transformer unit with a series voltage source that can represent the added fractional voltage. In the studies proposed next, a simulation scheme is followed where the network is modelled in OpenDSS with an additional controllable voltage source to represent the converter unit. Fig. 3.4 provides an overview of the quasi static simulation (QSS) scheme. The scheme involves solving a power flow problem to retrieve power flows. A DLL interface script is then written to compute the fractionally rated BTB unit's response to the local parameters. This generates the required injection magnitude and phase angle in response to the local parameters. This response is then fed back over a COM interface to

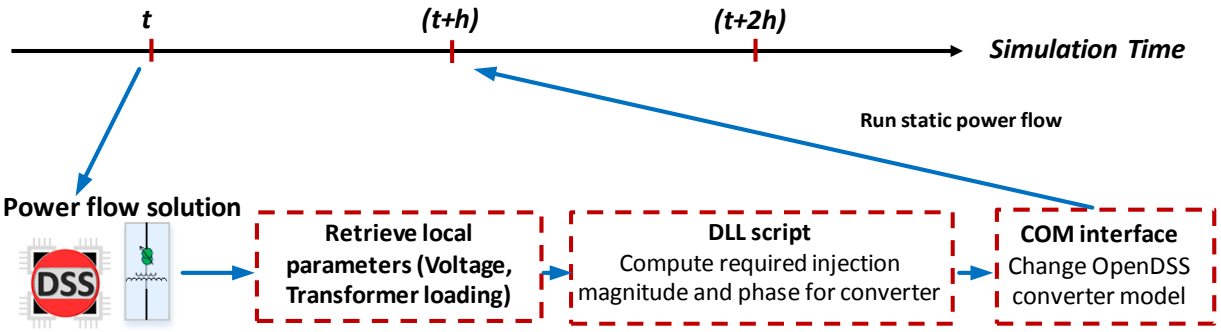

Figure 3.4 Simulation Scheme to analyze the system level impacts of hybrid transformers

the voltage source in the OpenDSS framework to represent the hybrid transformer's new control set point. The QSS scheme exercises control at discrete time steps. For the next few simulation studies this time step is set to 0.1 seconds.

3.3.2 Power Flow Control

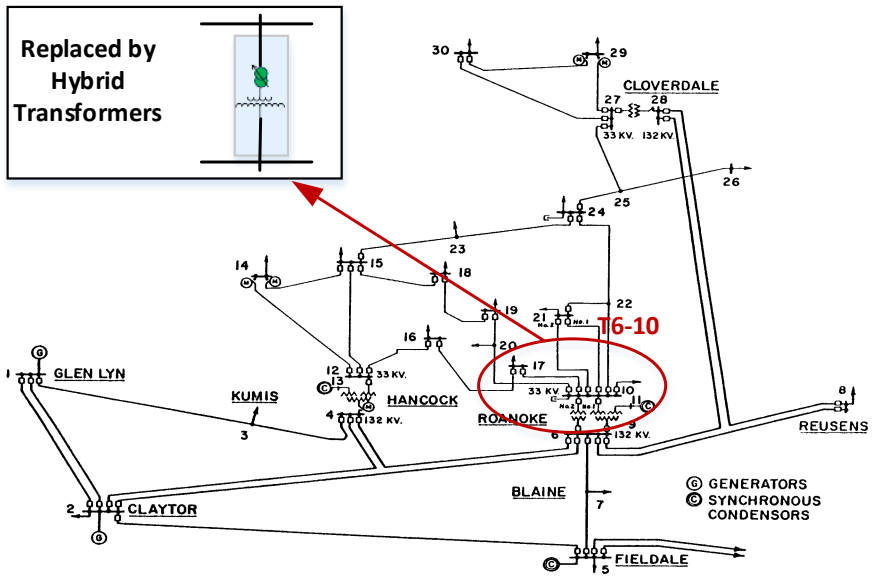

Figure 3.5 Modified IEEE 30 bus system with hybrid transformer (T6-10)

The system modelled in OpenDSS is a slightly modified IEEE 30 bus system as shown in Fig. 3.5. Transformer T6-10 is replaced with a hybrid transformer unit as the point of control with a 5 MVA converter. Thus, a 132/33 kV, 100 MVA control unit is

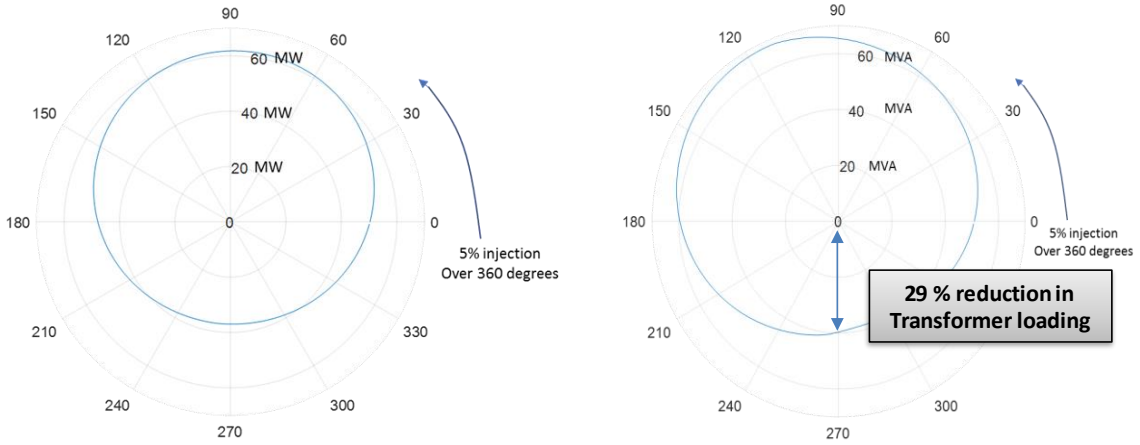

Figure 3.6 (a) Real power and (b) apparent power variation affected by hybrid transformer T6-10

realized in the form of hybrid transformers in this modified system. The nominal flow over this link in the modified system is 42.2 MVA.

In order to understand the full range of power flow control on this target system from the added point of control, a simulation case was generated where the COM interface was programmed to vary the phase angle of the injected voltage while keeping the magnitude fixed at 5% of the rated voltage. Thus, a 1.65 kV fractional voltage was maintained and varied over 360 degrees to the see the effect. Figs. 3.6 (a) and (b) show the variations in real and apparent power over the link in response to the injections. With just a 5% injection the loading levels on the transformer could be reduced by 29%. Active and reactive power flow could be controlled effectively on this corridor using the augmented converter. Thus, a fast power flow control device can be realized by simply augmenting an existing transformer on the system with a fractional converter.

3.3.3 Congestion control and DER management

With DERs like PV introducing enormous amount of volatility, existing dispatch procedures and expected power flow patterns get significantly disturbed. Unexpected power flow patterns may often create congestion and violate line capacity constraints. A use case is simulated on the system detailed in Fig. 3.5. A 1.1 MW PV plant is modelled in at bus 16. The plant is assumed to be operating based on an MPPT algorithm. Figure 3.7 (a) shows the modelled PV plant in the system.

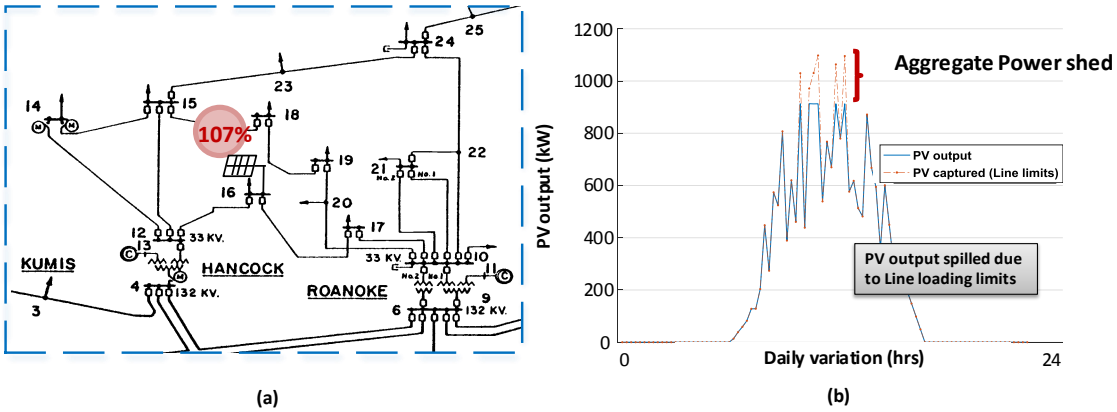

Figure 3.7 (a) Line 15-18 getting congested due to presence of PV plant (b) PV output and spilled output due to congestion

It is observed that owing to the excess energy, line 15-18 gets congested to a maximum of 107% of its rated capacity. This would result in the PV output being curtailed to avoid congestion patterns. Over a 24-hour cycle, the power being shed is shown in Fig. 3.7 (b). Hybrid transformers offer a fast and easy way to alleviate line loading concerns. Utilizing the hybrid transformer at T6- 10, the line loading across 15-18 can be kept under 100%. Fig. 3.8 shows the loading patterns across the line with the added control.

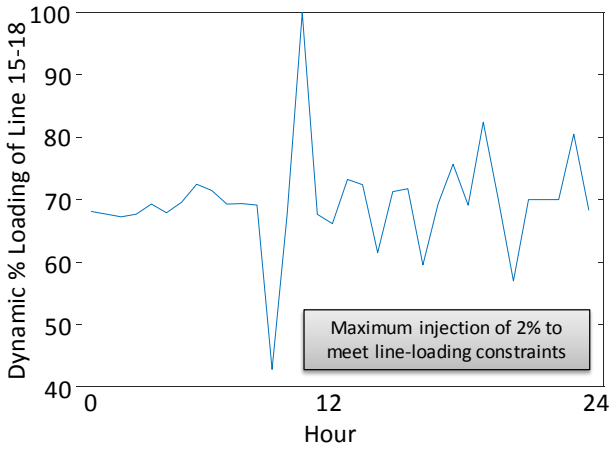

Figure 3.8 Dynamic congestion control on line 15-18

It is also important to note that by exercising control no other line across the system breaches its line capacity limit. The maximum injection required in quadrature is 2%. Thus, by utilizing a 5 MVA fractionally rated converter, alternative transmission paths can be utilized in real-time to maximize DER absorption without violating any physical constraints. Converters within these ratings are commonly available commercially, making this approach easily deployable.

3.3.4 Enhanced voltage management with high PV penetration

In addition to congestion issues, DERs also cause significant voltage volatility on the grid. Slow electromechanical solutions like Load Tap Changers (LTCs) or Line Voltage Regulator (LVRs) are commonly deployed at substations to manage this issue. A simulation case is presented here on a modified IEEE 13 bus system as shown in Fig. 3.9 (a). To understand the effect of PV penetration, a 0.5 MW PV plant is added to the system at the end of the feeder. The voltage variation seen at bus 650 is plotted in Fig. 3.9 (b). Even with the LTC deployed at bus 650, the voltage variation is only kept within 1% range. This is assuming that the switching action is without any delays. LTCs are typically

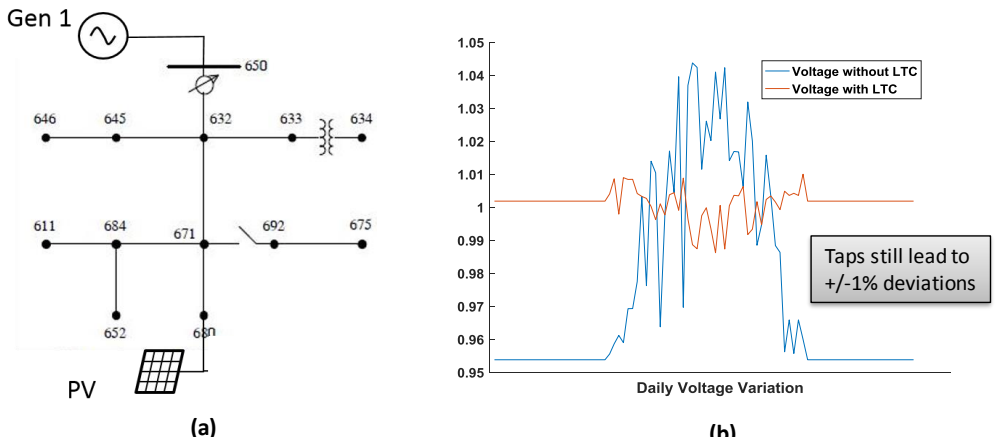

Figure 3.9 (a) 13 bus system with 0.5 MW PV farm (b) Voltage management with an LTC

designed to switch a few time (~10) on a daily basis but with high PV penetration on feeders, these devices are having to operate far more than they were designed for. The switching actions are often accompanied by significant delays making them an ineffective solution to deal with voltage volatility seen in DER heavy systems.

By deploying a hybrid transformer at bus 650, the voltage can be corrected extremely fast and in a precise and granular fashion. By simulating the hybrid transformer in voltage control mode using the COM object, the voltage profile attained is shown in Fig. 3.10. This shows that the hybrid transformer outperforms existing LTCs and LVRs while enabling

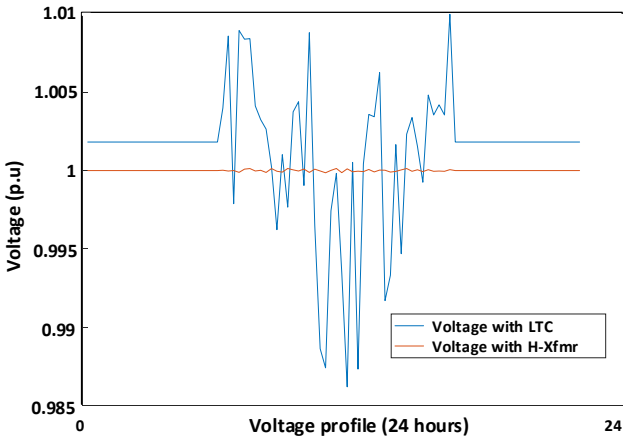

Figure 3.10 Comparison between voltage management using an LTC and a hybrid transformer

higher PV penetrations. The hybrid transformer approach allows numerous forms of control in a fast fashion across the grid.

3.4 Impact on Grid Resiliency

Large power transformers (LPTs) are highly custom components that are critical to the operation of power systems. The customized nature of these products has ensured long lead times for component replacement. Moreover, the logistics of installing the component once a replacement has arrived are challenging and further delay the restoration time. It is critical to develop solutions for this issue to ensure that the system remains resilient.

With all these vulnerabilities in mind, efforts have been made by federal bodies in the U.S to understand and improve the resiliency of critical pieces of infrastructure in the grid. In response to this a broad range of solutions were developed. In an attempt to minimize the recovery time following a power transformer failure, transformer manufacturers have developed mobile transformer units. These units typically consist of either a single-phase or three phase transformers mounted on a truck and characterized by compact form factors. By reducing the assembly time and transport time these units offer a fast and temporary solution to power transformer failures. Several efforts led by DOE, EEI and NERC have led to the RecX program. RecX transformers consist of single phase transformers transported on specialized assemblies to enable fast restoration and minimal installation time [116]. NERC and EEI have instituted transformer sharing programs like Spare Equipment Database (SED) as well as Spare Transformer Equipment Database (STEP) which encourage utilities to maintain and share power transformers [117].

The initiatives listed above only focus on minimizing recovery time and increasing redundancy. With limited flexibility incorporated in these LPT replacements, the resiliency assessment would largely be a function of the parameters of the replacement unit. Owing to the customized nature of these units, replacement transformers are bound to have differing impedance characteristics. Thus, maintaining a set of mismatched spares might not help in addressing resiliency issues associated with LPTs. Moreover, the power flows and voltage profiles within the network are sensitive to this change in impedance creating deviations in loading levels of other units spread out across the system. The efficiency of these fully rated mobile transformer units is also lower since these are temporary solutions.

The proposed hybrid transformer technology in the previous sections is extended to the transmission level. To promote lower probability of complete failure, the approach deals with splitting a large 200 MVA unit into multiple smaller modular units with

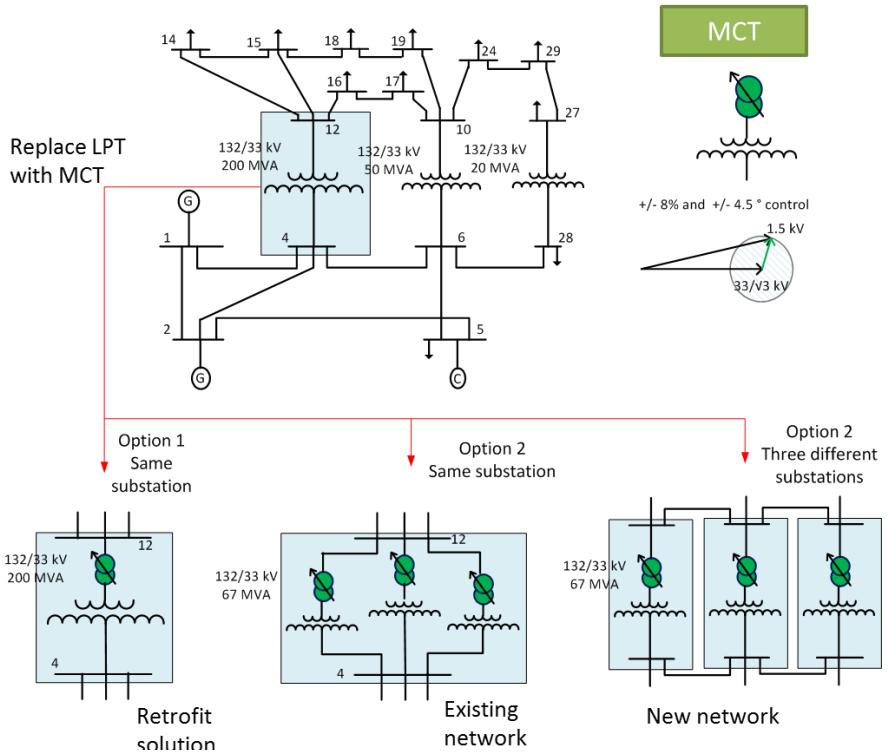

Figure 3.11 Concept of Modular Controllable Transformers (MCTs)

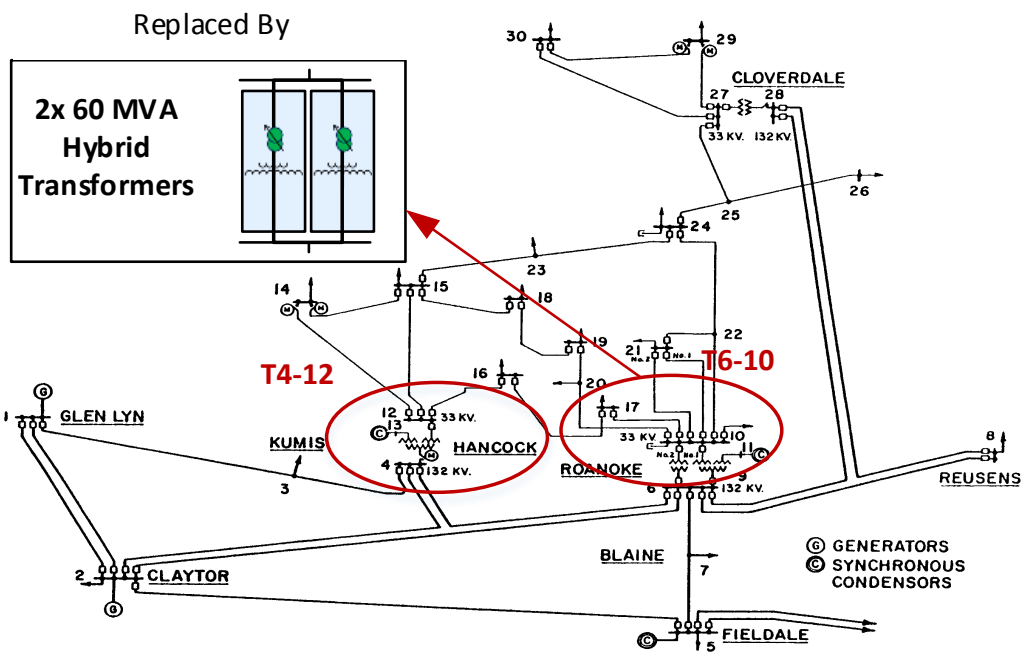

Figure 3.12 IEEE 30 bus system modelled with MCTs

augmented converters. Fig. 3.11 shows an illustration of the same. Thus, this technology is aptly name Modular Controllable Transformers (MCTs). These units can be standardized to enable fast replacement and manufacturing. However, on large transmission systems the power flow over any particular corridor is largely dependent on the apparent impedance seen. This makes the base power flow very sensitive to small variations in transformer impedances. As illustrated in Fig. 3.3 the augmented converter enables changes to be made to the apparent impedance over a corridor. Owing, to this, a large cache of smaller modular units can be maintained as replacement units while avoiding custom designs to meet strict impedance requirements. Grijalva et. Al have proposed a framework to quantify system level resiliency improvements while using this approach [118]

The same IEEE 30 bus system and the setup proposed in Section 3.3.1 is utilized to conduct some simulation studies. The two (LPTs) of interest are T4-12 and T6-10. Fig.

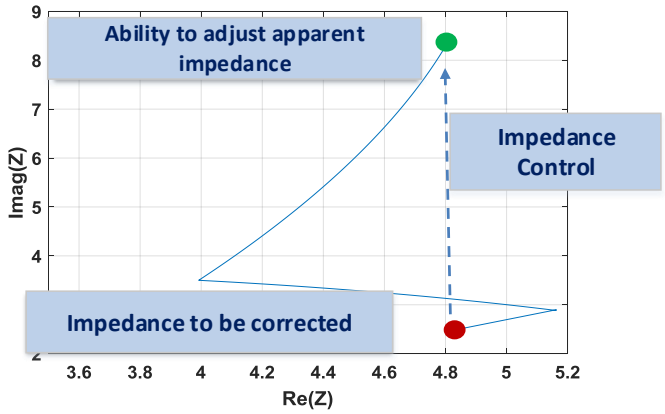

Figure 3.13 Impedance control to match replaced unit

3.12 shows the modular approach where one 100 MVA unit is replaced by two 60 MVA units. The MCT approach involves replacing the large LPT with two 60 MVA units with lower impedances and the same voltage ratings. This pushes the power flow through the corridor to 68 MVA. Corrective actions are taken by the MCT units to correct the mismatch. Fig. 3.13 shows the net impedance being altered by the MCT converters in response to the changed units. Fig. 3.14 shows the power flow reverting back to 42.2 MVA. This is achieved with a 5% voltage injection. Thus, replacement of damaged units becomes extremely easy owing to the MCT approach. Moreover, multiple modular units ensure partial operation in case of a single failure making the approach extremely resilient. By

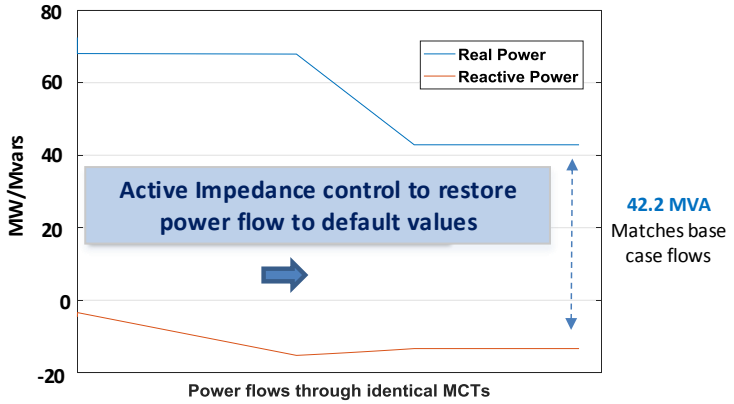

Figure 3.14 Power flow matched to base case using mismatched unit with added control

switching out one large unit for multiple modular ones the MCT approach reduces the probability of complete failure. Further, with the fail-normal approach, in the event of converter failure, the assets simply revert back to being passive transformers. The total loss of transmission corridors is minimized. Thus, the approach enables higher resistance to failures, redundancy and reliability.

3.5 Sensitivity of System Flows and the effect of Hybrid Transformers

The previous simulation studies prove that hybrid transformers can have enormous impact on making traditionally passive networks more active and flexible. However, the previous studies involve some system awareness to exercise the control. It is necessary to develop metrics to understand the effect of the added flexibility on passive parts of the network. The analysis presented in Section 3.3.1.1 allows the complete range of control for a hybrid transformer to be defined. This section proposes certain metrics to analytically define the effect of hybrid transformers on global system flows. These metrics will become a key component in defining autonomous control signals for such devices in a decentralized architecture. The system flows are a consequence of the base power flows over the passive network and the effect of the hybrid transformer itself. The next two sections present sensitivities that provide a framework to analyze the system.

3.5.1 Power Transfer Distribution Factors (PTDFs)

The power flows across different corridors in a given passive system are a function of the loading levels as well as the source dispatch pattern. This is the basis for generating power flow equations and solving a power flow. Thus, it is possible to derive power flows across any given line based on knowledge of the power injection or loading on any given

network. PTDFs are a measure of the sensitivity of line flows to these injection patterns. A brief review of the principle behind PTDFs is presented next. Equation (5) shows the power flow equations that are used to compute AC power flows.

$$\sum_{k=1}^{n} V_i V_k (G_{ik} \cos\theta_{ik} + B_{ik} \sin\theta_{ik}) = P_{Gi} - P_{Di} \quad (5)$$

$$\sum_{k=1}^{n} V_i V_k (G_{ik} \sin\theta_{ik} - B_{ik} \cos\theta_{ik}) = Q_{Gi} - Q_{Di} \quad (6)$$

Where,

n – number of buses

G_{ik} – conductance of link i,k

B_{ik} – susceptance of link i,k

θ_{ik} – phase angle difference between buses

P_{Gi}, Q_{Gi}- Active and reactive power injection at bus i

P_{Di}, Q_{Di} – Active and reactive power drawn at bus i

Equations (5) and (6) are iteratively solved using the Newton-Raphson method as shown in (7).

$$\begin{bmatrix} \Delta\theta \\ \Delta V \end{bmatrix} = -\begin{bmatrix} \frac{\partial P}{\partial \theta} & \frac{\partial P}{\partial V} \\ \frac{\partial Q}{\partial \theta} & \frac{\partial Q}{\partial V} \end{bmatrix}^{-1} \begin{bmatrix} \Delta P \\ \Delta Q \end{bmatrix} \quad (7)$$

The DC power flow approximation is a simplified version of the above process that is widely used in most economic optimization tools deployed today in SCADA and EMS systems. The DC power flows approximation is based off the assumption that only active

power flows are of consequence. Thus, reactive power flows and active power losses are neglected in this formulation. This means that $|G_{ik}| \ll |B_{ik}|$ and $\theta_{ik}$is very small. The consequence of these assumptions is that the partial differentials in the power flow solutions can now be simplified to (8)-(10)

$$\frac{\partial P_i}{\partial \theta_i} = \sum_{\substack{k=1 \\ k \neq i}}^{n} B_{ik} \tag{8}$$

$$\frac{\partial P_i}{\partial \theta_k} = -B_{ik} \tag{9}$$

$$\frac{\partial P_i}{\partial V_i} = \frac{\partial P_i}{\partial V_k} = 0 \tag{10}$$

Thus, the power flow solution presented in (7) can be simplified using this DC approximation. The DC power flows equations can then be summarized in (11).

$$\theta = -[B']^{-1}P \tag{11}$$

Where,

θ – vector of phase angles for all buses except the slack bus

B'- matrix of susceptances without the slack bus

P – vector of power injections at buses

Thus, for any given transfer of power between buses i and j, a transfer vector T can be developed. For instance, in a 5 bus system, a 1 MW transfer from 2 to 5 would imply a vector seen in (12). The slack bus (bus 1) entry is removed.

$$T = [\ 1\ 0\ 0\ \text{-}1] \tag{12}$$

For an arbitrary power 'p' to be transmitted between two nodes, the power flow equation presented in (11) becomes that seen in (13). The resultant relation shown in (14) denotes the sensitivity of phase angles to a given transfer of power in the system.

$$\Delta\theta = -[B']^{-1}pT \tag{13}$$

$$\left[\frac{\partial\theta}{\partial p}\right] = -[B']^{-1}T \tag{14}$$

For a given line '*lm'* on the same system, the sensitivity of a transfer *T* can be expressed by a PTDF metric like that seen in (15). Using the DC power flow assumptions (8)-(10), the PTDF for line '*lm',* for a transfer *T* becomes that seen in (16).

$$PTDF_{lm,T} = \frac{\partial P_{lm}}{\partial p} = \left(\frac{\partial P_{lm}}{\partial \theta_l}\frac{\partial \theta_l}{\partial p} + \frac{\partial P_{lm}}{\partial \theta_m}\frac{\partial \theta_m}{\partial p} + \frac{\partial P_{lm}}{\partial V_l}\frac{\partial V_l}{\partial p} + \frac{\partial P_{lm}}{\partial V_m}\frac{\partial V_m}{\partial p}\right)T \tag{15}$$

$$PTDF_{lm,T} = \left(\frac{\partial P_{lm}}{\partial \theta_l}\frac{\partial \theta_l}{\partial p} + \frac{\partial P_{lm}}{\partial \theta_m}\frac{\partial \theta_m}{\partial p}\right) \tag{16}$$

Thus, the sensitivity of power flow over a given line for a specific power transfer *pT* can be computed analytically using this formulation. This allows, the power flow sensitivity for a given line to be computed in a passive network. This methodology has been highlighted in detail in [60]. However, the sensitivity of any control action that the hybrid transformer may affect is yet to be calculated. The next subsection presents the same.

3.5.2 Flow Sensitivity to Hybrid Transformers

The passive system flows can be linearly captured using the PTDFs summarized above. However, the hybrid transformer significantly alters flows across the entire system due to its voltage injection. In this subsection, a methodology based on the PTDF sensitivities is presented to analyze the same. A similar approach has been presented by Thomas et.al in [119]. The hybrid transformer turns a passive link into a fully controllable one. This ensures, that any additional amount of power that the hybrid transformer may choose to dispatch over the link must loop all over the system and affect system flows.

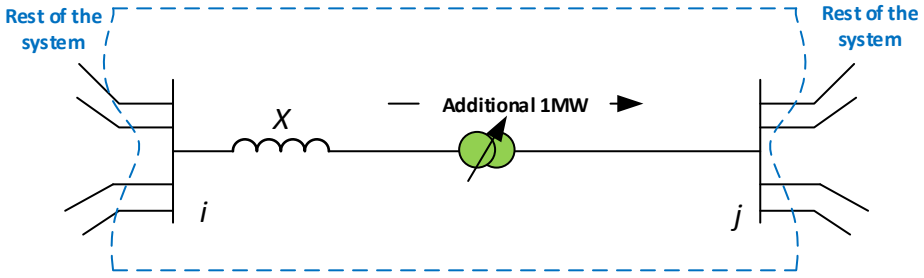

Figure 3.15 Link with hybrid transformer to add 1 MW above nominal flow

Figure 3.16 Equivalent to capture the effect of additional MW on other system flows

Consider the Fig. 3.15 which shows a link that may be equipped with a hybrid transformer. The effect of dispatching an additional MW of power over the link is the same as adding a generation unit to push and additional MW into the system at bus j and a 1 MW load at bus i. The increased power flow must loop through all the other meshed lines to

reach the load as seen in Fig. 3.16. This is equivalent to generating a transfer matrix *T* *b*etween bus j and i. The PTDFs of all the lines for this transfer indicate their sensitivity to the hybrid transformer itself. These PTDFs will be called hybrid transformer flow sensitivities (HTFS) in this document.

3.5.3 Power Flow Sensitivity with hybrid transformers- Simulation Study

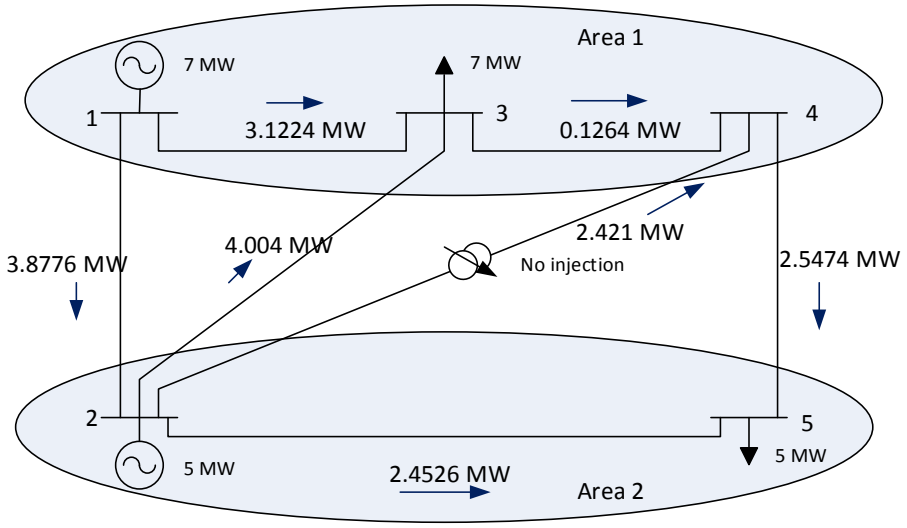

Figure 3.17 Base flows on passive 5 bus system

In order to verify these proposed sensitivities, a simulation study is conducted. Fig. 3.17 shows the network being simulated. Since, we are interested in steady state power flows, the MATPOWER package is utilized for this study. The system is divided into two areas with their respective loading. Source 1 is set to dispatch 7 MWs to it's own control area and Source 2 is set to dispatch 5 MWs. A hybrid transformer is placed on link 2-4 to add controllability. In the base case, the power flows without any added control from the hybrid transformer are seen in Fig. 3.17.

Analytically, the PTDFs are derived for each of these lines. First, the line PTDFs for a 7 MW transfer from bus 1 to 3 as well as a 5 MW transfer from bus 2 to 5 are derived

Table 2 PTDFs and system flows for passive 5-bus system

Line	PTDF (1 MW between bus 1-3) x7	PTDF (1 MW transfer bus 2-5) x5	Actual Flows on links
1-2	4.1006 MW	-0.2230 MW	3.8776 MW
1-3	2.8994 MW	0.2230 MW	3.1224 MW
2-3	3.2680 MW	0.7360 MW	4.0040 MW
2-4	0.5204 MW	1.9006 MW	2.4210 MW
2-5	0.3122 MW	2.1404 MW	2.4526 MW
3-4	-0.8326 MW	0.9560 MW	0.1264 MW
4-5	-0.3122 MW	2.8596 MW	2.5474 MW

and shown in Table 2. The actual system flows are a sum of these individual flows. Fig. 3.18 shows the system flows with an additional 1 MW being dispatched over link 2-4 by the hybrid transformer. The corresponding distribution factor sensitivities associated with a hybrid transformer are presented next. The sensitivities are then scaled to the transfer

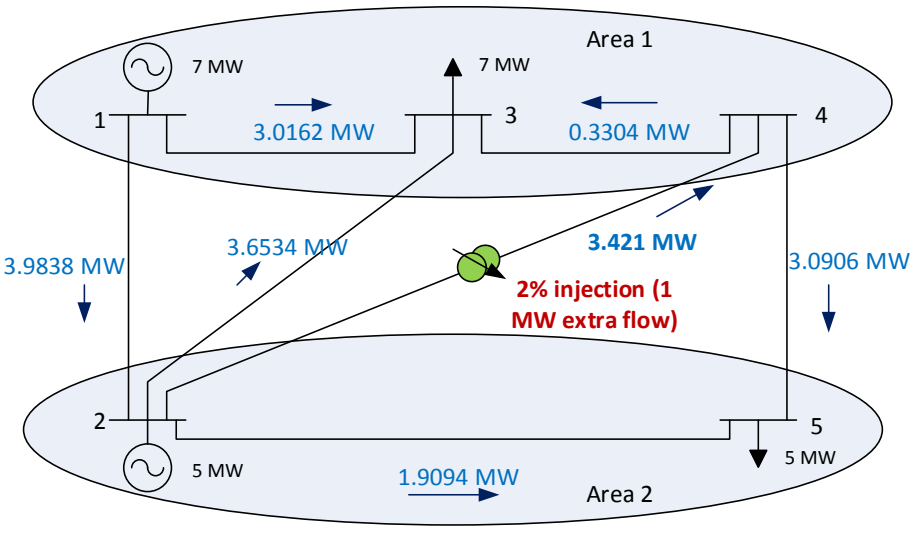

Figure 3.18 Power flows on 5-bus network (Hybrid transformer increasing flow by 1 MW)

Table 3 Hybrid Transformer Sensitivities

Line	Base Case Flows (MW)	HTFS (MW)	Actual Flows (MW)
1-2	3.8776	0.1062	3.9838
1-3	3.1224	-0.1062	3.0162
2-3	4.0040	-0.3506	3.6534
2-4	2.4210	1	3.4210
2-5	2.4526	-0.5432	1.9094
3-4	0.1264	-0.4568	-0.3304
4-5	2.5474	0.5432	3.0906

size. In this case since only 1 MW of additional power is being pushed, the sensitivities can be presented directly. Table 3 shows the calculated HTFS sensitivity. The net power flows across the system are a sum of the PTDFs for the passive system and the sensitivities associated with the hybrid transformer (HTFSs). Fig. 3.19 shows the methodology that could be followed to understand the effect of any hybrid transformer on any given system. It is key to note that in Fig. 3.19, the required global data is the matrix of power injections and loading levels. However, to make this a decentralized solution we propose an estimation scheme in a later section.

While the ability to exercise control over voltage and power flows across meshed bulk power systems has been achieved with hybrid transformers, implementing power electronic solutions becomes challenging in low voltage, high power systems where 50 kA fault current levels must be met. A retrofittable version of the hybrid transformer concept called Stacked Isolated Voltage Optimization Modules (SIVOM) is proposed for the same.

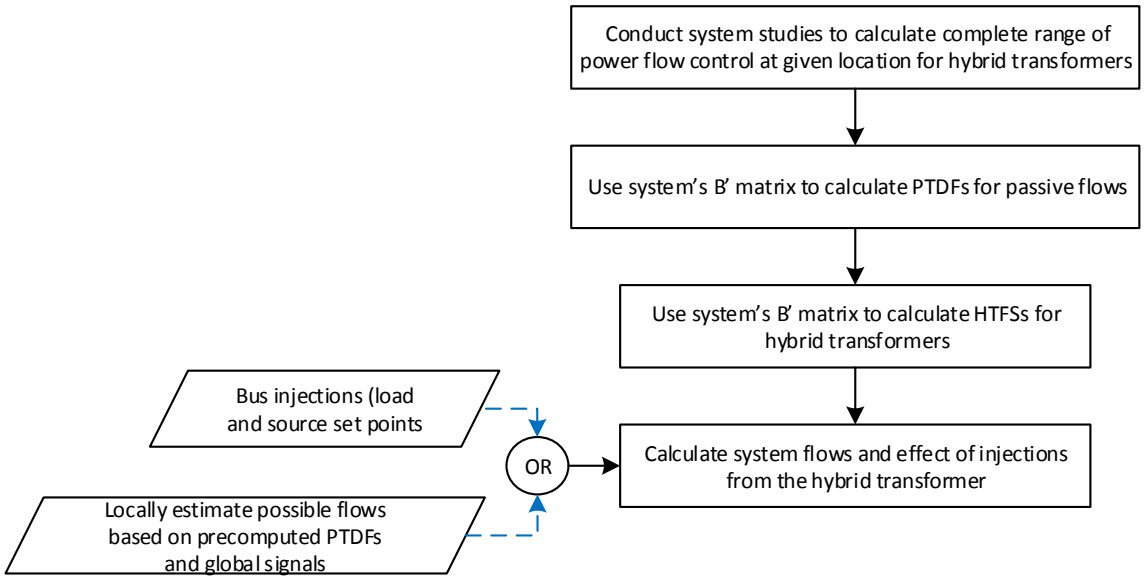

Figure 3.19 Methodology to analyze effect of hybrid transformers on arbitrary systems

The concept is elaborated in Appendix A along with promising use cases. The validity of this approach was ensured on Consolidated Edison's network as part of this study [120].

3.6 Discussion and Contributions

In contrast to relying on controlling power flows through centralized dispatch, low cost hardware control devices can be added to make passive networks controllable. Hybrid transformers provide control over numerous grid parameters at bulk power, medium voltage and low voltage levels, while being retrofittable and low cost. Moreover, the infrastructure cost of deploying these solutions is kept low since they do not require new links to be built.

Each of these solutions responds extremely fast to volatile phenomenon allowing management of congestion issues and voltage profiles in a precise granular fashion. Hybrid transformers may be controlled by a system operator by issuing set points for maintaining

desired system level flows. However, in the event of communication failure, hybrid transformers can still regulate the power on their respective links to safe levels and ensure that the line of interest does not get overloaded. This can dramatically increase the utilization of system capacity and promote the resiliency of the system.

In case of HILF events or cyber physical attacks where LPTs may be damaged and require replacement, the long turn around times and lack of replacements remain major issues. The hybrid transformer approach allows an LPT unit to be replaced with a slightly mismatched spare LPT unit, while controlling the apparent impedance of the corridor using the augmented power electronic converter. This greatly reduces post contingency recovery times and increased the resiliency of the system.

The ability of hybrid transformers to affect power flows and address congestion is showcased using some simulation studies in this chapter. Simulation studies have also been conducted to show that this technology far outperforms slow voltage regulating devices like OLTCs. A methodology was discussed to analyze the effect of hybrid transformers on system flows using PTDFs. This methodology will be utilized to intelligently operate hybrid transformers in the complete decentralized transactive and physical framework proposed in this research. Hybrid transformers thus, become a highly effective solution to tackling numerous problems associated with control over physical grid parameters.

Given that the physical layer of this architecture is managed in real-time, utilizing these devices to add flexibility, without affecting the economics of the system, the issue of creating a real-time decentralized marketplace for this multi-agent system remains. This

will be key to ensuring supply-demand balances in DER heavy grid structures. A decentralized architecture to manage the transactive layer is highlighted next.

CHAPTER 4. DECENTRALIZED TRANSACTIVE CONTROL ARCHITECTURE

Hybrid transformers show mechanisms to achieve unprecedented control over system flows and local parameters like voltage and congestion in a decentralized fashion. However, managing supply demand balances with ever changing resource availabilities and volatility is extremely challenging. The complexity is only accentuated when these assets belong to multiple owners across a system. There is a strong need to develop an architecture that can incentivize both demand and supply-side flexibility. Transactive mechanisms are key to ensuring that massively multi-agent systems can be stabilized effectively.

Real-time pricing is an efficient mechanism to achieve real-time stabilization through incentivization. However, centralized RTP mechanisms are often constrained by computation and communication bottlenecks. Thus, it is necessary to design a decentralized RTP mechanism that allows price to be derived instantaneously and locally, while reflecting grid constraints, without relying on central computations or low latency communications with a central controller. Moreover, an implementation that remains agnostic to topology information would be highly scalable and fractal, enabling operation even when parts of the system are damaged and separated. Such an architecture would allow the grid to be a means of enabling transactions, while independent devices such as hybrid transformers would ensure that physical grid limitations are not violated. Frequency is a ubiquitous signal that has been traditionally used to indicate the loading level of the system. This parameter could be used as a universal system-wide parameter that could

allow all loads and sources to transact and match supply-demand imbalances in real-time. This chapter proposes a frequency-based pricing transactive framework to achieve decentralized market operation and dynamic balancing. The chapter first discusses the role of frequency and how it can be leveraged as a signal and proposes market rules for different participating agents. A decentralized market architecture is then proposed. The proposed architecture is based on utilizing global signals to retrieve important system information to enable multiple geographically dispersed agents to transact power and contribute to grid stabilization.

4.1 Grid frequency as a global signal

Frequency is a key parameter that has been used to indicate imbalances between supply and demand levels. The nominal frequency is maintained at 60 Hz in the United States and 50 Hz in other parts of the world; a standard that was selected to ensure that direct grid connected electric machines and clocks can continue to operate safely and predictably. The frequency does however deviate in real-time. When the loading level rises, the frequency drops to a certain value and vice versa. The steady state settling frequency is a function of the droop curve for all the participating sources. Traditionally, droop was used as an indicator for the loading level across the system. By setting up a common droop curve for the entire system, the collective loading level of the system could be inferred. However, with the advent of modern control logic and fast communication infrastructure, the automatic generation control (AGC) and Area Control Error (ACE) schemes were implemented [121]. This was done to ensure that at any predefined dispatch point the frequency would be set back to 60 Hz irrespective of the loading level of the generators. This is done by introducing a bias to shift the droop curve [122].

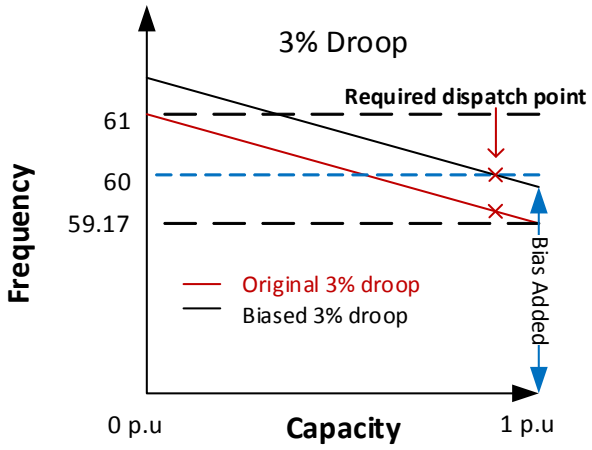

Figure 4.1 Droop curve and biasing mechanism

Fig. 4.1 shows an example of the biasing mechanism. The ACE parameter ensures that the other sources do not budge significantly from their predefined dispatch point and export excess power to different control areas. Thus, the grid frequency no longer indicates the net loading level, but a deviation from a predetermined operating point. The droop characteristic, however, is still implemented. This is done to ensure that the load sharing between sources can be managed if a transient occurs. However, one important development to note is that most modern devices do not require the frequency to be maintained strictly at 60 Hz. Since most frequency sensitive equipment is now interfaced to the grid through power electronics, the grid frequency could vary significantly. By letting the frequency vary, valuable information about the system's loading level can be derived. Moreover, transient phenomenon like ramp rates are made visible through frequency dynamics. Thus, by removing the AGC bias and reintroducing an open-loop droop implementation, the frequency can become a global parameter indicating the health of the system.

Although frequency has not been used traditionally as a system level pricing mechanism, some sparse adaptations have been found. Availability-based Tariff (ABT) is a scheme where a frequency dependent price is added to unscheduled interchange between different operating areas [123]. The unit commitment pattern for the sources is adjusted accordingly. Gupta et al. have proposed achieving load frequency control using demand response by assigning prices to frequency deviations [124]. Other approaches in literature have also been proposed to create an integrated mechanism for real-time markets and frequency regulation [125], [126]. Another adaptation of a frequency dependent pricing scheme is seen in [127]. This scheme uses a closed loop PI controller to generate prices that can stabilize the system based on frequency deviations. All these approaches either try to emulate some sort of frequency regulation scheme or leverage demand response while using the signals to perform a certain function. None of these schemes present a holistic and integrated market structure which performs like a regular wholesale market while embedding demand response, frequency regulation and economic dispatch. Moreover, even with these solutions, the other aspects of the grid architecture still remain centralized and coordinated rather than decentralized and distributed. The proposed approach in the subsequent subsection introduces a frequency dependent price that ensures that even with varying frequencies sources droop to the desired dispatch point that corresponds with their price preferences locally.

4.2 Decentralized Marketplace based on grid frequency

The approach proposed here relies on using global frequency signal to generate real-time prices in a distributed fashion. Frequency is a system-wide parameter reflecting the supply-demand imbalance. By using frequency to generate real-time prices, the need for

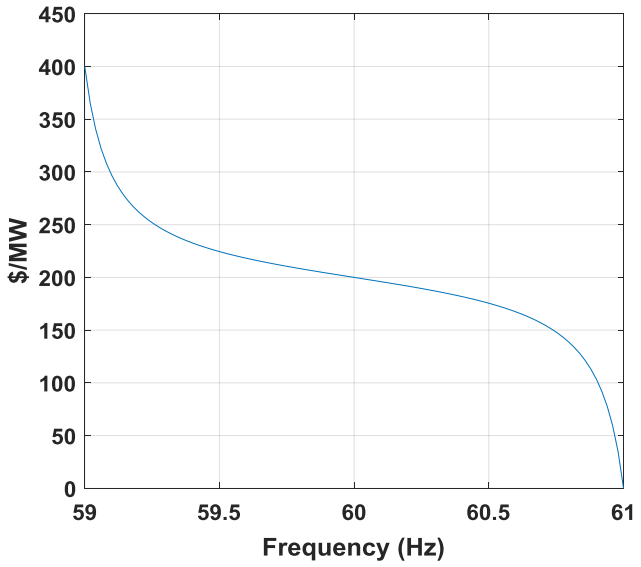

Figure 4.2 Real-time price vs frequency mapping

$$Price = -0.2492z^7 + 0.3864z^6 + 0.5796z^5 - 0.6244z^4 - 1.0397z^3 + 1.3161z^2 - 1.9701z + 22.4365 \quad (17)$$

$$where\ z = \frac{(frequency - 59.2420)}{0.4417} \qquad \forall\ 58.5 \leq frequency \leq 60$$

$$Price = -0.2492z^7 - 0.3864z^6 + 0.5796z^5 + 0.6244z^4 - 1.0397z^3 - 1.3161z^2 - 1.9701z + 17.5637 \quad (18)$$

$$where\ z = \frac{frequency - 60.758}{0.4417} \qquad \forall\ 60 \leq frequency \leq 61.5$$

extensive communication infrastructure can be eliminated. The real-time price for energy can be derived locally at every node.

Fig. 4.2 shows one possible mapping curve that could be used. The mapping is designed to leverage the exponential demand elasticity observed in literature as much as

possible. The mapping in Fig. 4.2 is designed using the relations (17) and (18). The seventh order polynomials closely approximate the exponential nature and allow the global characteristic to be updated by pushing 16 coefficients to all involved entities. The global characteristic for the whole system may be updated sporadically.

The intelligence of the system is then decentralized and distributed globally. Every node becomes a Universal Market Node (UMN) capable of sensing frequency, calculating the real-time price and making local decisions to alter behavior. Thus, an ecosystem of smart nodes is created where every node has visibility into price dynamics instantaneously. The approach tries to leverage a common economic principle while letting every agent incorporate that into their unique local controls. The local control and the required modifications are made locally to reflect autonomous operation. Every UMN possesses the ability to respond, to govern consumption, schedule generation, dispatch storage or participate in arbitrage. Moreover, by using price as reference, dispatch procedures may use local droops to enter a negotiation process that tries to settle to a common frequency which also reflects the transactive equilibrium. Each node then is exposed to market dynamics and can choose to balance local and global objectives. This allows all agents to have access to a market mechanism without adding costs of elaborate communication infrastructure and reducing complexity.

Fig. 4.3 shows the ecosystem and functionality that can be realized using the same global rule. These UMNs can be implemented on a low-cost Internet of Things (IoT) platform such as the GAMMA platform [128]. The platform provides ultra-low-cost sensing and computation hardware that helps in realizing this architecture. The nature of the curve incentivizes consumption when there is excess availability and the frequency is

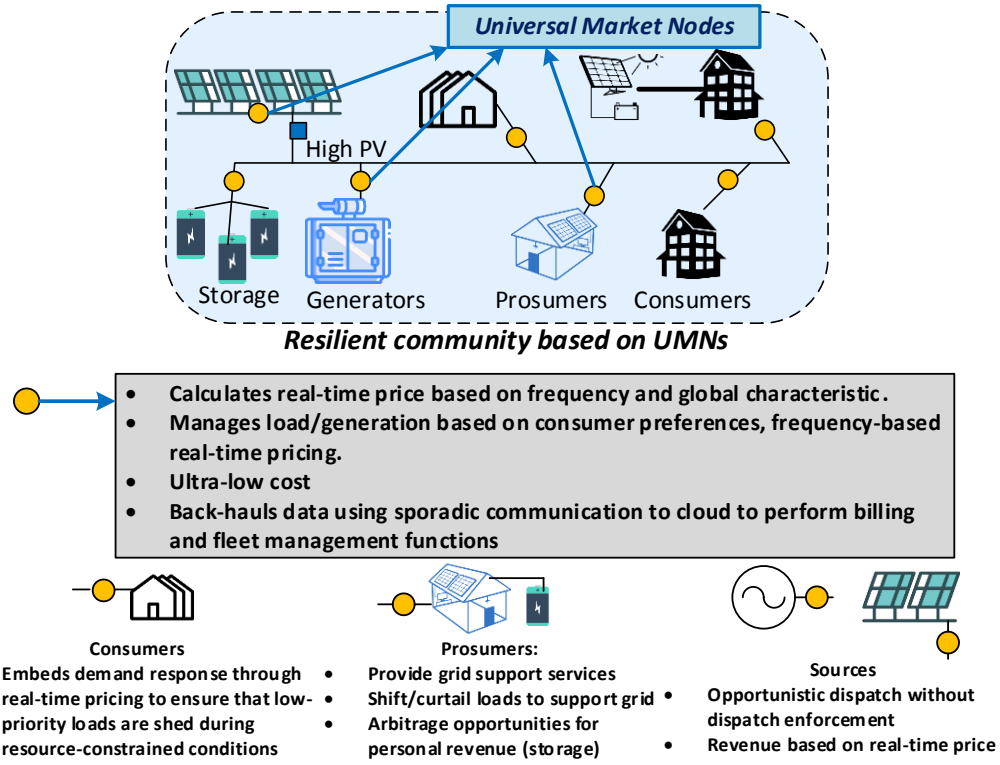

Figure 4.3 Decentralized transactive architecture based on global signals and edge intelligence

high and discourages it otherwise. This creates a framework for managing PV-dominant systems. All agents could then prioritize their consumption preferences and criticality of loads at the local level and react to changing global prices. Thus, frequency is not intrinsic to the system. It is merely a pricing mechanism that allows sources and consumers to transactively manage supply-demand ratios without any central coordination.

In extremely resource constrained situations in off-grid emerging grids, the real-time price reflects the availability and ensures that only critical loads are met at the high prices. Real-time prices reflects the availability of connected resources or contingencies, while ensuring the highest possible quality of service and respecting consumer preferences in such environments. One significant advantage of this approach is that the architecture does not require any information about the topology of the system, any knowledge of the system

states or reliance on AMI or PMU data. The universal market node paradigm allows for a day-ahead market optimization to set a baseline for calculations while deriving spot market prices in real-time, based on frequency. The approach can also work in real-time without elaborate day-ahead planning by utilizing droops while ignoring the AGC signals. By strongly integrating physical and transactive operations, every node contributes to collective stabilization of grid parameters. Moreover, the approach remains agnostic to system topology. Demand response becomes an integrated feature in this approach allowing higher flexibility. The variable nature of PV sources is actually reflected in the form of cheaper real-time prices. This ensures higher absorption of volatility using demand flexibility. Moreover, the cyclic nature of PV power outputs and lower prices during high PV intervals, ensures that consumers would actively consume power in intervals where the solar irradiation is higher.

Fast acting sources like batteries or flywheels may participate to provide quick responses without the need for a separate market structure for frequency support. This creates an ecosystem that strongly ties the physics of the network to the economics without relying on synchronous communication or central computation. This mapping becomes entirely scalable irrespective of the grid size. Thus, in the event of a HILF event, smaller broken grid sections can utilize the same control principle while utilizing energy at higher prices depending on the available resource mix, nature of the broken fractals and resource availability. This helps maintain a certain level of service rather than relying on central co-ordination to issue dispatch commands. Thus, by using price as a tool to leverage supply-demand flexibility a truly fractal, decentralized, and autonomous transactive architecture can be realized. In contrast to the approaches presented in literature, the proposed approach

creates a marketplace that centers on one global rule while letting the market dynamics dictate functionality and control. Hybrid transformers are key to ensuring that the physical grid phenomenon like congestion and voltage profiles are managed while letting the frequency-based market enable market dynamics to balance supply and demand in real-time.

The UMNs take on control actions based on the type of agent it represents. Thus, the local controls and their augmentations for different agents needs to be specified. The next two subsections aim to capture the nuances and complexity that need to be embedded to ensure that this architecture can be realized.

4.3 Market participation mechanism for Sources using Universal Market Nodes (UMNs)

One of the key issues with decentralized pricing schemes is market efficiency. Although, real-time prices may optimize load behavior, it is still important to ensure that the market prices are competitive. This involves ensuring that economic dispatch procedures are maintained. However, this needs to be done in a decentralized and autonomous manner. The subsequent section provides an overview of the conventional market procedure to derive merit order curves. The merit order curve determines dispatch procedures. Merit order curves do not capture the congestion costs and turn on and turn off costs. Since, hybrid transformers are proposed in this research to add flexibility, the cost of losses is socialized in the real-time pricing component. The subsequent sections show how decentralized economic dispatch can be attained in the proposed decentralized transactive framework based on the global frequency-price curve.

4.3.1 Conventional Merit Order Curves and Dispatch

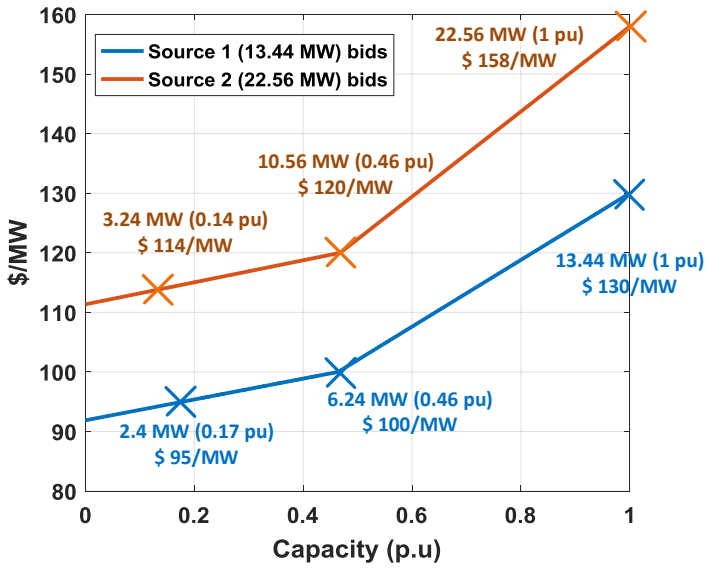

Figure 4.4 Production cost bids for two sample generators

Conventional economic dispatch is performed at the system level either by an Independent System Operator (ISO) or other system operator. This process involves a bidding procedure. Every participating source in the market structure submits a list of bids indicating the cost of each block of energy supplied. Fig. 4.4 shows [129] sample bids for two sources. The ISO then estimates the expected load profile for the next 24 hours based

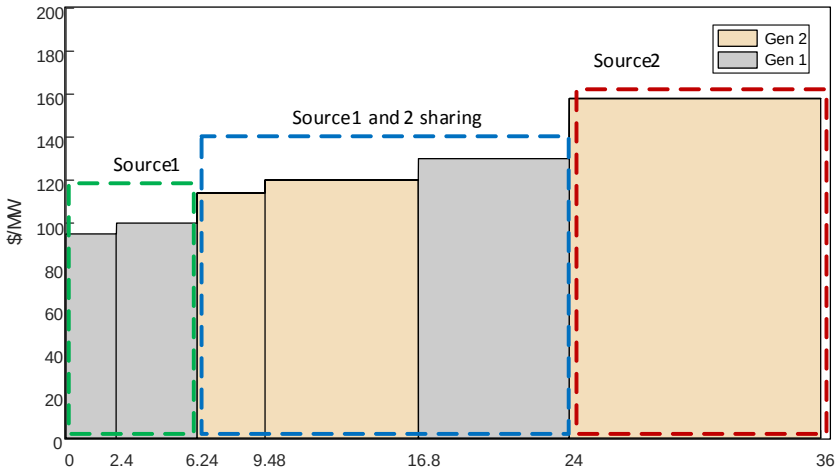

Figure 4.5 Economic dispatch (merit order curve) for the two participating sources

on historical data. At each point on this estimated load profile the cheapest combination of resources is then finalized in the form of an economic dispatch procedure. This generates a dispatch schedule for all the participating sources. This procedure is only adequate when the expected load profile is actually realized, which seldom happens. The consequence of this is that the economic dispatch procedure is updated on a periodic basis in real-time based on the current loading levels. For instance, in case the two sources shown here are the only participants, the economic dispatch schedule for increasing load is shown in Fig. 4.5. As illustrated, there are loading levels where Source 1 takes up the load, intervals where both the sources share and intervals where the larger source takes the peak load.

4.3.2 Source control using the price-frequency rule to achieve decentralized economic dispatch

The merit order curve from the previous section showcases how the economics of generation determine the dispatch pattern for multiple sources. This process requires retrieving bids from source and issuing AGC commands over low-latency communications in real-time. This is susceptible to failure in the event of damage to the communication infrastructure. A different way to realize this is proposed in this section based on the price-frequency mapping shown in Fig. 4.2. The dispatch procedure can be thought of as a way of calculating real-time price and dispatching the corresponding amount of power in the cheapest combination possible. In the proposed paradigm, the price-frequency mapping translates real-time frequency to price. The supply bids are a mapping between market price and supplied power. It is intuitive that using these two mappings, a curve relating frequency to power can be synthesized locally for each source. This curve would represent

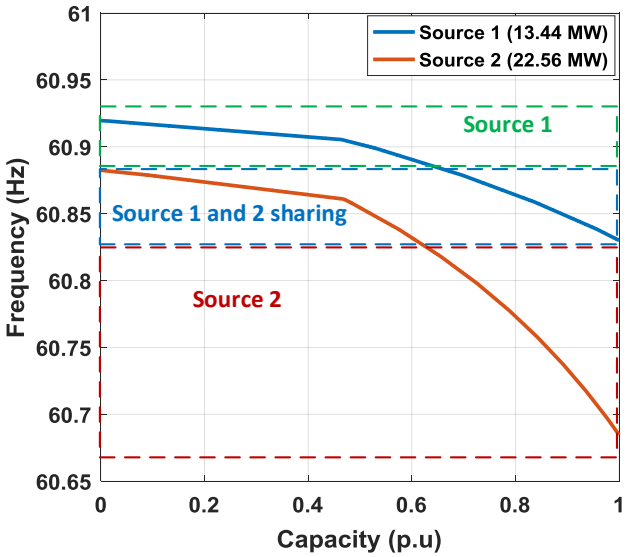

Figure 4.6 Nonlinear locally synthesized droops

a nonlinear droop curve. Nonlinear droop curves for the two sources shown in Fig. 4.4 are presented in Fig. 4.6.

The droops ensure that at every given frequency, the dispatch is always economical and that the power is shared in correct proportion within all sources. A similar procedure involving designing nonlinear droops is presented in [130]. However, this approach relies

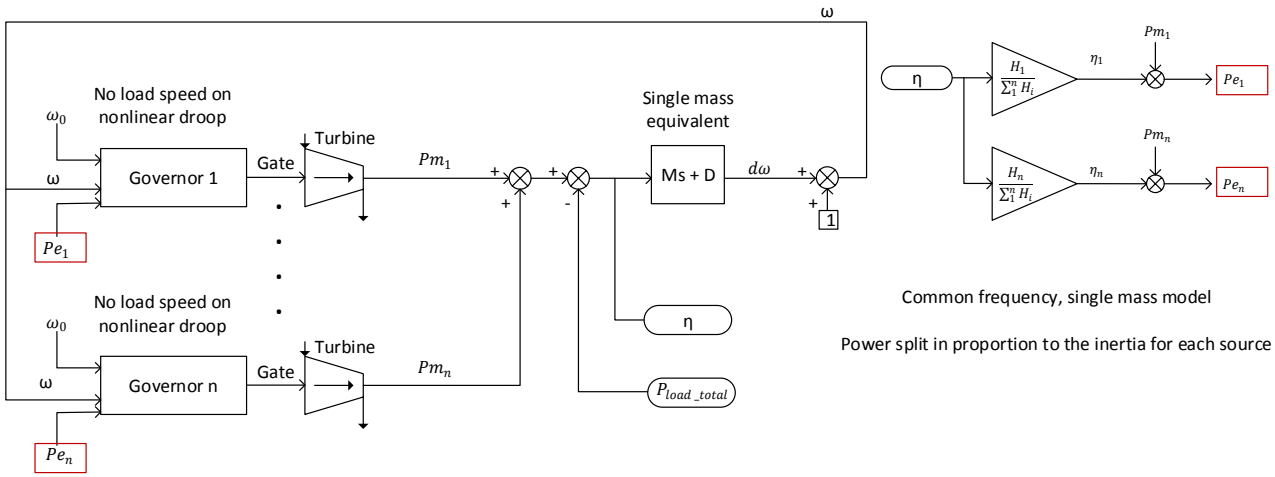

Figure 4.7 Two source test system with nonlinear droops

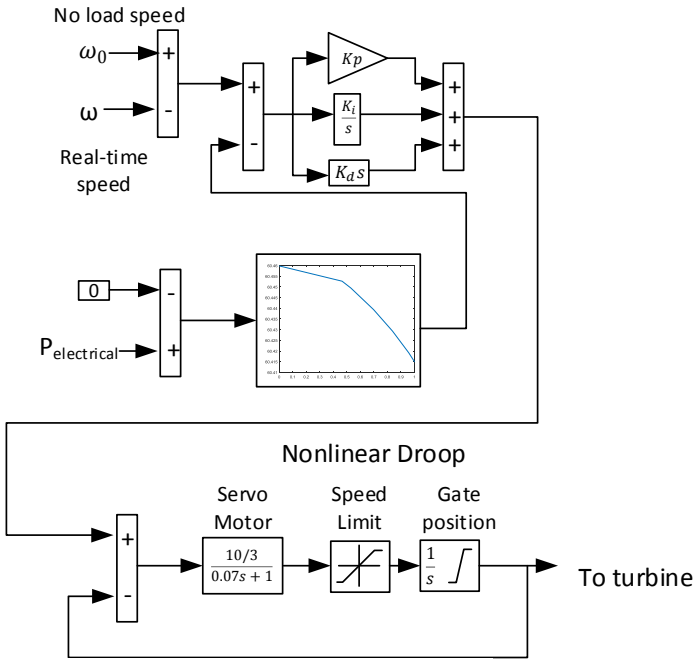

Figure 4.8 Detailed governor model with nonlinear droop

on every source having access to incremental costs for all involved units making it a centralized implementation.

A test system is utilized to showcase the proposed economic dispatch procedure. Fig. 4.7 shows the test system. The two sources involved, have the same cost curves as those shown in Fig. 4.4. The test system is run with the nonlinear droops from Fig. 4.6. It is important to note that the droops are derived locally based on personal cost preferences and the global price-frequency mapping that is common to all participants. A detailed model for the governor is presented in Fig. 4.8. This shows that the nonlinear droop can be implemented with just a slight modification to the existing droop controller on existing governor systems. Thus, the function of the UMN for sources would be synthesizing local droops based on the entities bids and interface these with the governor unit.

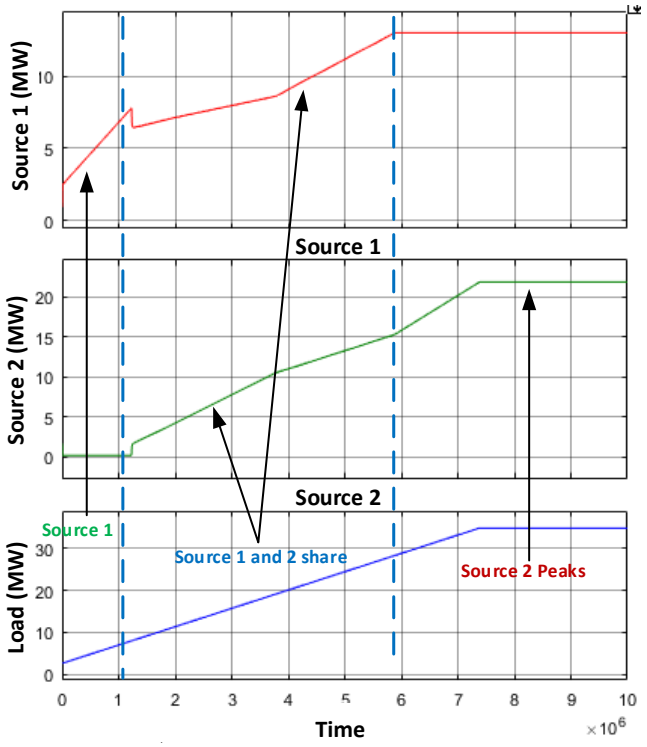

Figure 4.9 Power sharing corresponding to economic dispatch with nonlinear droops

A varying ramp of loads is applied to the test system. The droops create a power sharing pattern as seen in Fig. 4.9. This shows that the procedure is exactly equivalent to an economic dispatch procedure shown in Fig 4.5, in real-time, without elaborate co-ordination or communication mechanisms. Thus, this helps establish that the proposed price-frequency mapping can achieve the same performance as existing market procedures with no communication and co-ordination between the participants and the regulating body. It is however of interest to note that in large existing grids where such procedures are implemented, the requirements on frequency might be more stringent with a focus on operating closer to 60 Hz. The subsequent section details how the proposed nonlinear droops in this section can accommodate existing dispatch procedures while realizing an autonomous and decentralized frequency regulation market in real-time.

4.3.3 Source Control to achieve better transient performance while augmenting existing market processes in regulated environments

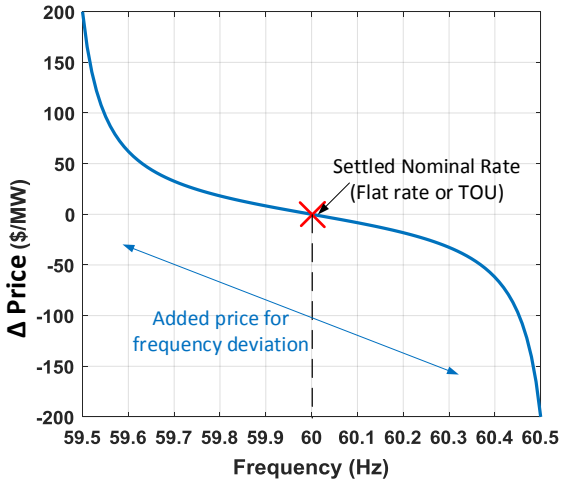

Figure 4.10 Modified price-frequency mapping for operation around day-ahead setpoints

In markets where a stricter control over range of frequencies is desired, control principles like Automatic Generation Control (AGC) and Area Control Error (ACE) are implemented. These signals ensure that every source adds a biasing term that sets the power output corresponding to the dispatch schedule at 60 Hz on the droop curve. In most cases a constant droop curve is implemented for all the sources that ensures that any disturbance is shared equally in proportion to each unit's capacity. While preserving the dispatch procedure decided by the ISO, it is possible to implement a modified price-frequency curve for frequency deviations. Fig. 4.10 shows one such curve. The implementation essentially augments the constant or TOU price set by the regulating authority. Thus, a frequency deviation indicates a deviation from the expected TOU or constant price in real-time.

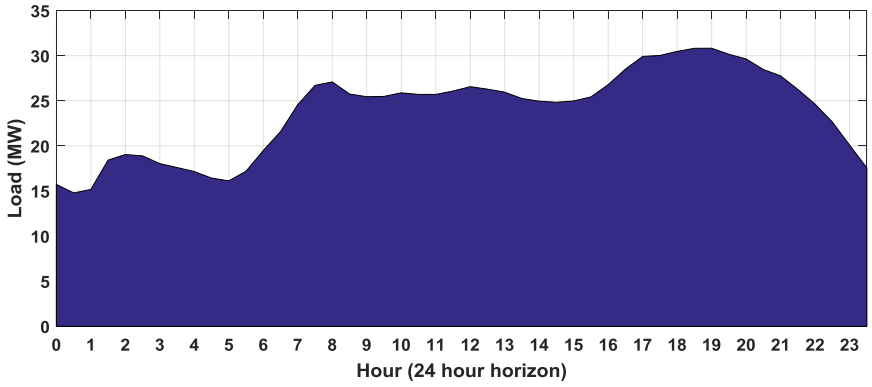

Figure 4.11 Sample load profile (15-minute intervals)

This implies that all sources only make the expected revenue when the frequency is 60 Hz. However, when a deviation occurs it is essential to re-dispatch the correct source in the correct order. The result is that at every dispatch point, a nonlinear droop curve can be realized which indicates the excess power that each source should supply when the frequency deviates. A load profile at 15-minute intervals is shown in Fig. 4.11. While utilizing the cost curves of the two sources shown in Fig. 4.4, the economic dispatch schedule can be computed for this load profile. The economic dispatch schedules for the two sources are shown in Fig. 4.12. This has two implications. The first one states that the two sources must follow the dispatch procedure if the real-time load is equal to that expected. The second implication is that the frequency should stay at 60 Hz if the economic

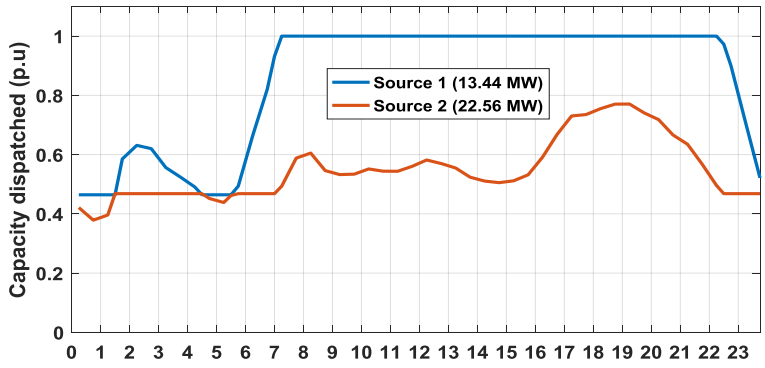

Figure 4.12 Economic dispatch set points for the given load curve

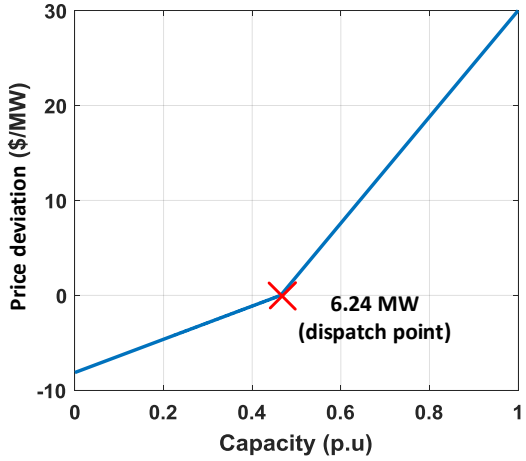

Figure 4.13 Desired deviation in price for deviation from dispatch

dispatch schedule is realized. However, it is of interest to note that the units are individually operating at cost points governed by their cost curves. In this case at 6.24 MW source 1 is being compensated $100/MWh. The regulating authority usually designs a flat rate or TOU scheme that generates equivalent total revenue and closes the market on a 24-hour basis. Thus, as the frequency deviates and a change in price is seen, each of the units will actually have varying preferences about the amount of power that they want to supply based on their current cost point of operation.

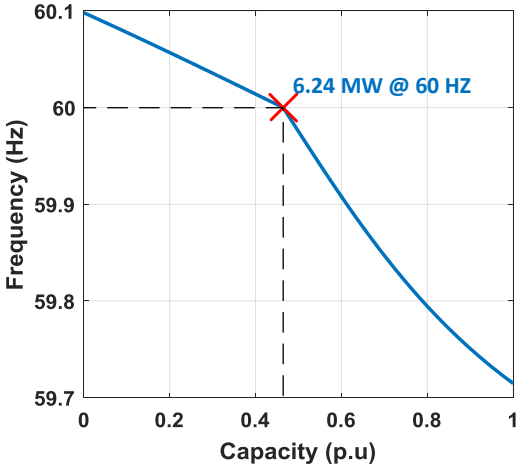

Figure 4.14 Nonlinear droop for one dispatch point

As an illustration, consider when source 1 is operating at 6.24 MW. As stated earlier the actual revenue source 1 is making is $100. The incremental price needed to ensure that operation is economical for source 1 is shown in Fig. 4.13. Considering the modified price-frequency curve shown in Fig. 4.10, this would mean that these operation points would be realized at certain frequencies resulting in a droop curve at this dispatch point shown in Fig. 4.14.

Thus, over the dispatch schedule shown in Fig. 4.12 a droop curve can be generated for each 15-minute interval or the rate at which economic dispatch signals are dispatched. It is important to note, that these curves are set locally while utilizing the dispatch schedule provided and the global price-frequency curve shown in Fig. 4.10. This is achieved without any coordination or communication between sources or with the ISO or regulating entity. The set of required droop curves generated locally, for source 1 and source 2 are shown in Fig. 4.15 and Fig. 4.16 respectively. The UMN then becomes a smart node that can retrieve local bids and market dispatch points to enforce time-varying droops on the governor of

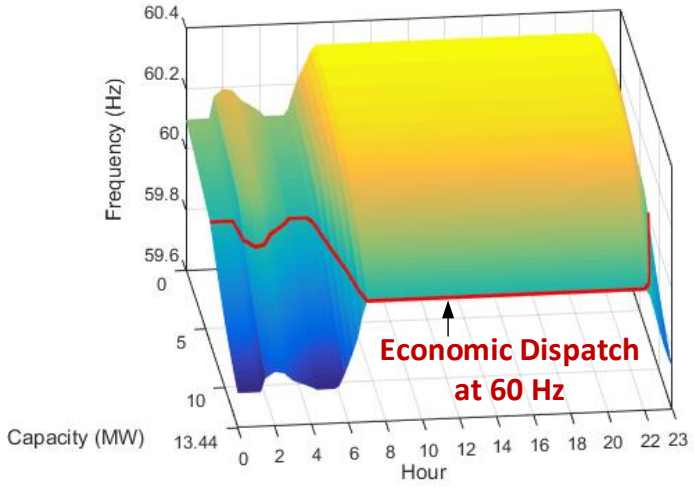

Figure 4.15 Nonlinear droops for all dispatch points (source 1)

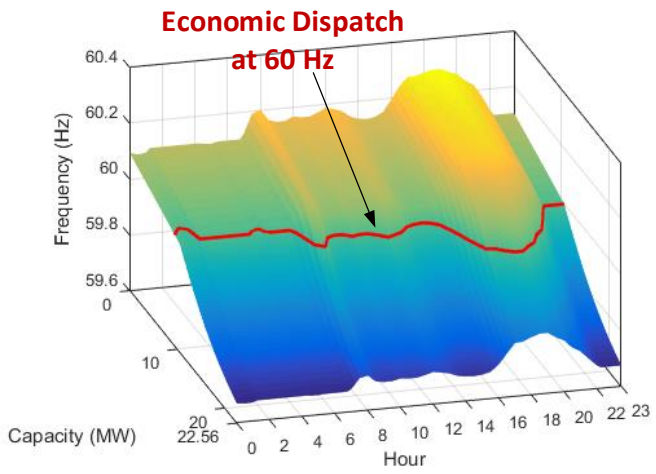

Figure 4.16 Nonlinear droops for all dispatch points (source 2)

each unit. In both these figures it is seen that the red line indicates the 60 Hz points of operation which correspond to the economic dispatch schedule.

This serves to establish a base line where current grid functionality can be realized in an equivalent if not better manner in most cases. This is achieved with lower reliance on continuous communication and co-ordination mechanisms. The approach proposed here for regulated market structures allows better performance to be achieved while ensuring that the existing market processes are maintained. A test scenario to showcase the distributed droop paradigm is shown here. For the purpose of this simulation the two dispatch points at hour 6 and 7 are considered. These dispatch points will have droop curves corresponding to these load intervals in Fig. 4.15 and 4.16. The simulation shows the loading level varying in each of these intervals. The performance with a standard 5% droop characteristic is compared here. The scenario is implemented on the same two source test system shown in figure 4.7.

A deviation from the economic operating point is created here. Fig. 4.17 shows the performance at these two points with the nonlinear droop curve. Fig. 4.18 shows the power

drawn from each of the sources with a standard uniform droop (5%) curve. It is seen that the sources share power in the most economic fashion for these intervals using the modified nonlinear droop curves. Thus, the UMN can embed these smart functionalities and augment existing sources and their control principles. The resultant framework allows resource availabilities and resource loading information to be embedded into the real-time price component. This information can be conveyed to every connected participant and made globally available through the real-time frequency.

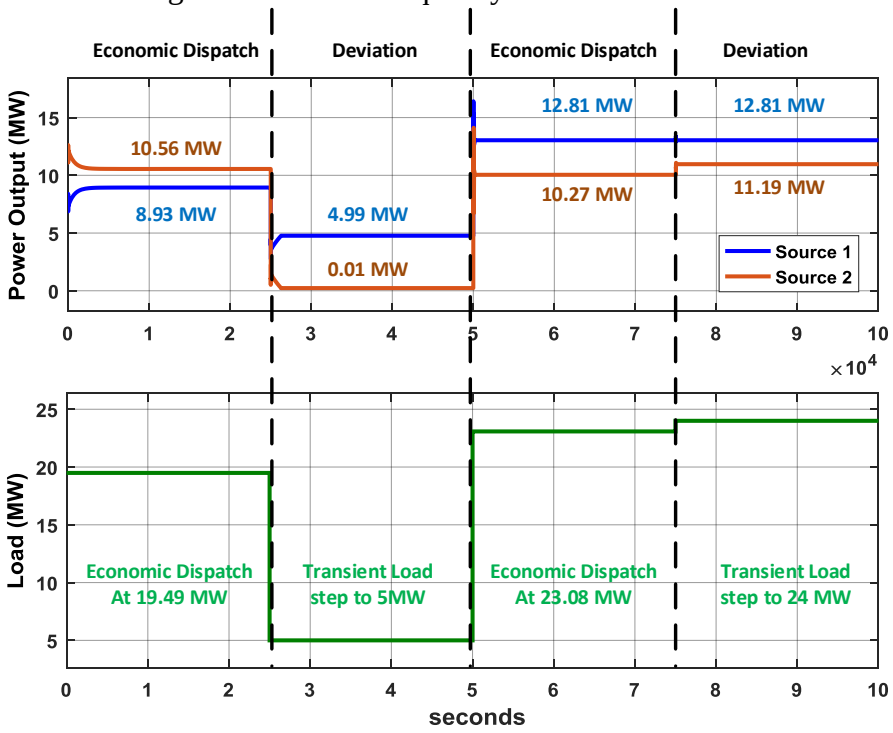

Figure 4.17 Economic power sharing between sources with nonlinear droops during disturbance on two dispatch points

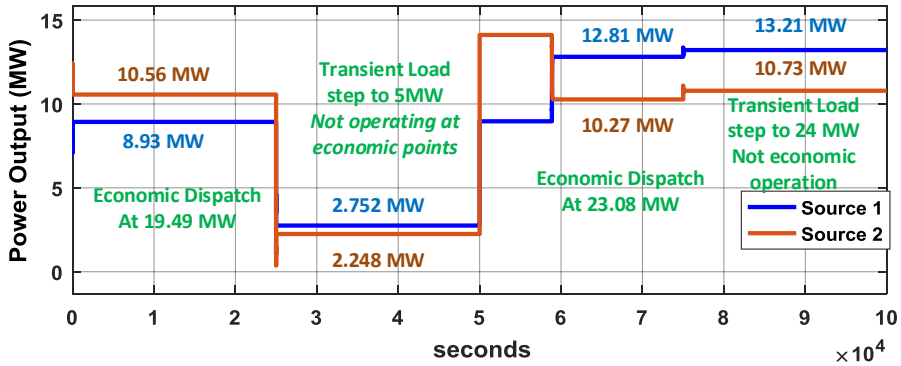

Figure 4.18 Incorrect sharing between sources during load disturbance (5% droop)

4.4 Distributed Demand Response through robust edge intelligence

The previous subsection shows that by embedding edge intelligence, sources in the system can be regulated based on the new transactive framework while achieving decentralized economic dispatch. However, the true merit of this architecture lies in the ability to leverage demand flexibility successfully in a way that supports grid behavior. The architecture highlighted above relies on UMNs with edge intelligence, that can prioritize consumption in a real-time pricing framework. It is important for this embedded intelligence to consider individual consumer preferences as well as global conditions of the entire system. These considerations would play a key role in developing a robust algorithm to leverage demand flexibility in a multi-agent system and assessing the efficacy of the architecture. This section summarizes the constraints and nuances that need to be captured to develop a robust control framework. An optimization algorithm to effectively leverage demand flexibility is then presented in this section. This algorithm will be deployed on UMNs on the consumer side in this architecture.

4.4.1 Edge intelligence constraints and nuances

The edge intelligence needs to use the entire temporal flexibility rather than only during certain critical intervals [131], [132]. This section discusses the different nuances of consumer behavior that need to be considered to leverage this flexibility. A given consumer may require certain loads must be consumed at their designated times to derive any benefit at all. This could be any critical load like lighting loads or life support equipment depending on whether the agent is a consumer or a critical community load like a hospital. Similarly, there may be other loads that could be moved to different times of the

day but may cause some discomfort to the consumer. These could include flexible loads like the dishwasher or washing machines. Lastly, there may be low priority loads that could be consumed opportunistically. These typically would provide low benefit values. Thus, it is apparent that different loads possess different temporal characteristics and differing benefits. A simplified approach towards modelling load behavior is presented below.

Based on this, each agent's loads could be thought of as lying within 3 priorities for any given consumer with the actual contents of each priority level being subjective to the agent or value of the service to the community. Priority 1 loads would be those that have extremely high benefits associated with them and are largely inflexible. Priority 2 loads are moderate benefit loads that are relatively flexible, but any temporal movement of loads comes at a slight discomfort. Priority 3 loads could be thought of as the lowest benefit loads that may be consumed or curtailed freely across a 24-hour cycle when the opportunity presents itself. A consumer's willingness to reschedule loads would largely depend on their flexibility as well as personal discomfort associated with the same. Finally, it is also important to state that within each priority level, different loads may provide different amounts of value from consumption. The classification of loads into these priority levels ensures that a consumer can actively decide or change the priorities for any given load without having to rely on detailed disaggregation approaches [133]. It is also important to levy certain rules that ensure that any agent does not destabilize the system. Every agent is free to perform arbitrage or schedule consumption as long as they do not consume erratically and create instabilities.

The proposed decentralized transactive architecture allows the real-time price to be derived instantly and locally. However, in PV dominant system with volatility there is only

a slight notion of the possible future prices. Further, ramp-rate issues are prevalent in PV dominant systems and are typically addressed by using storage. This makes it challenging to scale optimization approaches [134], [135] where all data points about price and consumer loads are known. At any given time 't' every agent can derive the global real-time price of energy based on the frequency being observed, but the future prices over the remaining $24-t$ intervals are still uncertain. If an agent is to defer a certain amount of load into the remaining time horizon, the agent algorithm must consider the uncertainty of price, personal discomfort and the benefit derived from deferring loads to make the decision.

Thus, the intelligence that is built into each UMN must account for past decisions, future uncertainties, local consumer preferences and grid-friendly constraints. A robust approach over a receding horizon is proposed in the next section to achieve the same. The algorithm relies on sporadic communications to receive the global price vs frequency mapping and a rough forecast of possible prices from the market operator. Based on local preferences about flexibility, sensitivity to uncertainty and criticality of loads the proposed algorithm optimizes consumption for each agent at the current instant of time t while capturing future uncertainty.

4.4.2 Local Optimization Framework for UMNs

In any transactive framework, the market structure is only efficient if all associated parties derive as much benefit as possible from the service. A social welfare function can be defined to capture and maximize the net benefit derived [136].

$$Min_{e_t} \sum_{t=1}^{24} \lambda_t e_t - U_t(e_t) \quad (19a)$$

$$where\ U_t(e_t) = b.e_t \quad (19b)$$

Equations (19a-19b) present the conventional social welfare maximization problem. Here, λ_t represents the varying prices. In a dynamic pricing framework, $\lambda_t e_t$ corresponds to the cost of consuming a given amount of energy e_t in each interval *t.* Similarly, *U(t)* represents the value or benefit derived from the consumption. A benefit function where the benefit is linearly proportional to the load consumed is considered in (19b). The benefit *b* may correspond to the criticality of the load or value of service each consumer derives from the consumed load. It is apparent that the solution to the minimization problem set in (19) would enable each agent to get the best value of service. However, none of the considerations presented in Section 4.4.1 are captured in this problem. Thus, using this minimization problem as a basis, the problem is progressively modified to incorporate the nuances highlighted earlier.

4.4.2.1 Priority Levels and Varying Benefit Levels

To accommodate for the three levels of priorities that were described earlier, the problem's benefit function is modified as shown in (20). This helps account for each consumer's varying benefits associated with consuming loads within each priority level. Here, b_1, b_2 and b_3 represent the benefits associated with consuming priority 1,2 and 3 loads. The decision variables are now the vectors $\{e_1, e_2, e_3\}$. The solution to (20) would determine the optimal consumption patterns for loads within each priority level based on the benefits a consumer may derive.

$$\underset{e_1,e_2,e_3}{Min} \sum_{t=1}^{24} \begin{matrix} \{\lambda_t - b_1(t)\}e_1 + \{\lambda_t - b_2(t)\}e_2 \\ +\{\lambda_t - b_3(t)\}e_3 \end{matrix} \tag{20}$$

4.4.2.2 Consumer discomfort and load rescheduling

While it is desirable to have each consumer shift their consumption to peak PV intervals, this can often be challenging owing to consumer preferences and discomfort. Any connected consumer would only prefer to reschedule consumption in a dynamic pricing framework to a later point, if the value of service derived at a later point outweighs the sum of the cost of consumption now and the cost of discomfort associated with rescheduling. Thus, we define a cost of discomfort c_d which is proportional with the number of intervals a given load is shifted [137]. As an example, if at time t the price is λ_t and the price at $(t+h)$ it is λ_{t+h}, a consumer would only shift consumption of energy e_x with a benefit b from t to $(t+h)$ if the condition in (21) and subsequently (22) is met. Thus, an augmented shifted benefit ($bshift$) can be defined as a benefit function that accounts for the cost of discomfort associated with rescheduling consumption and is summarized in (23).

$$\lambda_t e_x - b e_x > \lambda_{t+h} e_x + c_d . h . e_x - b e_x \tag{21}$$

$$or \quad (\lambda_t - b) e_x \; > (\lambda_{t+h} - bshift_{t,t+h}) e_x \tag{22}$$

$$where, bshift_{t,t+h} = b - c_d . h \tag{23}$$

The indices under $bshift$ operator indicate the interval the load is being shifted from and the interval the load is being shifted to in that order. It is important to note that in accordance with the discussion in Section 4.4.1, only priority 2 and 3 loads can be temporally shifted. While priority 3 loads can be shifted with ease, priority 2 loads are the

ones that have some discomfort associated with them. $bshift$ only captures the augmented shifted benefit associated with all priority 2 loads.

$$Min_{\{e_{1,t} \cup e_{2,t} \cup e_{3,t} \cup eshift_{i,j}\}}$$

$$\sum_{t=1}^{24} \{\lambda_t - b_1(t)\}e_1 + \{\lambda_t - b_2(t)\}e_2 + \{\lambda_t - b_3(t)\}e_3$$

$$+ \sum_{i=1}^{24} \sum_{j=1}^{24} \{\lambda_t - bshift_{\mathrm{i,j}}\}.eshift_{i,j} \quad (24)$$

Formulation (24) here incorporates these shifting characteristics into the problem shown in (20). These indicate the optimal patterns to consume energy within the 3 priority levels as well as optimal rescheduling patterns for priority 2 loads to maximize consumer benefit. Any non-zero values in the in the solution corresponding to the vector $eshift_{i,j}$ would indicate possible shifts in priority 2 loads that could maximize the consumer's derived value of service. The actual priority 2 consumption at t would be that seen in (25).

$$e_2(t) + \sum_{i=t}^{24} eshift_{i,t} \quad (25)$$

This shows that for a given amount of consumer discomfort and a given set of benefits a consumer may derive, the solution to (24) would indicate the optimal consumption and rescheduling pattern.

4.4.2.3 Uncertain Prices in the Receding Horizon and 'Grid-friendly' Behavior

The minimization problem summarized in (24) works well in terms of scheduling consumption while accounting for temporal shifts in consumption. However, one key

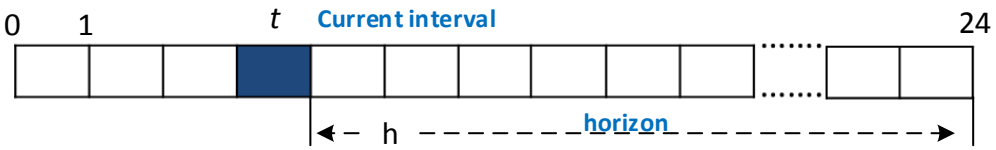

Figure 4.19 Notation used to signify time intervals

assumption in the formulation is that prices over the entire horizon are completely known. This is seldom the case in any real-time market. At best, a consumer agent has a rough forecast of future prices with a varied amount of uncertainty. In a PV dominant network, it is expected that with high PV outputs around solar noon the frequency is higher and consequently the price is the lowest. Each agent has complete knowledge of the price at the current time instant t based on the real-time frequency and has a forecast of the future prices over $(t+1)$ to 24 provided by the market operator which may or may not be realized. These parameters are sent once a day to each agent by the market operator. Fig. 4.19 provides a clarification for the notation being used to denote time intervals. Certain consumers may want their edge intelligence to be more wary to uncertainty while others may want to be more opportunistic in their response. To incorporate this sensitivity to risk in future prices into the algorithmic framework, each user may add a band of prices to their UMN that they are willing to tolerate throughout the day. This means that an opportunistic consumer would prefer a band of prices $(\lambda_{max,t+h} - \lambda_{min,t+h})$ like those seen in Fig. 4.21 while an extravagant consumer may prefer a range of prices as seen in Fig. 4.20.

An optimization problem is presented in (26) by considering certainty intervals at the α confidence levels within the band of prices $(\lambda_{max,t+h} - \lambda_{min,t+h})$. The formulation considers all the local constraints specified above to solve an optimization problem to reschedule, curtail or consume with the given parameters. The first part of the problem (26)

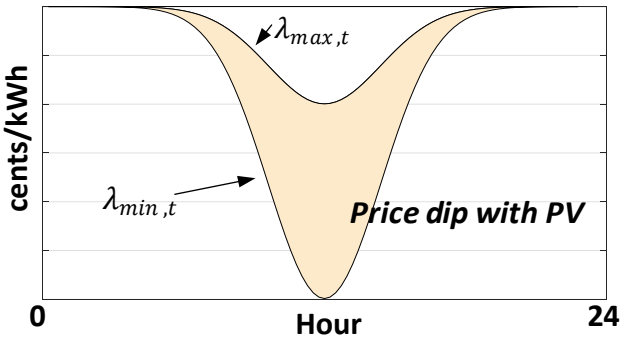

Figure 4.20 Acceptable band of prices for a risk averse consumer

is based on known quantities at the current interval t, while the second part is based on predictions with uncertainties. The second part of the minimization problem formulated here is created using well known techniques [138] to create a dual of the problem. It is the important to note that at each interval t the algorithm solves the optimization problem for current instant t as well as the entire future horizon $(24 - t)$ based on the forecasts. Thus, all considerations about rescheduling and discomfort are captured while ensuring that the uncertainty in future forecasts is embedded in the solution. At each interval the consumption pattern determined by the solution to (26) for the current instant t is followed. This process is repeated at each interval as the real-time price changes and the 24 hour horizon shortens.

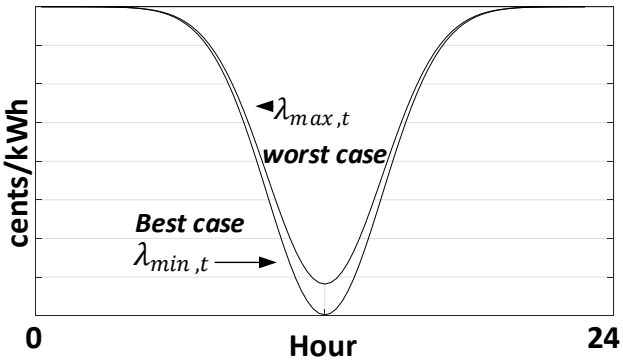

Figure 4.21 Acceptable band of prices for an opportunistic consumer

$$Min_{\{e_{1,t},e_{2,t},e_{3,t},e_{1,t+h},e_{2,t+h},e_{3,t+h},eshift,d_{1,t+h},d_{2,t+h},d_{3,t+h},\xi_{t+h},\beta,y_{t+h}\}}$$

$$\{\lambda_t - b_{1,t}\}e_{1,t} + \{\lambda_t - b_{2,t}\}e_{2,t} + \{\lambda_t - b_{3,t}\}e_{3,t}$$

$$+\sum_{h=1}^{24-t}\{\lambda_t - bshift_{t+h,t}\}eshift_{t+h,t}$$

$$+\sum_{h=1}^{24-t}\{\lambda_{min,t+h} - b_{1,t+h}\}e_{1,t+h} + \{\lambda_{min,t+h} - b_{2,t+h}\}e_{2,t+h}$$

$$+\{\lambda_{min,t+h} - b_{3,t+h}\}e_{3,t+h}$$

$$+\sum_{h=1}^{24-t}\sum_{i=t}^{24-t}\{\lambda_{min,t+h} - bshift_{i,t+h}\}eshift_{i,t+h}$$

$$+\beta\Gamma + \sum_{h=1}^{24-t}\xi_{\mathrm{t+h}} \dots\dots\dots\dots\dots\dots\dots\dots\dots\dots\dots\dots\dots\dots\dots\dots\dots\dots\dots\dots\dots\dots\dots\dots\dots\dots\dots\dots (26)$$

subject to,

$$e_{1,t+h} = \frac{d_{1,t+h} + d_{1,t+h+1}}{2} \qquad \forall\ h = 0, \dots, 24 - t\ (26a)$$

$$e_{2,t+h} + \sum_{i=1}^{24} eshifts_{i,t+h} = \frac{d_{2,t+h} + d_{2,t+h+1}}{2} \qquad \forall\ h = 0, \dots .24 - t\ (26b)$$

$$e_{3,t+h} = \frac{d_{3,t+h} + d_{3,t+h+1}}{2} \qquad \forall\ h = 0, \dots .24 - t\ (26c)$$

$$\{d_{1,t+h+1} + d_{2,t+h+1} + d_{3,t+h+1}\} - (1 + r_u)\{d_{1,t+h} + d_{2,t+h} + d_{3,t+h}\} \leq 0$$

$$\forall\ h = 0, \dots .24 - t\ (26d)$$

$$(1 - r_d)\{d_{1,t+h} + d_{2,t+h} + d_{3,t+h}\} - \{d_{1,t+h+1} + d_{2,t+h+1} + d_{3,t+h+1}\} \leq 0$$

$$\forall\ h = 0, \dots .24 - t\ (26e)$$

$$e_{3,t} + \sum_{h=1}^{24-t} e_{3,t+h} \leq e_{3,des} - \sum_{h=1}^{t-1} e_{3,h} \qquad \forall\, t = 1,.,24 \; (26f)$$

$$\sum_{t=1}^{24} (e_{1,t} + e_{2,t} + e_{3,t}\} + \sum_{i=1}^{24} \sum_{j=1}^{24} eshift_{i,j}$$

$$\leq \sum e_{1,des} + \sum e_{2,des} + \sum e_{3,des} \qquad (26g)$$

$$\sum_{h=t}^{24} \left[\sum_{i=t}^{24} eshift_{i,h} + e_{2,h} \right] \leq \{ \sum e_{2,des} - \sum_{h=1}^{t-1} e_{2,h} - \sum_{h=1}^{t-1} \sum_{i=1}^{24} eshifts_{i,h} \}$$

$$\forall\, t = 1, \ldots..,24 \; (26h)$$

$$\sum_{j=1}^{24} eshift_{t,j} + e_{2,t} \leq e_{2,des}(t) \qquad \forall\, t = 1, \ldots\ldots,24 \; (26i)$$

$$eshift_{i,i} = 0 \qquad \forall\, i = 1, \ldots..,24 \; (26j)$$

$$\beta + \xi_{t+h} \geq \left(\lambda_{max,t+h} - \lambda_{min,t+h}\right) y_{t+h} \qquad \forall h = 1,.,24 - t \; (26k)$$

$$e_{1,t+h} + e_{2,t+h} + e_{3,t+h} + \sum_{i=1}^{24} eshifts_{i,t+h} \leq y_{t+h} \qquad \forall\, h = 1,.,24 - t \; (26l)$$

$$0 \leq e_{1,t+h} \leq e_{1,des}(t+h) \qquad \forall\, h = 0,.,24 - t \; (26m)$$

$$d_{1,t+h}, d_{2,t+h}, d_{3,t+h}, eshifts_{i,j} \geq 0 \qquad \forall\, h = 0, \ldots.24 - t \;\; \forall\, i, j = 1, \ldots..24 \; (26n)$$

$$\beta \geq 0\,, \xi_{t+h} \geq 0, y_{t+h} \geq 0 \qquad \forall\, h = 1, \ldots.24 - t \; (26o)$$

The decision variables for problem (26) are $\{e_{1,t} \cup e_{2,t} \cup e_{3,t} \cup\ e_{1,t+h} \cup e_{2,t+h} \cup e_{3,t+h} \cup eshift \cup d_{1,t+h} \cup d_{2,t+h} \cup d_{3,t+h} \cup \xi_{t+h} \cup \beta \cup y_{t+h}\}\, \forall\, h = 0, \ldots,24 - t.$ The variables β and ξ are dual variables to the initial problem meant to capture the uncertainty

in the prices. The variable Γ models how conservative the solution tends to be. Γ takes values based on the number of intervals left in the horizon. So, over 24-hourly intervals throughout a day, Γ starts out with 23 and ends with 0. Thus, as the problem is solved at every interval and the horizon recedes, the conservativeness of the solutions drops. This is valuable as it makes the algorithm greedier as the horizon recedes. Moreover, the problem still attempts to capture all possible shifts in case the forecast $\lambda_{min,t+h}$ is realized.

Constraints (27a-26c) relate energy $(e_{1,t}, e_{2,t}, e_{3,t})$consumed within each of the priority levels to demand $(d_{1,t}, d_{2,t}, d_{3,t})$ using a trapezoidal summation approach. In order to ensure that none of the agents engage in erratic behavior to destabilize the system, a set of grid-friendly constraints are imposed. Constraint (26d) and (26e) ensure that the ramp up and down rate is limited to $r_u$and r_d respectively. So, for a maximum ramp up or down rate of 5%, $r_u$or r_d would be 0.05. These may correspond to rules set up by the market operator for residential, commercial and industrial customers. Constraints (26f-26h) limit the total consumption over a 24-hour period as well as within each priority category. These limits reflect each agent's desired consumption within each priority level. The constraint (26i) ensures that the load being shifted is limited to that specified in $e_{2,des}$. This ensures that the movement of priority 2 loads is tracked. Constraints (26j-26o) capture the constraints embedding uncertainty into the problem as well as bounds on all variables. Thus, a robust algorithm is presented that can control every consumer's consumption in a decentralized manner without real-time coordination or communication, to maximize personal benefit while contributing to grid stabilization.

4.4.2.4 Implementation of Edge Intelligence

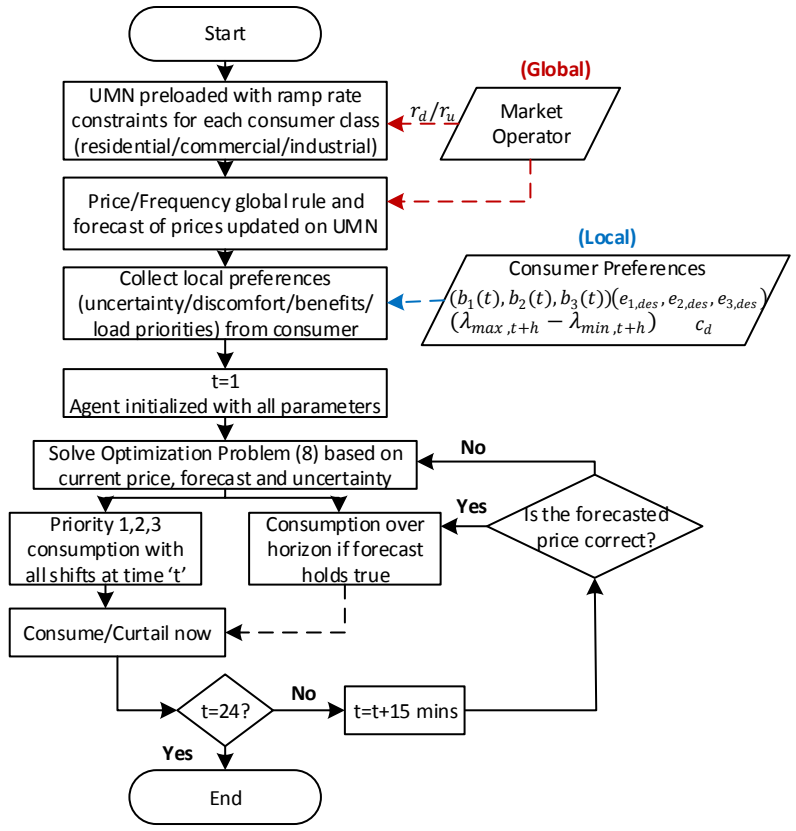

Figure 4.22 Implementation scheme for algorithm (26) on UMNs

The edge intelligence operates on some global rules and some local ones. The global price to frequency mapping is updated once a day by the system operator and sent to each agent along with a forecast of expected intra-day prices. Each UMN then collects information about the user's preferences about the desired consumption within each priority level $(e_{1,des}, e_{2,des}, e_{3,des})$, the time varying benefits associated with consuming these loads $(b_1(t), b_2(t), b_3(t))$, their personal discomfort associated with rescheduling loads (c_d) and their averseness to uncertainty in future prices in the form of the band $(\lambda_{max,t+h} - \lambda_{min,t+h})$. The forecasted intra-day prices sent by the market operator are assumed to be λ_{min} for all consumers. Depending on the nature of each consumer

(residential, commercial or industrial), certain ramp rate limits are already built into the edge intelligence. These characteristics may be updated by the operator. The robust model (26) is implemented on each individual agent. The algorithm is recursively solved at each interval with knowledge of past decisions and uncertainty about the future prices. Fig. 4.22 shows a flowchart of the implementation.

In each interval t the problem considers the past consumption within each priority level, calculates the known current price and solves problem (26) over the receding horizon. The solution then computes the optimal consumption for the current interval as well as a projection for future intervals. This whole process is repeated every 15 minutes locally. Moreover, at any point a given agent can change their preferences about flexibility or consumption preferences. These are reflected in the solution generated in the next 15-minute interval. The UMNs can directly control connected loads within each priority level. It is intuitive to see that if the price is high enough to outweigh any benefit in any priority category, formulation (26) would curtail the load. This is key in contingency scenarios where the demand reduction could support operation of resource constrained communities. This allows an edge intelligence algorithm to be realized that dynamically reacts within reasonable parameters to the state of the grid and collectively realizes demand response.

4.4.2.5 Simulation Test Case for Consumer UMN

In order to show the algorithm's efficacy a couple of simulation studies are presented in this subsection. A single consumer is modelled with the profile shown in Fig. 4.23. The three priorities of loads are assumed to be those shown in the same figure. The time varying

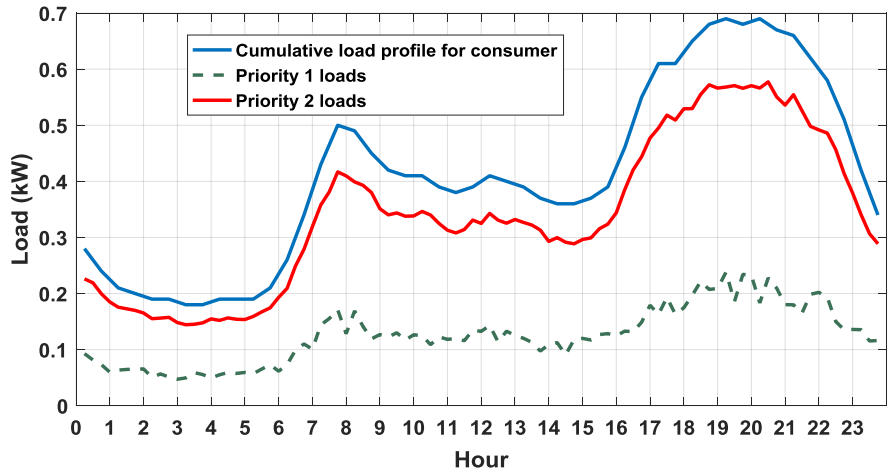

Figure 4.23 Sample residential consumer profile with three priority categories

benefits for priority 2 loads are shown in Fig. 4.24. These correspond to the time varying priority 2 load shown in Fig. 4.23. The personal benefits for priority 1 loads are modelled to be a constant 120 cents/kWh to convey that these are critical while the priority 3 benefits are kept at 10.5 cents/kWh to convey that these are lower in terms of criticality to the consumer. The ramp up and down rate r_d/r_u is limited to 8%. A price variation is simulated to analyze the behavior of this agent and it shown in Fig. 4.25. With these parameters a

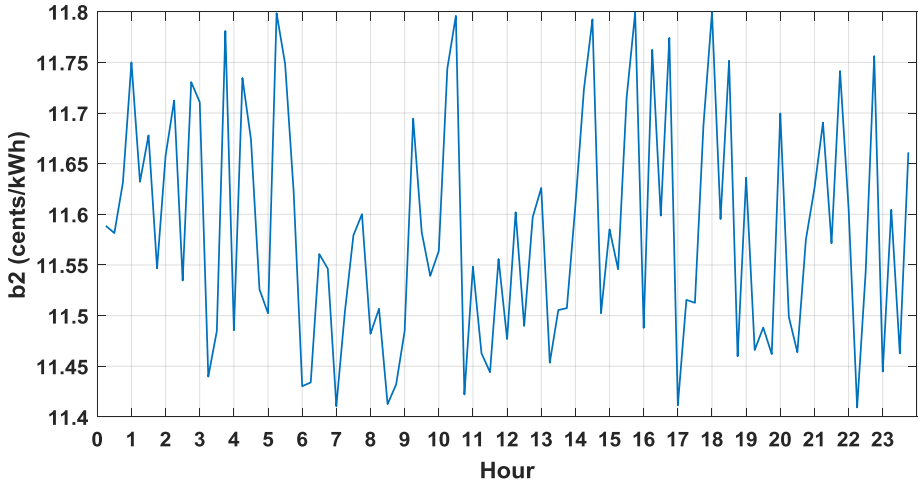

Figure 4.24 Modelled time varying benefits for priority 2 loads

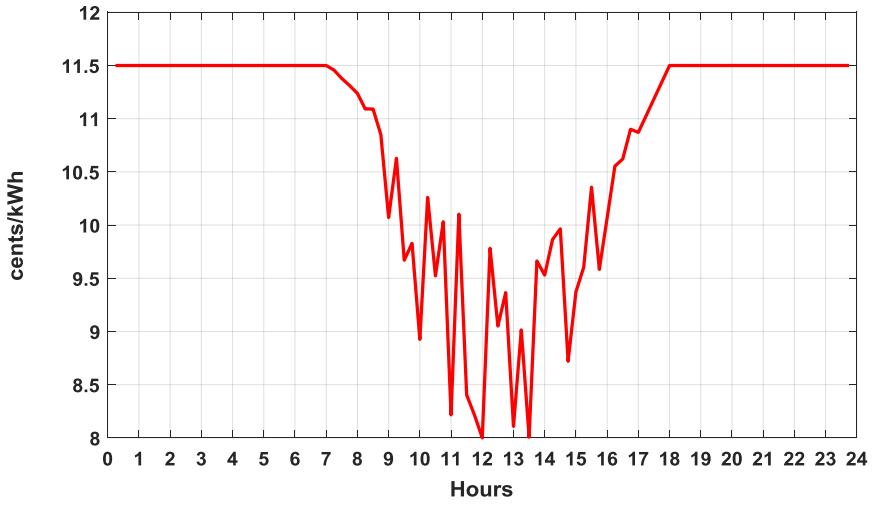

Figure 4.25 Sample real-time price profile

first study is done to analyze the effect of varying levels of discomfort that users may have locally and how the algorithm responds in response to the changing price. The value of c_d is varied between 0.1 to 0.6. This would imply a consumer that is extremely opportunistic or extremely extravagant respectively. Fig. 4.26 shows the varying consumption patterns that the local optimization framework would generate based on different discomfort values. The extreme ends of Fig. 4.26 are also shown in the Figs. 4.27 and 4.28.

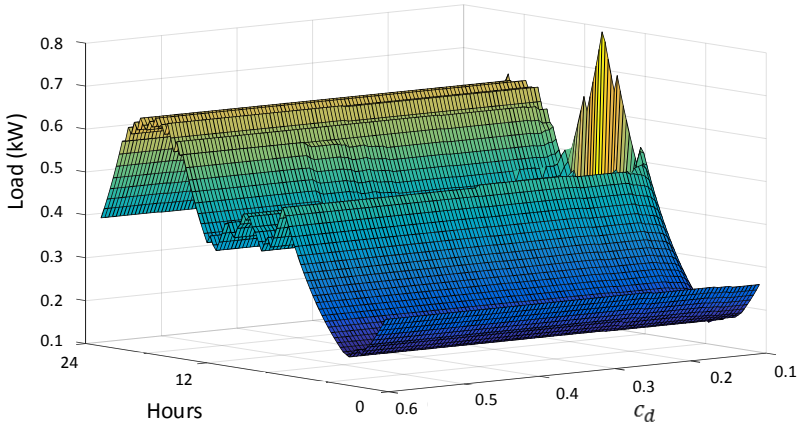

Figure 4.26 UMN response to varying consumer discomfort

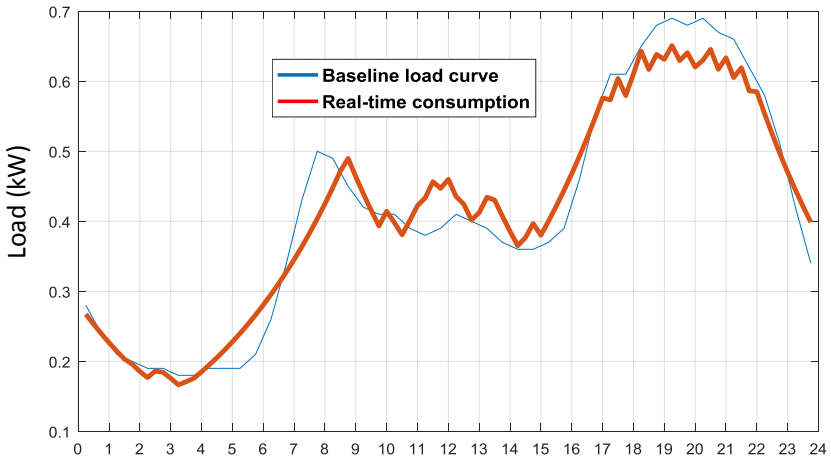

Figure 4.27 UMN real-time consumption for extravagant consumer

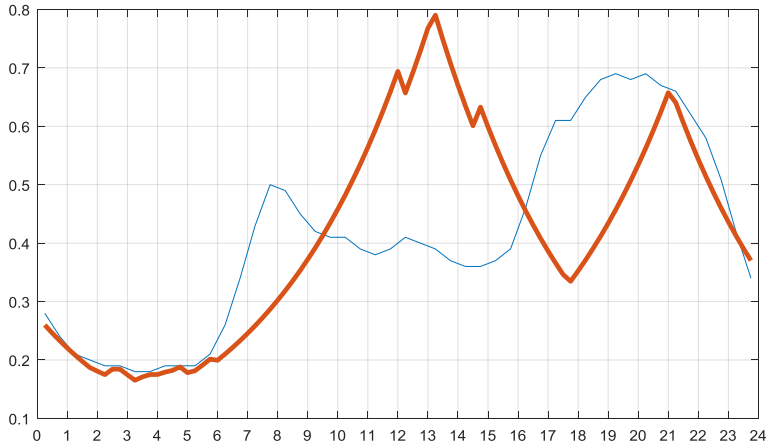

Figure 4.28 UMN real-time consumption for an opportunistic consumer

Another important scenario to analyze is contingencies where the resource availability is extremely scarce. In this scenario, the observed prices would be consistently high. This is simulated by charging the same agent a constant price of 20 cents/ kWh with

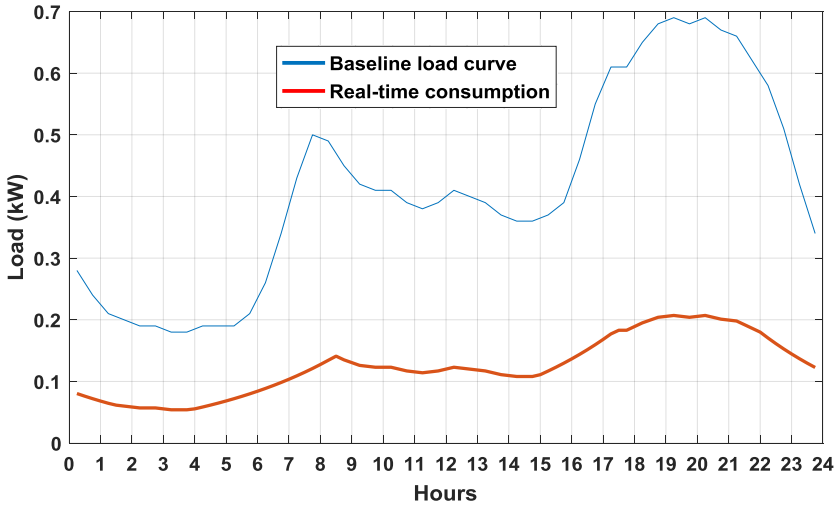

Figure 4.29 UMN drops consumption to priority 1 loads during high price contingency intervals

the same set of parameters. Fig. 4.29 shows the resultant consumption pattern. The UMN algorithm sheds both the priority 2 and 3 loads in this scenario while only operating the highest priority tier 1 loads for this agent. Thus, based on local parameters the intelligence algorithm can scale and react to the same varying global prices. Moreover, in the event of a HILF event, the UMN algorithm can prioritize critical loads and sustain small resource constrained communities till restoration actions can be taken.

4.5 Need for Physical Grid Control in Transactive Frameworks

The proposed transactive framework allows real-time stabilization of grid structures by utilizing edge intelligence and incentivizing participants through price dynamics. While, power balance constraints across the network can be managed effectively, the transactive architecture allows little control over the physical distribution of grid flows. Line congestion management and voltage management becomes challenging without visibility into the precise geospatial distribution of sources and loads and their power injections.

Hybrid transformers are an effective distributed mechanism to manage these physical constraints on grid structures. These devices could function in parallel with the transactive framework and allow control over physical aspects of power delivery. The next subsection highlights the role of hybrid transformers in the proposed decentralized transactive framework.

4.6 Role of Hybrid Transformers in a Decentralized Transactive Framework

The dynamics of the transactive mechanisms have an effect on physical parameters like line flows and voltage patterns on the system. Hybrid transformers have been proposed to address these challenges. Hybrid transformers are power control solutions that can be augmented to address congestion issues and alter power flows in meshed networks. However, the metrics proposed in Section 3.5 rely on knowledge of power injections to estimate flows. In order to realize an autonomous implementation however, it is important recognize the parameters that the hybrid transformer in a given system has access to.

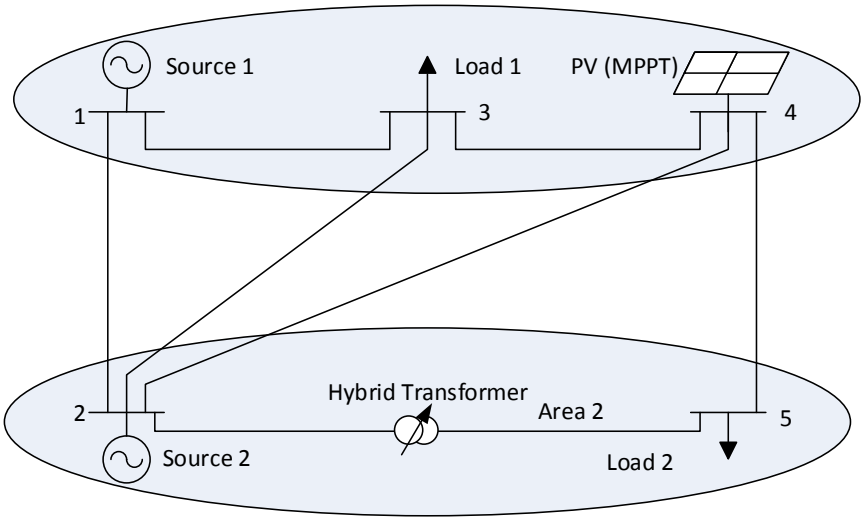

Figure 4.30 5-bus system with two areas

Consider a 5-bus system shown in Fig. 4.30. The system is divided into two areas each with a source and a load bus. Area 1 also has a community PV plant. The two sources have nonlinear droops embedded based on their production cost. The PV plant is assumed to function on a maximum power point tracking (MPPT) basis. The hybrid transformer is located on link 2-5.

In this particular system, the hybrid transformer has access to the loading level of its own link and the current frequency of the system. While, the current injections from the sources are not accessible to the unit, historical dispatch points for the given frequency can be made available to the hybrid transformer unit. This allows a local estimate of the power injections from sources 1 and 2 to be extrapolated locally at the hybrid transformer. The three variables in this system are the loading levels at buses 3 and 5 as well as the PV plants injection. The load being supplied by sources at buses 1 and 2 may be distributed between buses 3 and 5 in any combination. This information cannot be extracted from global variables. However, the PTDFs as well as HTFSs are based on the impedance characteristics of the network. These parameters are known and fixed unless the system changes. The next section presents a methodology to use this information to extrapolate the flows on other lines based on these known parameters.

4.6.1 Estimation of system flows

The example system presented in Fig. 4.30 is utilized to illustrate the methodology. In this system 5 key PTDF patterns for all lines need to be precalculated based on system impedances. The first transfer pattern T_1 is for a 1 MW transfer from source 1 to load 1. The second is a transfer pattern T_2 for a transfer of 1 MW from source 2 to load 2. The third

is T_3 for a transfer of 1 MW from bus 3 to bus 5. The fourth pattern is T_4 that implies a transfer of 1 MW from bus 4 to bus 3 that implies a 1 MW transfer from the PV plant to load 1. Finally, the fourth PTDF vector is for a 1 MW transfer between bus 4 and bus 5 which implies a transfer from the PV plant to load 2. The 5 transfer vectors for this 5 bus system are presented in (27a)-(27e). The index for the slack bus is removed form each of these vectors.

$$T_1 = [0 \; -1 \; 0 \; 0] \tag{27a}$$

$$T_2 = [1 \; 0 \; 0 \; -1] \tag{27b}$$

$$T_3 = [0 \; -1 \; 0 \; 1] \tag{27c}$$

$$T_4 = [0 \; -1 \; 1 \; 0] \tag{27d}$$

$$T_5 = [0 \; 0 \; 1 \; -1] \tag{27e}$$

The PTDFs for all lines for each of these transfer patterns can be precalculated. These PTDFs would indicate a sensitivity for the flow on each line for any of these transfer patterns. Since, PTDFs are a linear metric, the effect of two such transfers would simple be a summation of the PTDF vectors. PTDF vectors can defined for each of these transfer patterns. $PTDF_{T_m}^{n}$ is the notation used for the same where n indicates the line of interest and m stands for the transfer pattern of interest. T_1 and T_2 stand for a transfer from the source to load within their respective control areas. However, it is possible that the net load may be unevenly distributed between buses 3 and 5. T_3stands for a fictitious transfer between the two loads. The effect of this is the same as shifting a MW of load from bus 3 to 5. Similarly, T_4 and T_5 imply a portion of the load that is not reflected in the frequency and is

being supplied by the PV plant. HTFSs are also precalculated. Based on these sensitivities, a 2-step process is proposed to allow the power flow patterns to be estimated.

4.6.1.1 Assumption of base case loading in control areas

The initial assumption that the hybrid transformer algorithm locally makes is to assume that source 1 is supplying all it's power to load 1 and vice versa. Here G_1 and G_2 are the outputs of sources 1 and 2 while L_1 and L_2 represent the load at buses 3 and 5 respectively. The PTDFs computed above for patterns T_1 and T_2 should corroborate the system flow on the hybrid transformers own link if this is the case. Thus, the hybrid transformer unit locally computes, the theoretical line flow over its own link based on these expected load values L_{1exp} and L_{2exp} based on the formulation (28).

$$Expected\ flow_{25} = PTFD_{T_1}^{25}.L_{1exp} + PTFD_{T_2}^{25}.L_{2exp} \quad (28)$$

However, if the expected flow over its own link doesn't match the $Actual\ flow_{25}$ on its own link it is the effect of a combination of transfers T_3-T_5.

4.6.1.2 Estimation of worst-case system flows based on error

Uneven loading between buses 3 and 5 as well as unknown PV injections may result in $Actual\ flow_{25} \neq Expected\ flows_{25}$. Multiple solutions may exist where the line loading across the link 25 matches the $Actual\ flow_{25}$ However, the function of the hybrid transformer in this self-stabilizing framework is to simply estimate the worst case line loading that could take place on the system and prevent it. Thus, it is possible to estimate the worst-case loading levels on the other links in the system by formulating a maximization problem based on T_3-T_5 and take remedial action.

Formulation (29) is a maximization problem that can be used to estimate the worst possible loading on any line 'n' across the system, subject to certain constraints. The decision variables are PV_{L1}, PV_{L2} and ΔL_1. The decision variables PV_{L1} and PV_{L2} imply any load at bus 3 and bus 5 that may be supplied by some power from the PV plant at bus 4. Similarly, ΔL_1 aims to capture the spatial variation in the loading level between bus3 and 5 for the same total load being supplied by sources 1 and 2.

$$Max\ \{PTDF^n_{T3}.\Delta L_1 + PTDF^n_{T4}.PV_{L1} + PTDF^n_{T5}.PV_{L2}\} \quad (29)$$

Subject to,

$$PV_{L1} + PV_{L2} \leq 1.05.PV_{forecast}(t) \quad (29a)$$

$$-L_{2exp} \leq \Delta L_1 \leq L_{1exp} \quad (29b)$$

$$PTDF^{25}_{T3}.\Delta L_1 + PTDF^{25}_{T4}.PV_{L1} + PTDF^{25}_{T5}.PV_{L2} = Expected\ flow_{25} - Actual\ flow_{25} \quad (29c)$$

$$0 \leq PV_{L1} \leq 1.05.PV_{forecast}(t) \quad (29d)$$

$$0 \leq PV_{L2} \leq 1.05.PV_{forecast}(t) \quad (29e)$$

Constraint (29c) imposes the known quantity which is the difference between the expected and actual flow as an effect of a combination of T_3-T_5. Constraint (29a), (29d) and (29e) limit the expected total PV injection to 5% above the expected forecast. Similarly, $\Delta L_1$is bound in (29b) to ensure that the spatial loading is limited to that which is feasible. This implies the maximum load that can be shifted from bus 3 to bus 5 to capture the spatial loading is limited to the loading seen by sources 1 and 2. The lower bound on

the variables $PV_{L1}$and PV_{L2} is kept at zero to capture the worst case loading condition for each respective line in case the PV output completely drops. Thus, using a relatively simple formulation, the worst-case loading for each line 'n' can be computed to achieve the load flow that is being seen by the hybrid transformer.

In case that the estimates show that a line across the system may be loaded heavily, the hybrid transformer then uses the precomputed HTFSs to change its own flow to remedy this situation. In the eventuality, that the hybrid transformer is unable to relieve load on the given line without overloading another based on its estimates, the hybrid transformer sends an alert to the operator.

4.7 Discussion and Contributions

The approaches highlighted above present a set of principles for all connected agents to participate in a transactive platform. The real-time pricing mechanism proposed in this section relies on one global rule while allowing local entities to change their control principles based on personal objectives and on ensuring that the grid operates as an ecosystem of UMNs. The price allows numerous phenomena like resource constraints and system loading levels to be expressed in the form of a locally derived global price. Rather than designing an architecture that focuses on generation following loads, the architecture implements demand response, autonomous economic dispatch and frequency regulation into one common and integrated control structure which ensures that loads and sources can interact better. All this is achieved without any low latency peer-to-peer communication or any communication with centralized supervisory control schemes. The architecture also paves the way for deploying very low-cost grid microgrid structures with a PV dominant

resource mix in developing economies. The system framework remains extremely lightweight, highly resilient, dependent on edge intelligence and resilient to communication failures making it ideal for these environments.

This chapter highlighted the nuances of such a decentralized architecture. A robust set of rules and mechanisms for operating such systems was highlighted in this chapter. A methodology to operate sources in the form of local nonlinear droops was proposed. In addition to this a methodology to exercise better load sharing between dispatched sources in regulated market structures was also showcased. The results showed the ability to enable economic dispatch for multiple sources without any central coordination. The proposed methodology will be a key feature embedded in UMNs responsible for controlling sources.

Demand flexibility is a key feature of this framework. Modelling consumer behavior is key to extracting all the possible flexibility from the system. An approach towards modelling nuances of consumer behavior was proposed in this chapter. A robust algorithm was then proposed to allow consumers to react to varying global prices in the transactive framework while ensuring that their local objectives and constraints were satisfied. The ability to leverage demand flexibility under varying resource availabilities was shown through simulation studies. The developed algorithm will be deployed in this multi-agent system at every node and be incorporated into the UMNs.

The role of hybrid transformers in managing the physical flows across such decentralized market structures was then highlighted. Using global signals like frequency and the local flows across the hybrid transformer link, an estimate can be developed for system flows across the grid structure. The hybrid transformer then attempts to calculate a

worst-case overloading pattern and attempts to alleviate it. The system operator may issue signals to the hybrid transformer sporadically to issue set points based on centralized computations. However, the device can continue operation based on historical knowledge of the system.

Analyzing such a complex multi-agent system over long periods of time while capturing physical and transactive dynamics is often challenging. A simulation framework is presented in the next chapter to address the same. The framework is designed to understand the behavior of both the physical and transactive aspects to ensure the efficacy of this integrated decentralized physical and transactive architecture.

CHAPTER 5. SIMULATION PLATFORM FOR MASSIVELY DISTRIBUTED MULTI-AGENT SYSTEMS

The solutions presented in this work solve a range of issues from a transactive and physical perspective. However, it is computationally challenging to simulate the effect of a massively distributed multi-agent system with many nodes reacting in different ways. Since, frequency is a key parameter in the proposed real-time transactive framework it is essential to capture some dynamics on a continuous basis. Thus, a design of a novel simulation platform was required for the same. Similarly, each agent only observes local signals and frequency to decide their local behavior. All these agents decide their next control action in parallel. Consequently, the result of these actions is a change in frequency. Another key aspect is the role of hybrid transformers. Hybrid transformers have tremendous value when the flows in the system are known, these devices will have very little access to global system flows in this decentralized architecture. However, these devices are capable of exercising control based on some global variables and historical knowledge of system parameters as suggested in Chapter 4 making them another independent agent in this multi-agent system. This section proposes a simulation scheme that can enable the analysis of such a distributed multi-agent architecture.

5.1 Simulation platform for long-term studies involving frequency dynamics

This section highlights a methodology developed to capture frequency dynamics in the this transactive framework to allow the efficacy of the platform to be tested for multi-agent systems. The platform is based on the quasi-steady state (QSS) approximation that

is typically used to analyze long term voltage and frequency dynamics. The distinguishing factor however, is that the platform proposed here also captures the multi-agent response of the system based on those frequency dynamics. A brief overview of the QSS method is presented here. Then an overview of the implementation to couple the frequency domain and multi-agent network is presented next.

5.1.1 Power System Equation Types and Characteristics

For the purpose of stability studies, the power system equations cane be widely divided into the three types [139] shown in (30), (31) and (32).

$$0 = g(x, y, z) \tag{30}$$

$$\dot{x} = f(x, y, z) \tag{31}$$

$$z(t_{k+1}) = h(x, y, z(t_k)) \tag{32}$$

Where,

x – state terms which evolve with differential equations

y – linear terms in balance equations or algebraic variables

z – states of components with discrete switching actions

Here, the equation (30) denotes the network equations that enforce constraints about power balance at buses or Kirchhoff's current law (KCL). Equation (31) comprises of the differential equations that determine the dynamics for state variables like frequency or voltage. These embed all the dynamics associated governors, turbines and automatic

voltage regulators. The equations (32) capture the dynamics of components with discrete switching actions like OLTCs or capacitor banks.

The QSS technique focuses on decomposing the state variables x into different categories based on the speed of their evolution. For instance, the dynamics governing frequency are much slower than those governing voltage. For long term analyses based off frequency only the dynamics of the slow components need to be captured. The QSS technique breaks down the vector x into a fast component x_1 and a slow component x_2. The fast component can then be assumed to be infinitely fast and become a discrete switching variable while the differential equations governing the slow variables are preserved. Thus, the new power system equations (33)-(36) can be summarized as follows.

$$0 = g(x_1, x_2, y, z) \tag{33}$$

$$0 = f_1(x_1, x_2, y, z) \tag{34}$$

$$\dot{x_2} = f_2(x_1, x_2, y, z) \tag{35}$$

$$z(t_{k+1}) = h(x_1, x_2, y, z) \tag{36}$$

The equations f_1 and f_2 represent the fast and slow parts of the state equations. Using this theory, a simulator design is proposed in the next section.

5.1.2 QSS simulator with frequency dynamics

For the research presented in this document, the frequency dynamics are of interest. Thus, the entire mechanical dynamics of a governor-turbine-generator (GTG) need to be captured. However, the rest of the system is assumed to be infinitely fast in accordance with the QSS framework.

A full model of the network can be constructed in OpenDSS. OpenDSS can programmatically solve a static load flow at each instant in time. In this instance two sources are modelled into the OpenDSS framework as voltage sources. The full dynamic model including the GTG dynamics is modelled in Simulink. Both the governors embed the nonlinear droops that are a result of their own local bids as well as the price frequency curve. Automatic voltage control (AVR) and exciter dynamics are neglected, and the voltage is assumed to be held by both sources at 1p.u. Thus, for the proposed framework, all dynamic equations such as governor reactions, turbine dynamics as well as the effect of generator masses on frequency dynamics are maintained and correspond to x_2 from the previous discussion. All the network level dynamics such as travelling waves, voltage transients are assumed to be infinitely fast from timestep to timestep and are updated by solving a static load flow. These states correspond to the variables x_1 in the previous simulation.

The simulation scheme then goes as follows and is represented in Fig. 5.1. A static load flow is first run in the OpenDSS solver. The loading level on each source is then retrieved. This loading level is then updated in the dynamic simulator in Simulink and the resultant frequency dynamics are simulated for one timestep h. The load is picked up by both sources in accordance to their locally synthesized droop curves.

The new loading level for both sources is then converter to rotor angles that the voltage sources in the static OpenDSS domain must follow. Similarly, the resultant frequency from the dynamic simulation is sent to all the independent consumer agents in the MATLAB script to curtail, consume or shift load. The resultant control action is then

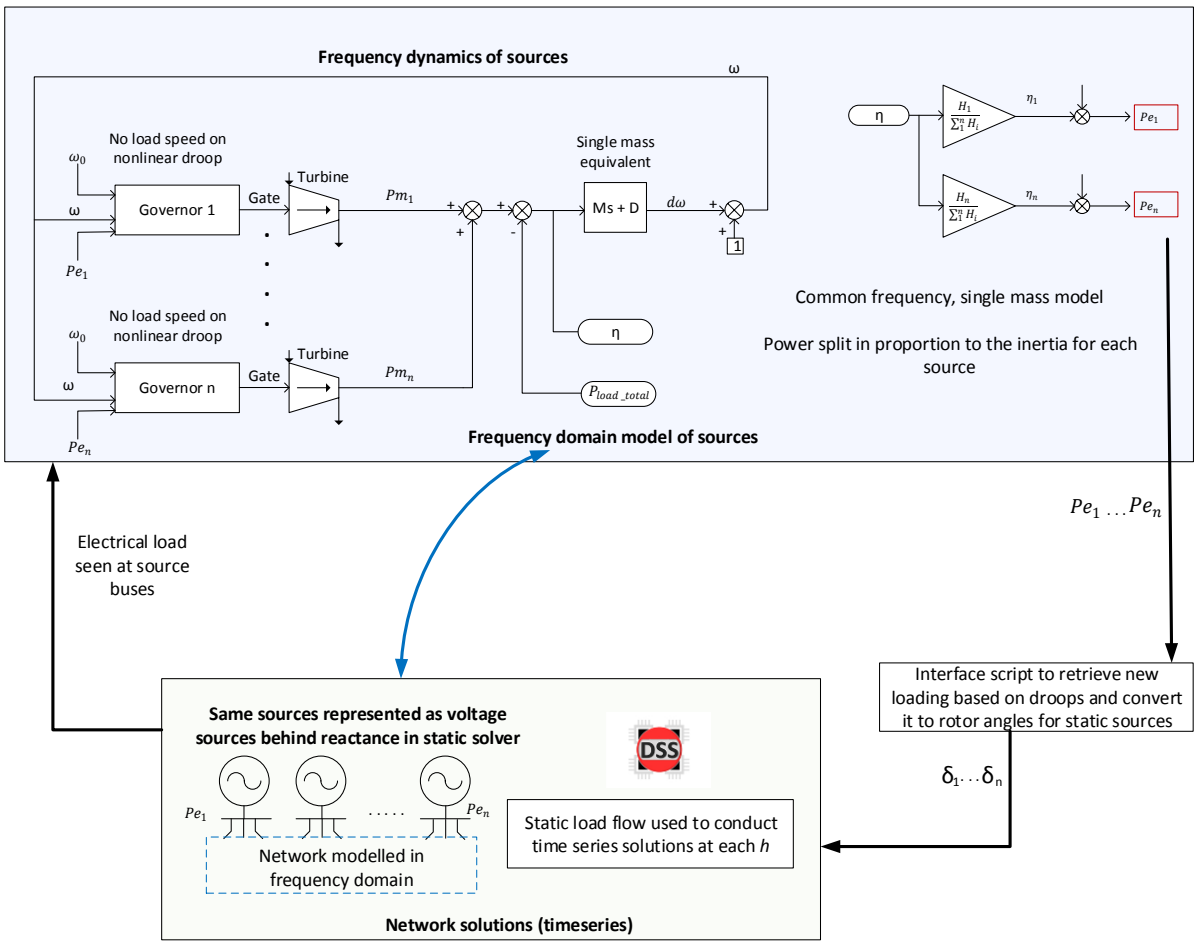

Figure 5.1 Simulation Scheme based on QSS approach

reflected in the OpenDSS domain in the next time step and the whole loop is repeated for the duration of the simulation. By reducing the number of dynamics that have to be simulated, the simulation time can be driven down, and the complexity can be lowered. Further, by allowing a script that simulates the reaction of all UMNs in response to the frequency to be inserted, the effect of the multi-agent framework in response to the dynamic can be analyzed. Previous studies have benchmarked the performance of such a QSS framework in terms of analyzing long term frequencies and the error observed is quite minimal [140]. Thus, a robust method to analyze network dynamics of multi-agent systems while capturing the continuous frequency dynamics is proposed here.

5.2 Multi-agent System Simulation Scheme

A complex architecture with numerous intelligent agents is realized when the transactive and physical elements proposed above are coupled. This needs to be effectively captured in simulation scheme to capture the effect. A simulation scheme is proposed here to achieve the same. The simulation scheme has numerous stages that use serial or parallel computing. Fig. 5.2 shows an overview of the same. The execution begins with initializing all connected agents. All agents are initialized with the global price-frequency mapping as well as some price forecasts. These agents are initialized as independent scripts in MATLAB with their local preferences. For clusters of consumers this implies the nuance such as consumer discomfort, sensitivity to forecast errors as well as personal priority levels for load blocks. This information is local and unique to each agent. Similarly, sources can synthesize their own local bids and production cost preferences into nonlinear droops based on the global characteristic. Hybrid transformers across the system also receive the same global data as well as any updates to topology since the previous market clearing cycle. Thus, all agent scripts in MATLAB initialize their own frameworks based on the global parameter.

These agents then show up as loads, voltage sources for generators and series voltage sources for hybrid transformers in the static OpenDSS framework. OpenDSS is used to create snapshots of static power flows. A static load flow solution is then run in OpenDSS. The physical aspects of the network in terms of flows as well as voltages are analyzed using

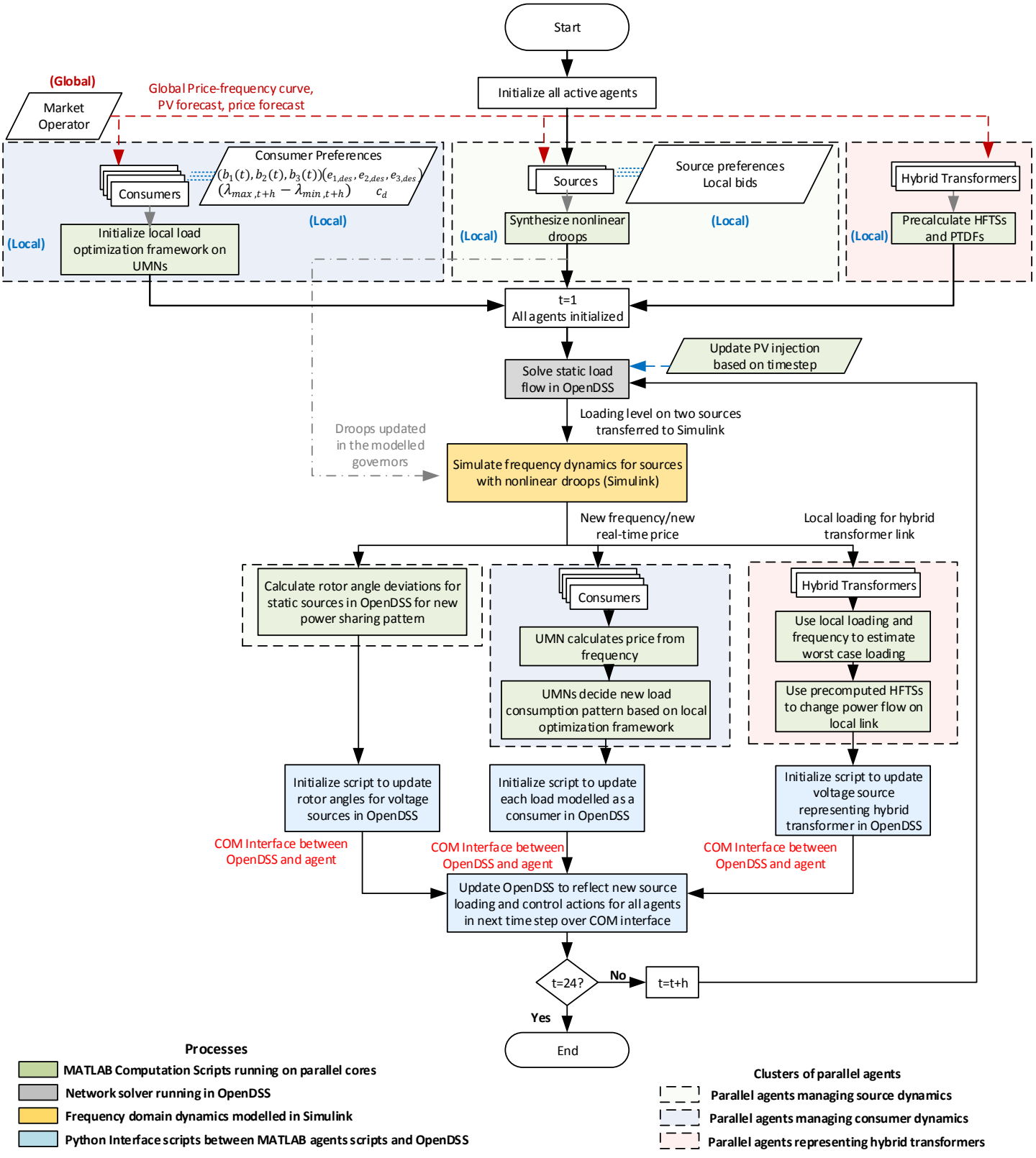

Figure 5.2 Multi-agent simulation scheme to analyze the effects of the proposed transactive and physical architecture

this solver. From the OpenDSS load flow, the loading levels of the two sources being represented as voltage sources is retrieved. The total load is then retrieved over a COM interface from OpenDSS and used as an initialization parameter for the frequency domain simulation in Simulink. The model in Simulink contains the detailed GTG models with all their parameters. The continuous simulation with frequency dynamics is run for a timestep and paused. The new distribution of the load between two sources as well as the new frequency is retrieved at the end of this time step. This information is fed to all the independent scripts representing the consumers and hybrid transformers in the system. In addition, the nonlinear droops ensure that the load is shared in a certain pattern. To capture, the same the required power angles for the static simulation in OpenDSS are calculated. This ensures that the voltage sources representing the two sources share load in the same pattern that the dynamics dictate.

Locally, the frequency and local parameters are used by each agent to compute their action over the next time step. This could mean decisions about curtailing, consuming or load rescheduling for consumers or changes in control actions for the hybrid transformers. Each agent script then runs in parallel. Multiple computational cores have been used to parallelly allow algorithms on each agent to be executed. Parallel execution ensures that the simulation time can be driven down. Each agent then initiates a python script that allows their next control action to be conveyed to the OpenDSS network over a COM interface. The execution loop is then repeated for the next time step. Thus, a scheme is realized where the physical flows and network dynamics are captured in OpenDSS, the frequency dynamics are simulated in Simulink, agent dynamics and computations are carried out in

MATLAB and the interfaces between the physical and frequency domain are executed in Python.

The notation for clustering as well as the different platforms used in each time step are conveyed in the legend in Fig. 5.2. The control flow for the executing the entire flow chart and calling respective platforms through scripts is managed in MATLAB. This creates a powerful platform to simulate such multi-agent systems while using parallel resources effectively.

5.3 Contributions

The architecture and control solutions presented in this research involve numerous agents exercising control based on some global signals. However, the challenge with analyzing the impact and efficacy of such frameworks is the computational complexity. Different agents respond to changing conditions based on the local and global preferences.

A robust scheme was developed to enable modelling of such systems. In order to leverage different platforms, the scheme utilizes different existing platforms and packages to analyze steady state power flow and frequency dynamics. Each agent is also modelled in with varying local preferences and their suitable UMN algorithms. Parallel processing is utilized to allow the reaction of every agent to be calculated in a computationally efficient manner. This scheme will be utilized as the platform to prove the efficacy of the proposed solutions as well as to analyze their role in this multiagent architecture.

CHAPTER 6. DECENTRALIZED INTEGRATED TRANSACTIVE AND PHYSICAL ARCHITECTURE

The proposed approaches present techniques to add flexibility to grid structures. The transactive framework proposed here is one that relies on edge intelligence to stabilize the system using global signals to signify market dynamics. This allows supply-demand imbalances to me stabilized through the transactive layer. Hybrid transformers add a significant amount of flexibility on physical grid structures to allow this transactive mechanism to be exercised. This section validates these mechanisms by presenting simulation studies to support the claim. The section also showcases the ability to use global and local signals to ensure that a resilient architecture is realized while effectively using edge intelligence.

The simulation test case is first presented. The case is modelled with nuances of all agents. The simulation scheme presented in Chapter 5 will be utilized. The setup is designed to showcase the integration of the physical and transactive solutions presented in this research. The test bed also captures the multi-agent and multi-objective nature of this system.

6.1 Multi-Agent Test Bed

Fig. 6.1 shows a schematic of the test bed. The test bed consists of 2 sources (1.344 MW and 2.256 MW) and a PV plant (2.5 MW). There are two communities of consumers modelled into the system. A hybrid transformer is placed on the link 2-5 as well and will

operate on the estimation principles highlighted in Section 4.5.1. Different aspects of the agents are specified in the next few subsections.

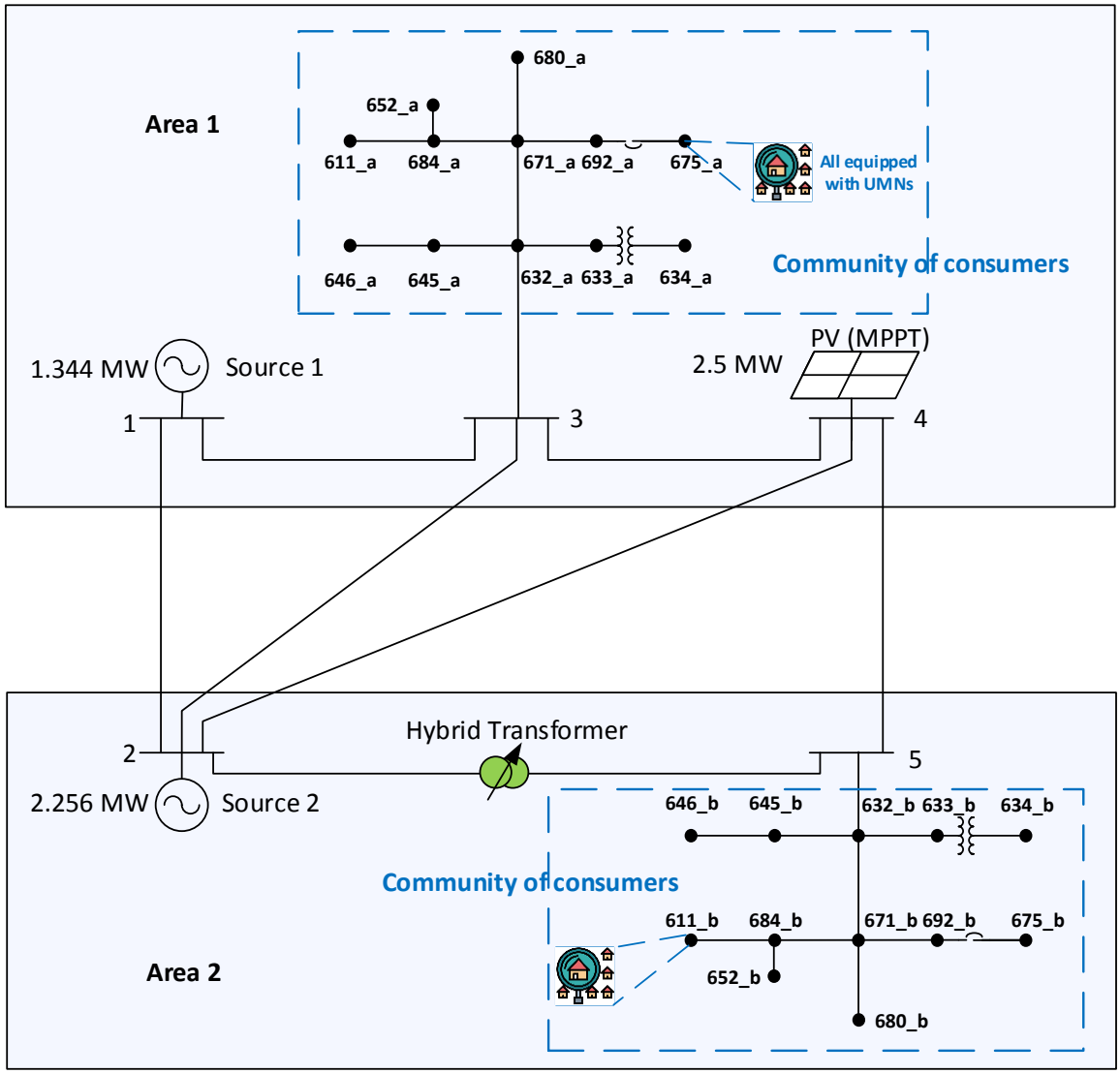

Figure 6.1 Multi-agent test bed

6.1.1 Source UMN Agents

Two sources are modelled into the system at buses 1 and 2. These units represent the areas 1 and 2 being represented. Unit 1 and 2 are sized at 1.344 MWs and 2.256 MWs respectively. The local bids for the two sources are those shown in Fig 4.4 and are scaled

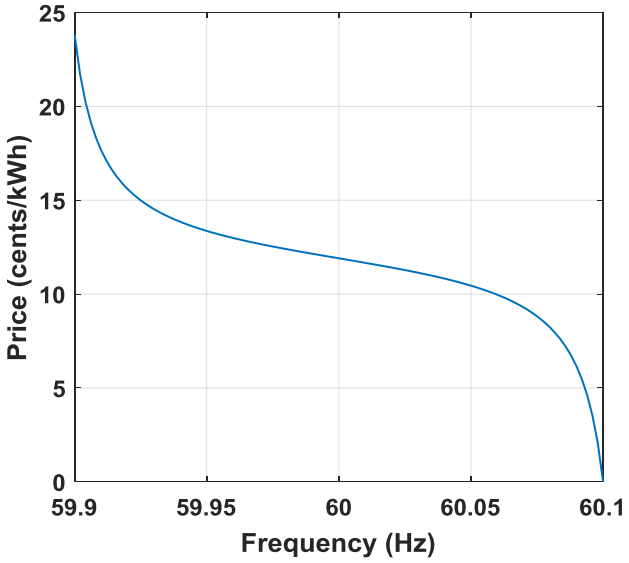

Figure 6.2 Price-frequency characteristic deployed on test bed

down by a factor of 10 for this system. In accordance with the approach highlighted in Section 4.3.2, the sources possess local information about their bids as well as the global price frequency curve. The price frequency curve utilized for the studies presented in this section is shown in Fig. 6.2.

The modelled PV output pattern in shown in Fig. 6.3. The PV plant is modelled to function in MPPT mode. The two source bids are locally synthesized as nonlinear droops

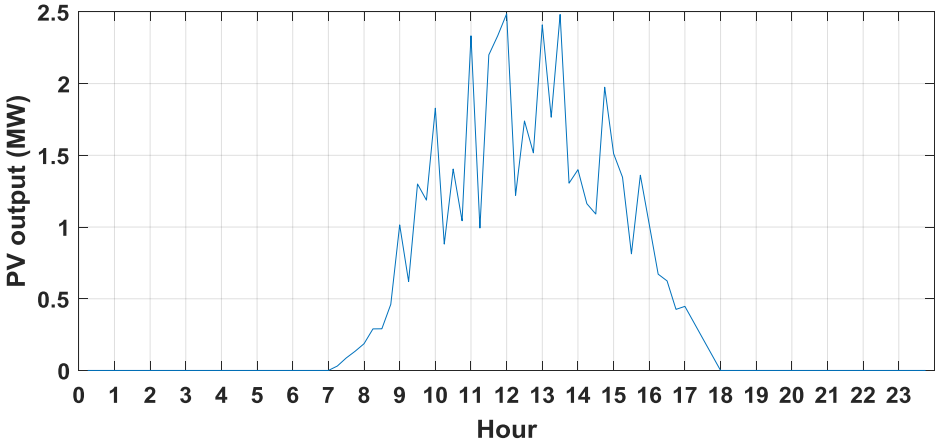

Figure 6.3 PV output pattern

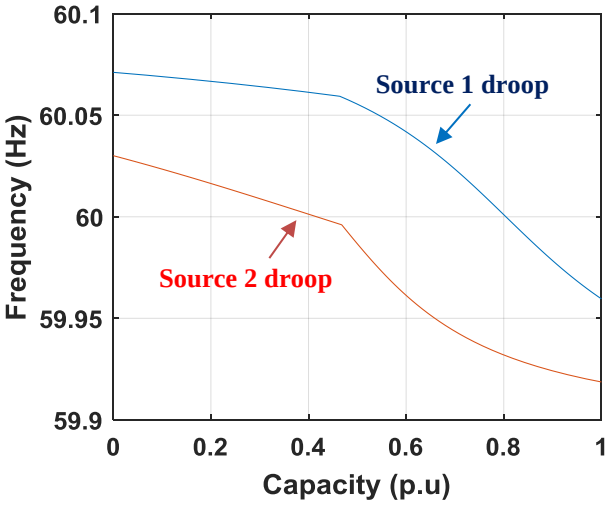

Figure 6.4 Locally synthesized nonlinear droops with global characteristic and local preferences

and are illustrated in Fig. 6.4. Thus, the frequency is a true reflection of the production cost of the dispatchable sources.

6.1.2 Consumer UMN Agents

The two communities modelled in at buses 3 and 5 and are represented by IEEE 13-bus feeders [141]. Each node on the IEEE 13-bus feeder is modelled as a cluster of consumers. The modelled consumers are a mix of residential, commercial and industrial profiles. Baseline profiles used for these consumers are those seen in [142] and shown in Fig. 6.5.

A total of 1111 unique agents including 754 residential, 60 commercial and 297 industrial consumers are modelled in and dispersed in these clusters. Some of these agents are duplicated to realize the baseline load curve shown in Fig 6.6. Each agent is assigned a random variation of benefits, breakdowns for the priority levels as well as a randomly

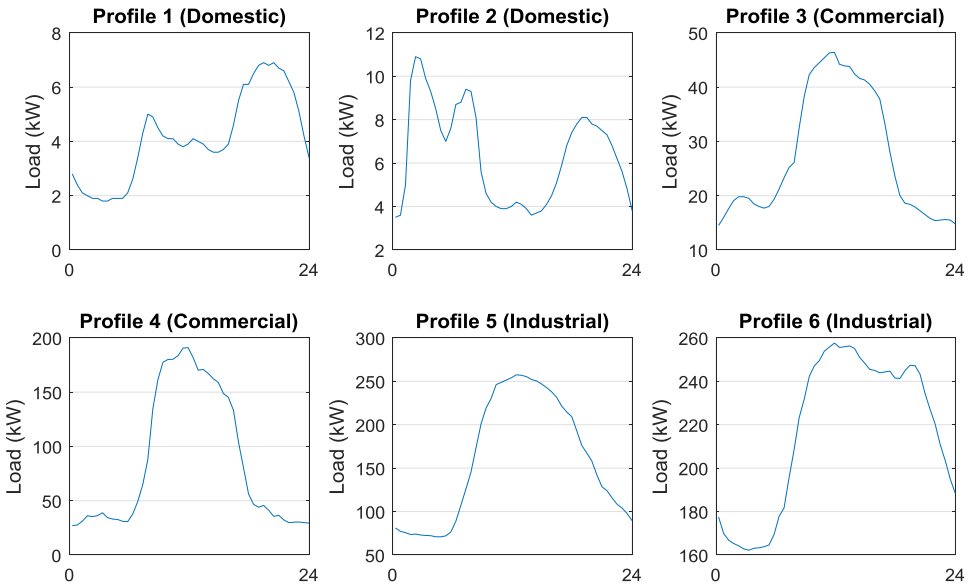

Figure 6.5 Baseline load profiles for modelled consumers

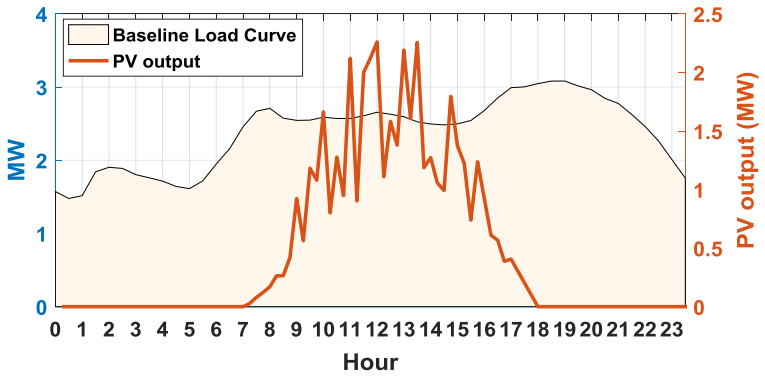

Figure 6.6 Baseline load curve and expected PV output

assigned cost of discomfort within certain bounds. Residential consumers have fewer critical loads and a lower discomfort cost while commercial and industrial agents may have a larger portion of their loads being critical and higher discomfort costs associated with rescheduling them.

Similarly, the ramp rate limits are tighter for large industrial consumers to avoid large load steps on the system. Table 4 shows the ranges used for these parameters for each

Table 4 Characteristics of the 1111 modelled agents

Profile	Type	Number of agents	c_d (Range)	b_2 (Range)	b_3 (Range)	Priority 1 loads (% of total load)	Priority 2 loads (% of total load)	r_d / r_u
Profile 1	Residential	454	0.1-0.2	11.4-11.8	10.5-10.6	25-35%	45-60%	0.08
Profile 2	Residential	300	0.45-0.75	11.4-12.1	10-11.4	20-25%	45-60%	0.1
Profile 3	Commercial	40	1-1.4	12.4-12.5	11.8-11.9	50-60%	25-40%	0.3
Profile 4	Commercial	20	0.7-1.02	12.25-12.35	11.8-11.85	30-60%	20-55%	0.3
Profile 5	Industrial	115	0.7-0.8	13-13.5	12-12.5	50-60%	28-40%	0.05
Profile 6	Industrial	182	1.2-1.5	13-14.5	12.9-13.05	50-70%	20-45%	0.02

profile and its associated agents. The ramp rate limits are enforced by the system operator to ensure that stability is ensured and are encoded into the UMNs as a rule for connection. The value for b_1 is fixed at 50 for all critical loads for the purposes of this simulation study. The priority 3 loads are any loads that remain after the priority 1 and 2 loads are decided. The personal time varying benefits are modelled for each consumer by randomly varying the value between the given ranges for b_1 and b_3. Thus, unique consumers with their individual preferences can be modelled. Each UMN has the global characteristic shown in Fig 6.2 built into it to derive price and is modelled with the algorithm presented in (26).

6.1.3 Hybrid Transformer UMN Agents

A hybrid transformer unit is modelled into the system on link 2-5. The architecture involves using historic data about the sources and their droops to extrapolate data about the system To this end, the nonlinear droops shown in Fig. 6.4 are made available to the hybrid transformer agent along with the $[B']$ matrix representing the system impedances. The subsequent section presents the results of a simulation study with all these agents.

6.2 Simulation Study

With all the parameters specified, a 24-hour simulation study is conducted using the simulation scheme presented in Section 5.2. As the PV output starts increasing throughout the day, the frequency starts increasing. The real-time price starts dropping as cheap PV energy starts flooding the test system as shown in Fig. 6.7. It is important to note that the real-time price reflects the resource mix as well as the loading level of the system. The dispatchable sources maintain economic dispatch in accordance with their merit order curves in an autonomous fashion.

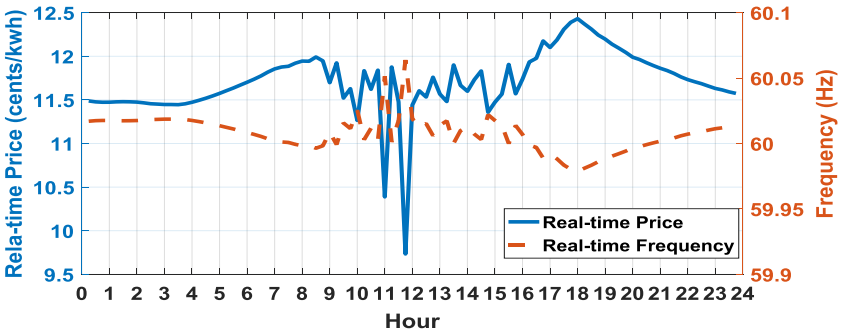

Figure 6.7 Real-time price variation in response to changing frequency

Each consumer UMN agent then reacts based on their local preferences as well as the global price that is derived locally. Fig. 6.8 shows the behavior of the 1111 agents across the system in response to changing prices. Each UMN updates its consumption pattern based on the real-time price. It is important to note how every agent takes a conservative approach in the beginning and becomes more opportunistic moving forward owing to the decreasing value of Γ. This is the desired behavior and a feature of the UMN consumer optimization framework detailed in Section 4.4.2. It is also seen in Fig. 6.8 that

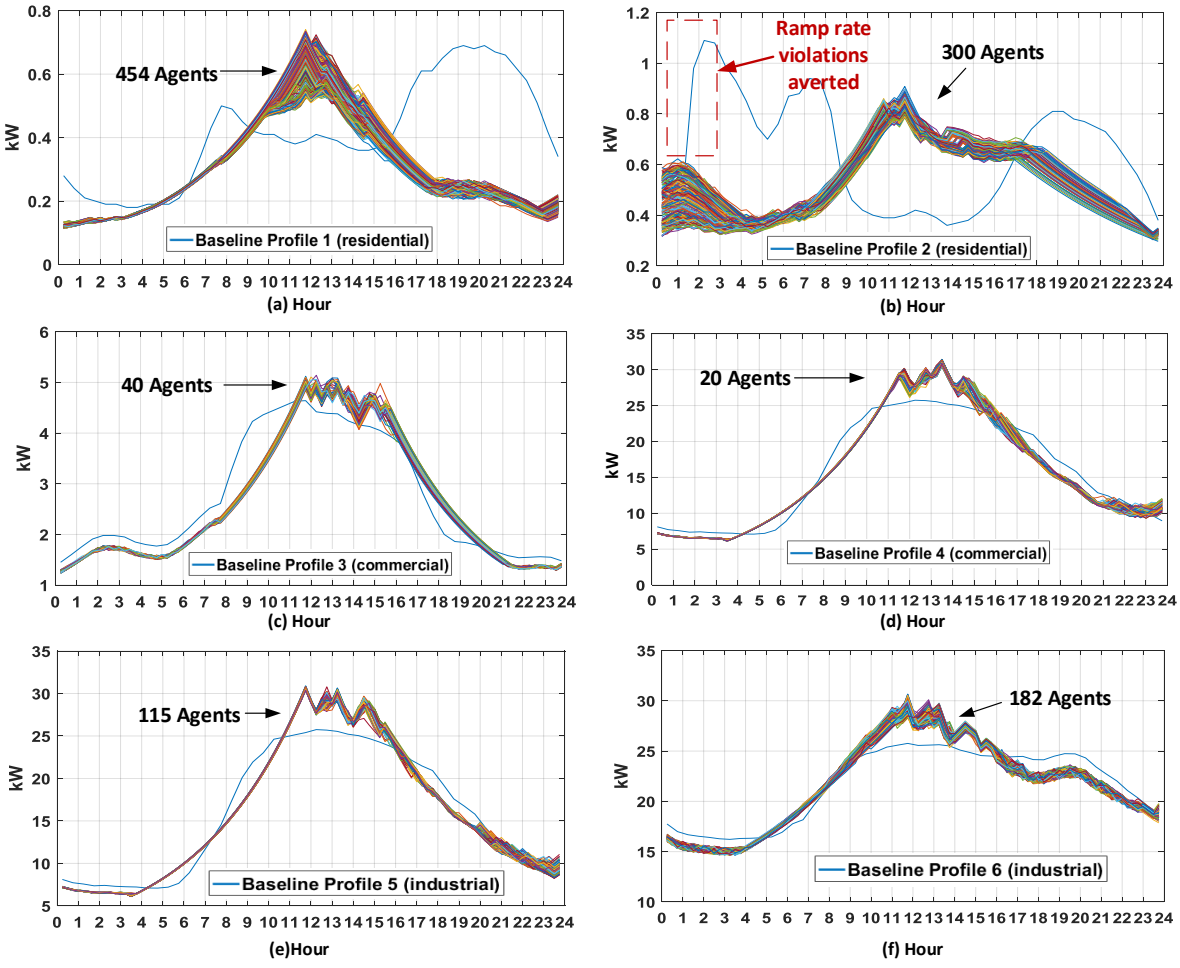

Figure 6.8 Behavior of 1111 consumers in response to real-time prices

the grid-friendly ramp rate constraints prevent erratic consumption behavior in consumers following Profile 2.

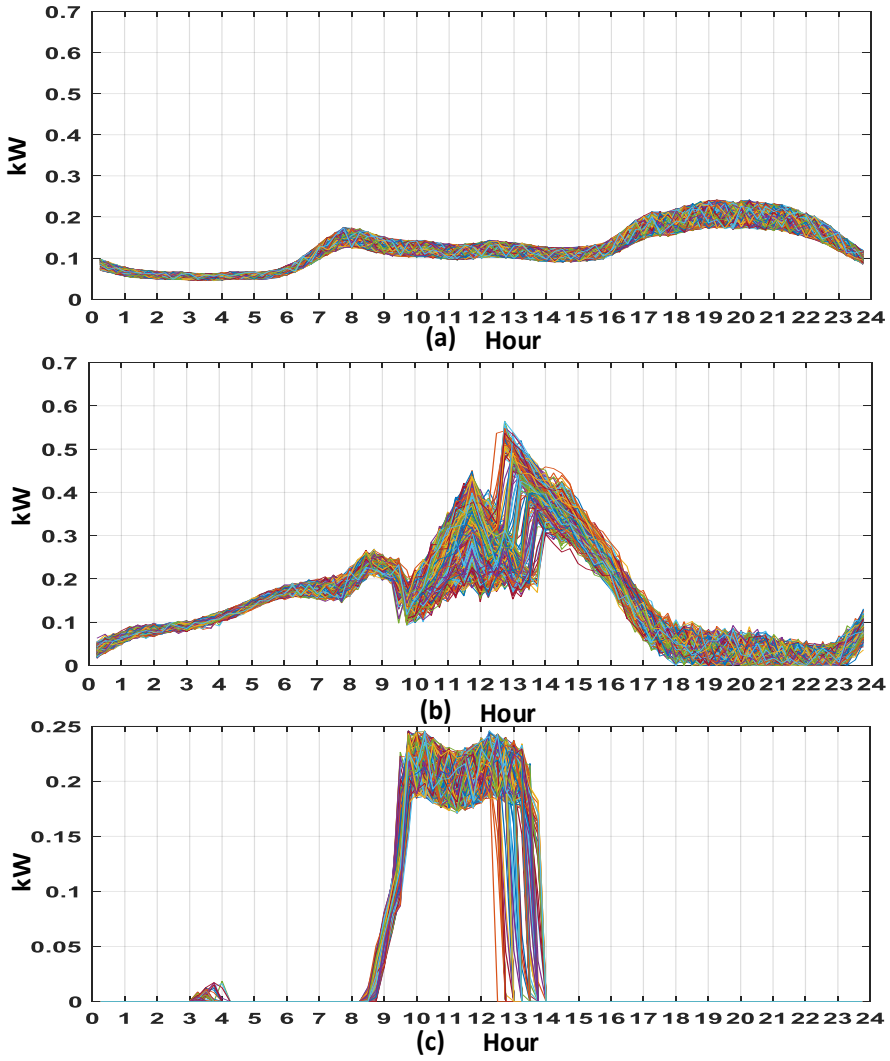

Figure 6.9 Consumption pattern for 454 agents (Profile 1) for (a) priority 1 (b) priority 2 and (c) priority 3 loads

Fig 6.9(a), (b) and (c) show the consumption within the 3 priority levels for 454 agents following Profile 1. While critical priority 1 loads are always consumed priority 2 loads are shifted as much as possible by each UMN while respecting each consumer's individual cost of discomfort. Similarly, it is seen that the lowest priority loads are

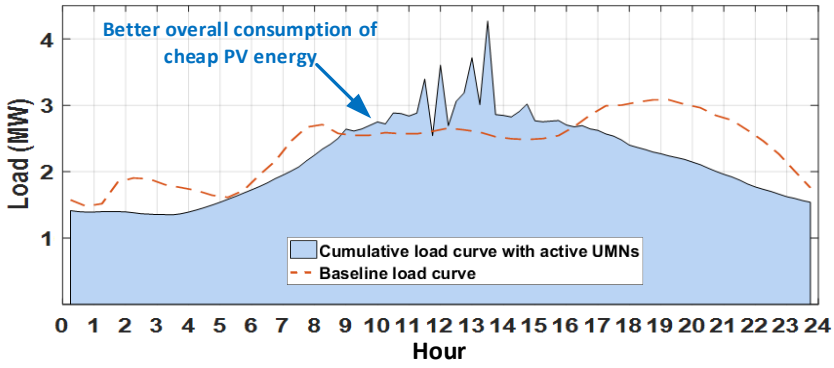

Figure 6.10 Load flexibility leveraged using edge intelligence to achieve better consumption patterns in PV dominant systems

exclusively consumed when energy is the cheapest. Thus, an approach is created that can enable the operation of communities in a resilient manner while reducing the dependence on real-time communications and coordination. Fig. 6.10 shows how the edge intelligence embedded in every UMN collectively alters the net load profile. All of this is achieved while ensuring that the constraints set by the consumer are respected. Rather than leverage supply flexibility to balance loads in a generation follows load paradigm an architecture is created where the supply availability is conveyed in real-time to leverage flexibility from both ends of the system. Moreover, when the price is higher in the event of resource scarcity, the price conveys this information ensuring that critical loads can be supplied while flexible loads are voluntary curtailed.

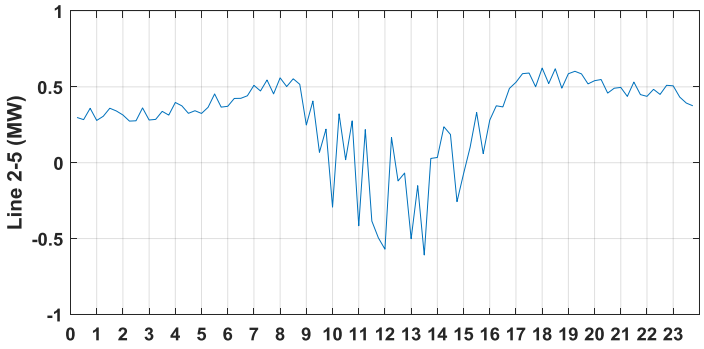

Figure 6.11 Controlled local power flow on 2-5 by hybrid transformer

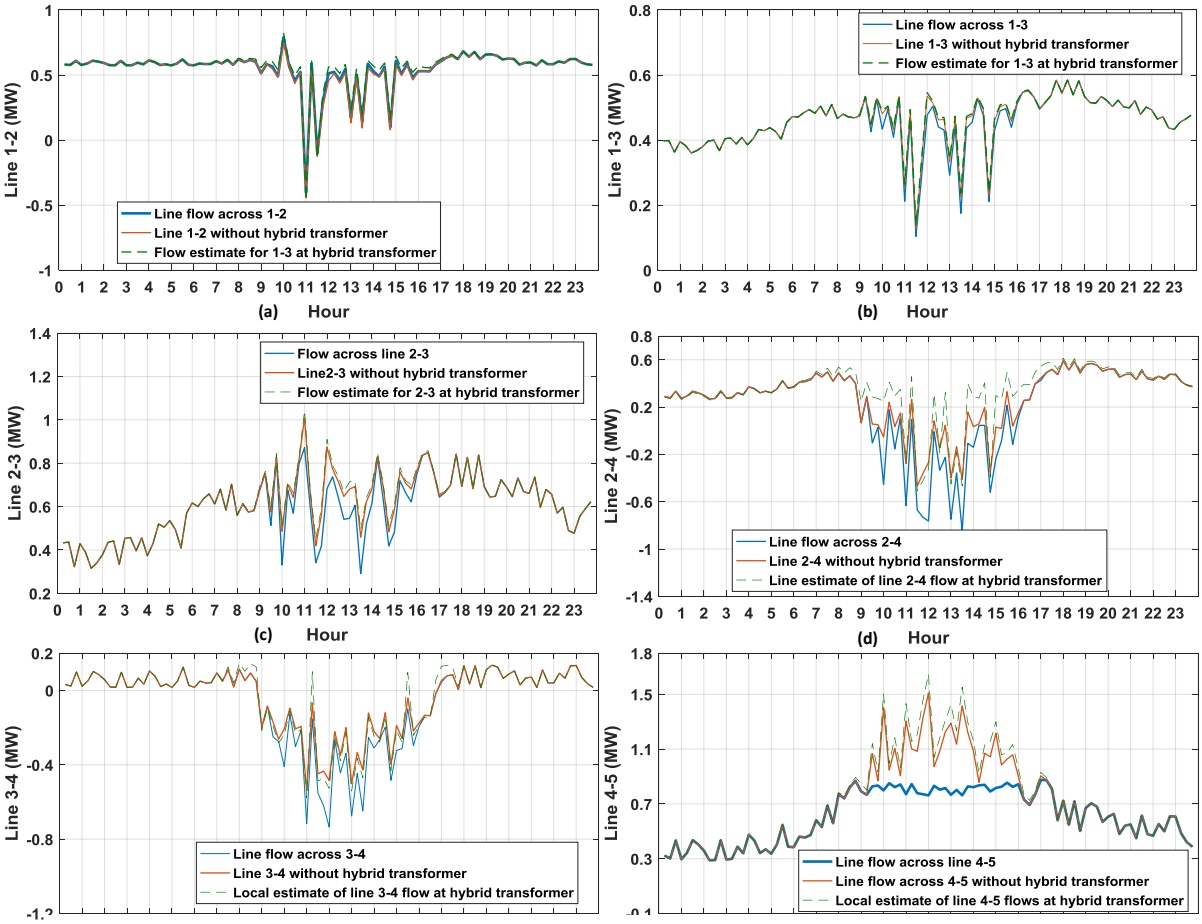

Figure 6.12 Line flows controlled by hybrid transformer to avoid congestion

In addition, as this transactive framework attempts to balance supply-demand imbalances in real-time, the power flow patterns vary significantly over the test case. The hybrid transformer modelled in uses the frequency and local line flow to estimate global flows. All lines across the network are assumed to have a capacity of 1 MW. Fig. 6.11 shows the power flow being controlled on link 2-5 in this test system. The hybrid transformer makes local decisions based on global estimates.

Fig. 6.12 shows the actual line flows as well as the hybrid transformer estimates of line flows. The estimates are locally derived using local line flow and frequency with an estimate of the amount of PV energy flooding the system. Line flows are shown to be

positive or negative depending on the flow direction across the line. The figure also shows the passive flows that would have occurred without a hybrid transformer unit on line 2-5. It is seen in the same figure that the hybrid transformer estimates a possible congestion pattern on line 4-5 and diverts power based on its own HTFSs. While, hybrid transformers show great potential, there are certain extreme scenarios where the solution's efficacy is limited. An example of such a scenario is presented in Appendix B.

Thus, a self-stabilizing physical grid is achieved. A grid architecture is achieved where a robust transactive mechanism allows supply-demand balances to be met in real-time without any communication while ensuring that all physical grid constraints are met.

CHAPTER 7. CONCLUSIONS, CONTRIBUTIONS AND FUTURE WORK

7.1 Conclusions

Future grid architectures are bound to be ones characterized by huge amounts of PV due to lower LCOEs as well as federal mandates and incentives associated with grid independence. Distributed ownership of assets makes coordination of such grid structures extremely challenging. Physical aspects such as volatility and congestion will become commonplace in such structures. Supply-demand imbalances are challenging to stabilize in such milt-agent grid structures Moreover, today's transactive framework lacks scalability to accommodate millions of active agents with varying personal objectives and transactive goals. Reliance on continuous and synchronous communications for operation also compromises the resiliency of the system as a whole. Thus, a new architecture that can leverage more flexibility on both the transactive and physical sides of the grid is the need of the hour.

The work presented in this research attempts to create a robust transactive framework to allow supply-demand balances to be met in real-time while leveraging flexibility from all connected agents in the system. This creates an ecosystem of nodes that balance local objectives while actively contributing to global goals. The architecture is designed around utilizing edge intelligence without relying on continuous communication and computations at central entities. By using global signals effectively, the architecture eliminates the need for low latency communication and makes the system highly robust and resilient. The

architecture shows enormous value in sustaining operations in periods of lower resource availability while encouraging consumption in situations with resource surplus. Rather than designing an architecture that focuses on generation following loads, the architecture implements demand response and autonomous economic dispatch into one common and integrated control structure. A completely decentralized operational and market architecture is thus achieved.

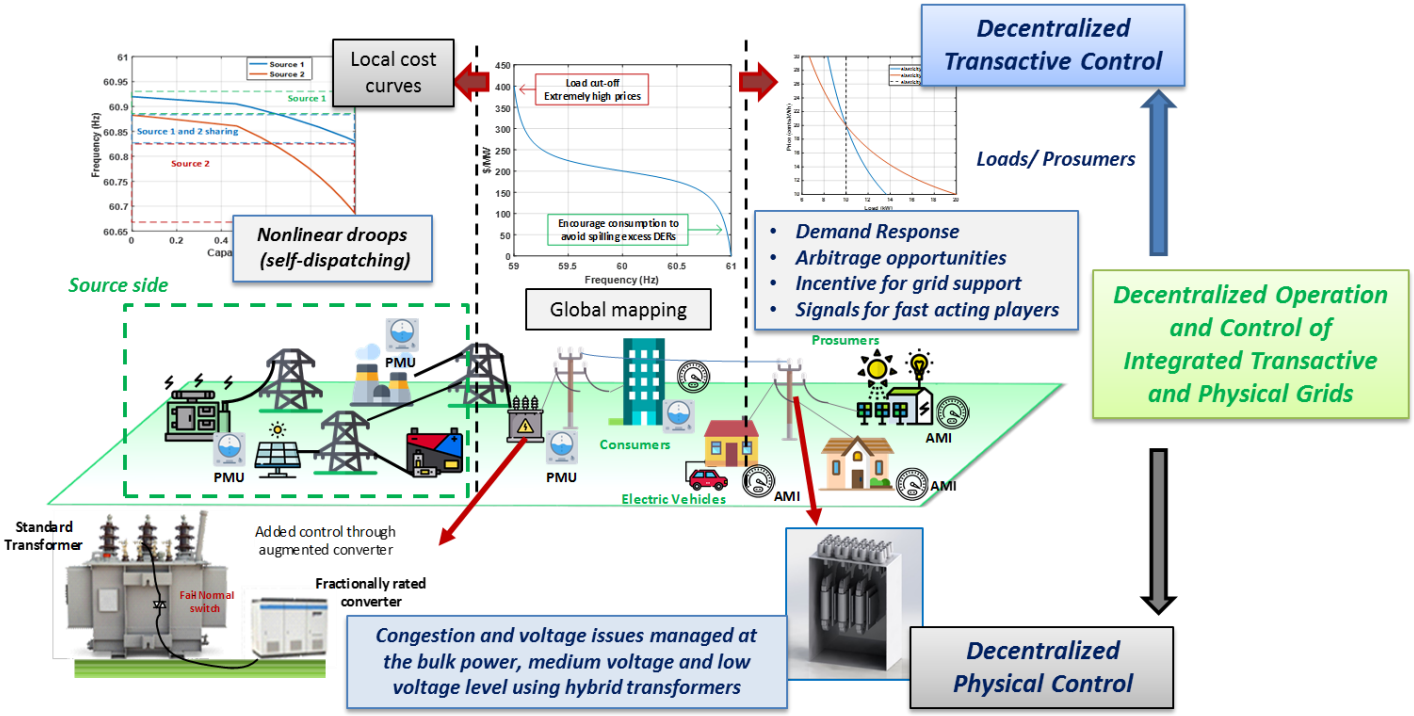

Figure 7.1 Decentralized Integrated Physical and Transactive Architecture

A system based on transactive principles is often challenging to manage from a perspective of managing physical constraints. Dynamic control on the grid is becoming increasingly necessary to handle the fast volatility introduced by DERs. Hybrid transformers are proposed in this research as an elegant solution to achieve high amounts

of flexibility in a cost-effective fashion. The approach shows enormous resiliency compared to other FACTS based counterparts. Precise and dynamic control over voltages, power flows and impedances across any given network. The devices show merit in addressing congestion related issues and maximize efficient usage of transmission capacity. Fig. 7.1 shows a picture of the framework when it's integrated. Thus, a decentralized integrated transactive and physical control architecture for such grid structures can be realized.

7.2 Contributions

7.2.1 Analysis of hybrid transformers as an effective grid control tool

System operators utilize source controls and dispatch procedures to control flows across the grid. This is going to be extremely challenging in future grids with a large number of active agents with varying objectives. Source side controls also affect the economics of generation. Distributed hardware devices like hybrid transformer can affect changes in power flows by making traditionally passive meshed networks active.

The efficacy of the hybrid transformer approach as a grid control tool was analyzed in this work. The system level impacts of this approach were also analyzed to evaluate the value of power flow control and voltage management. Further some metrics were developed to allow hybrid transformers to be integrated with the proposed decentralized transactive framework. This work has enabled one DOE report, one NEETRAC report and two conference publications.

7.2.2 Novel Decentralized Transactive Architecture

Managing supply-demand imbalances in geographically dispersed, DER-heavy multi-agent systems is extremely challenging using centralized management approaches. Moreover, the reliance on low-latency communications and complex computations could make the system vulnerable during failure modes. Yet, the ability to operate critical loads operation based on locally available sources is extremely valuable.

In order to enable such a paradigm, a novel decentralized transactive architecture was proposed. The architecture relies on global signals to manage the transactions across the system. Each connected agent controls their own consumption, dispatch or rescheduling decisions based on global frequency. The framework enables the architecture to become an ecosystem with millions of active agents. Further, the control principles remain fractal and agnostic to topology. The resiliency of this approach as well as the scalability was shown in this work. The architecture shows tremendous value in terms of operating grid structures with high penetration of volatile resource. Local control methodologies for sources and consumers in such systems were developed in this work. These algorithms become key elements of the local intelligence and allow such an architecture to be exercised. This work has enabled two journal publications and three conference publications.

7.2.3 Simulation engine to analyse multi-agent decentralized architectures

A large part of this work was developing tools to understand the effect of edge intelligence on grid structures. A novel simulation engine was developed using numerous packages to allow rigorous analysis of such systems. The tool allowed the effects of agents

to be captured on physical grid flows while providing a platform to model individual agents.

7.3 Future Work

In this work a novel mechanism of managing PV dominant grid structures is presented. There are still some concepts that could be explored further to prove the efficacy of this approach.

7.3.1 Quantification of Stability

While, the architecture proposed above does show value in managing real-time supply-demand imbalances as well as ways to address volatility, it is quite challenging to quantify the stability for such massively distributed multi-agent frameworks. Formulations that can identify modes of potential instability in such systems need to be quantified. These metrics then need to be translated to robust rules that would apply to all connected nodes.

7.3.2 Policy, Regulation and Role of the System Operator

The architecture highlighted above allows transactions between different entities without requiring any central coordination entity. However, a system operator is still essential to ensuring that the network is maintained and serviced. The grid-as-a-service paradigm seems to be a logical application. Grid operators could operate as a co-op while simply charging a service fee to connected agents. Correct regulations and policies for such operators (DSOs or aggregators) need to be designed and explored. The procedures to update the price-frequency characteristics and the associated algorithm need to be developed.

7.3.3 Rules of Connection, penalties and load tripping

While the architecture does provide key signals to convey resource adequacy, it is often challenging to ensure that an extravagant consumer doesn't hit the grid structure with a large load step. Rules need to be built in to every UMN to gauge the impact a load step may have on the system and it's impacts on stability. Further, if a load step does occur and the energy is being transiently supplied by some other agent, adequate penalties and compensation mechanisms need to be established.

An investigation into embedding open ledger functionality typically seen in blockchain frameworks needs to be conducted. As with any multi-agent transactive system, there may be potential for gaming between agents. Sufficient rules and policies need to be designed to prevent gaming and to levy penalties in case it does occur. Compliance rules need to be designed and enforced by the system operator in charge.

7.3.4 Role of Storage and Prosumers

The work presented in this research allows grid structures to be operated with large DER penetration levels. However, the local optimization framework and it's nuances need to be explored for prosumers. Adequate set of rules and optimization algorithms need to be deployed for the same.

Storage adds tremendous value in terms of aiding transient stability as well as arbitrage opportunities. Local optimization frameworks also need to be designed for storage entities in such architectures. A rigorous approach towards identifying the impact of storage on both the proposed transactive and physical elements needs to be developed.

It may be possible for the system operator to deploy the storage as a community asset. Quantifying the minimum amount of storage, nature of subscriptions to this service for connected agents, its structure and role in the proposed transactive mechanism could be key to making this approach more robust.

7.4 Acknowledgement

This work was supported by the Center for Distributed Energy (CDE). Parts of this work were enabled through support from some key sponsors. The work related to hybrid transformers presented in this research was supported through a DOE grant. The work wouldn't have been possible without key inputs from Deepak Divan (Georgia Tech), Marion Jaroszewski (Delta-Star transformers) and Kerry Cheung (program director – DOE). The development of the retrofittable hybrid transformers for low voltage meshed grids couldn't have been possible without inputs and support from key personnel at Consolidated Edison.

APPENDIX A. RETROFITTABLE HYBRID TRANSFORMERS FOR LOW-VOLTAGE MESHED GRIDS

While the ability to exercise control over voltage and power flows across meshed bulk power systems has been achieved with hybrid transformers, implementing power electronic solutions becomes challenging in low voltage, high power systems where 50 kA fault current levels must be met. A retrofittable version of the hybrid transformer concept is proposed for the same. Geospatial loading across meshed low voltage networks causes overloads in nearby transformers. Moreover, uneven loading of transformers also ensures that a poor voltage profile might be observed. Volt-VAR control on radial systems has been achieved with capacitor banks. However, in highly coupled systems like these underground low voltage meshed networks, single-point bulk Volt-VAR solutions often lead to unexpected reactive power loops. Operators of such systems have often resorted to replacing overloaded transformer units on these grids with larger ones, which is often an expensive approach. Thus, there is a need for deploying the same fractional control approach seen in hybrid transformers in these low voltage systems.

Stacked Isolated Voltage Optimization Modules (SIVOM) are presented here as a scaled retrofittable implementation of hybrid transformers for low voltages meshed grids. SIVOM units are implemented using coaxial winding transformers (CWTs). CWTs are single turn transformers with a multi-turn secondary as shown in Fig. A.1. CWT geometries are highly robust, can withstand high fault currents and show extremely low leakage impedances [143], [144]. The configuration in which these would be deployed is shown in Fig. A.2. SIVOM units are connected in series with the 26.4 KV/208 V transformers

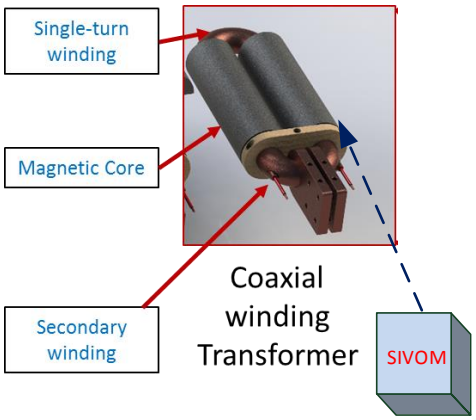

A. 1 Coaxial Winding Transformers

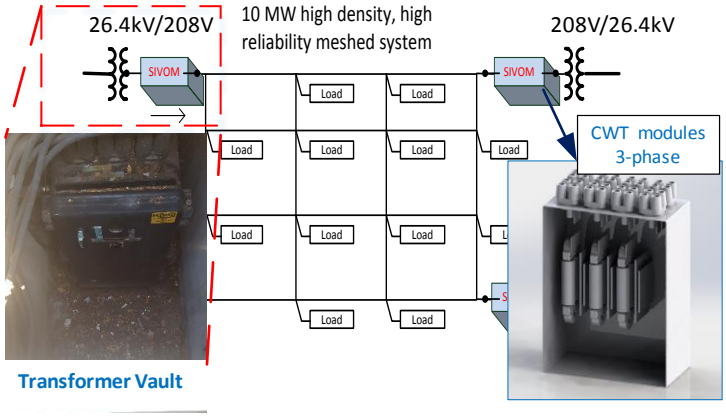

A. 2 SIVOM deployment in meshed LV systems

on the secondary. The single turn primary copper tube is connected in series with the line. By injecting an out-of-phase voltage on the multi-turn secondary, a fractional out-of-phase voltage can be reflected in series with the primary voltage. Moreover, this out-of-phase voltage is synthesized by using the existing phase connections at the 208 V terminal. As shown in Fig A.3, a quadrature voltage to phase A can be synthesized using the line-to-line voltage vector BC. Thus, using the other phases, a quadrature voltage can be synthesized

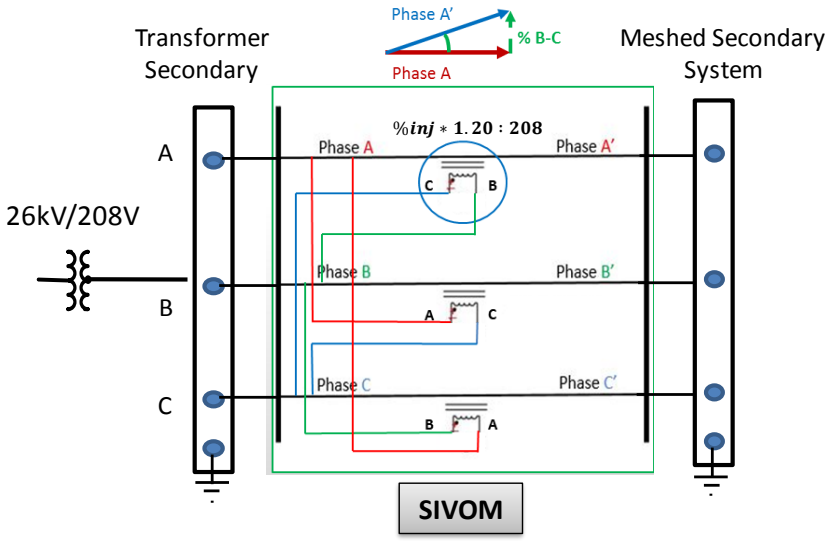

A. 3 Configuration to achieve quadrature injection

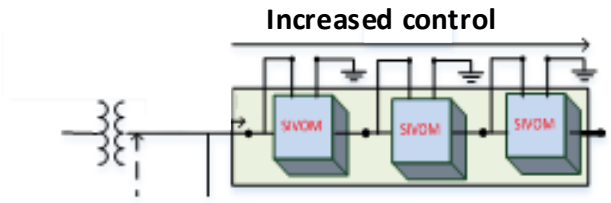

A. 4 Stackability of SIVOM Modules

for all three phases. In order to add more control at any geospatial location, these units can be stacked to increase the injection magnitudes as shown in Fig A.4. Thus, a modular, low-loss, compact, stackable and retrofittable realization of hybrid transformers is achieved. These units can also be bypassed to achieve the 'fail-normal' mode of operation where the outer copper tube simply becomes a current carrying conductor.

The key difference here is that only certain injection patterns can be achieved based on the phase connections available at 208 V secondary. Another key difference is that the injection magnitude remains fixed with the turn ratio of the CWT unit. Increased injection can be achieved with stacking units. However, the value in this approach is that it can be

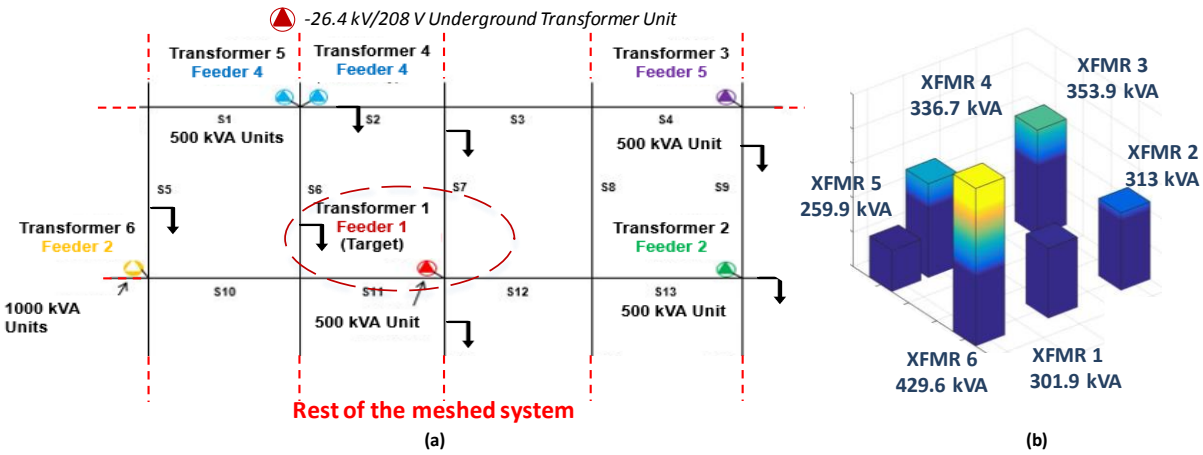

A. 5 (a)Target low voltage sub grid (b) Base case loading pattern for 6 transformers.

retrofitted into small tight spaces such as underground mains to provide the same functionality in meshed low voltage systems. Since these are passive transformers with added controls, they are very robust, can survive faults, can sustain extreme temperatures and could sustain operation even under water-logged conditions. A few simulation cases are presented next to showcase the value of this approach.

Consolidated Edison operates a highly meshed low voltage underground system in the Manhattan area. This makes it a prime use case to test out the concept. The area network was modelled in OpenDSS and the model was carefully benchmarked to confirm its validity. Although the entire system was modelled, a small sub grid with 6 relevant transformers is presented here. The sub grid of interest is illustrated in Fig. A.5 (a). The base case loading pattern for the 6 transformers is shown in Fig. A.5 (b). Transformer 1 is identified as the target transformer that will be retrofitted with the SIVOM units. SIVOM units are modelled into the OpenDSS system as simple series transformers with a fixed turns ratio. The unit can switch between injection modes by changing the phase

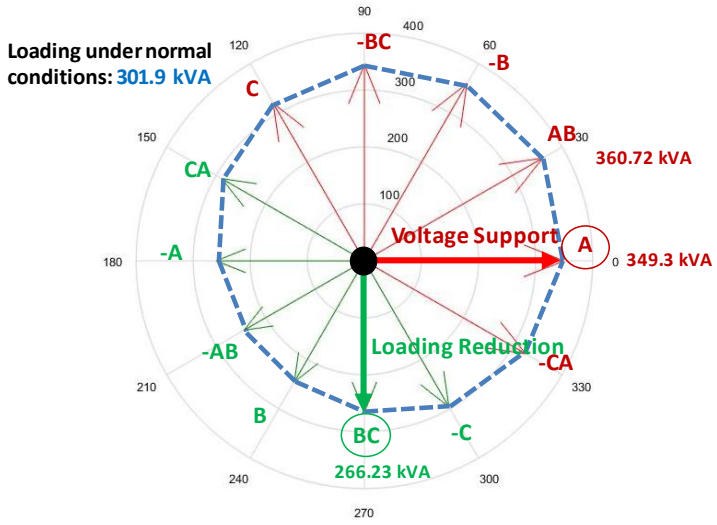

A. 6 Power flow variation with 12 injection patterns

connections to the CWT unit. These control actions are modelled as a DLL script that interacts with the simulation over a COM interface.

In order to study the effect of various injection modes, a 1% injection is carried out in all 12 patterns on the target transformer. A 1% injection magnitude is achieved by setting the turns ratio for the CWTs and rounding to the nearest integer. The loading variation in response to these injection patterns is shown in Fig. A.6. From this analysis, two modes of operation stand out as the ones of interest – loading reduction (quadrature injection) and voltage support (inline injection) as shown in Fig. A.7. These modes help address overloads on certain transformer units in the meshed system or provide Volt-VAR support in a given area. A few simulation cases were generated to understand the effect of different injection magnitudes in these two modes. While keeping the SIVOM unit at transformer 1, the turn

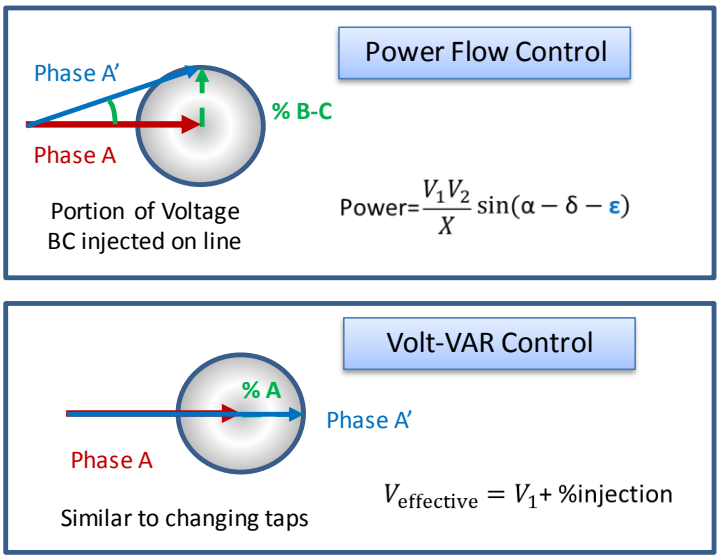

A. 7 Two necessary modes of operation

ratio is varied to achieve a 1% and 2% injection. Fig. A.8 (a) shows the power flow control that can be achieved with these injections in loading reduction mode. Thus, better load sharing between connected transformers can be achieved while alleviating heavily loaded units. Similarly, the effect of the voltage boost mode is shown in Fig. A.8 (b) where the area voltage profile can be improved using these units.

Meshed low voltage systems are designed to be highly tolerant to contingencies. However, depending on the contingency's spatial location and the coupling between

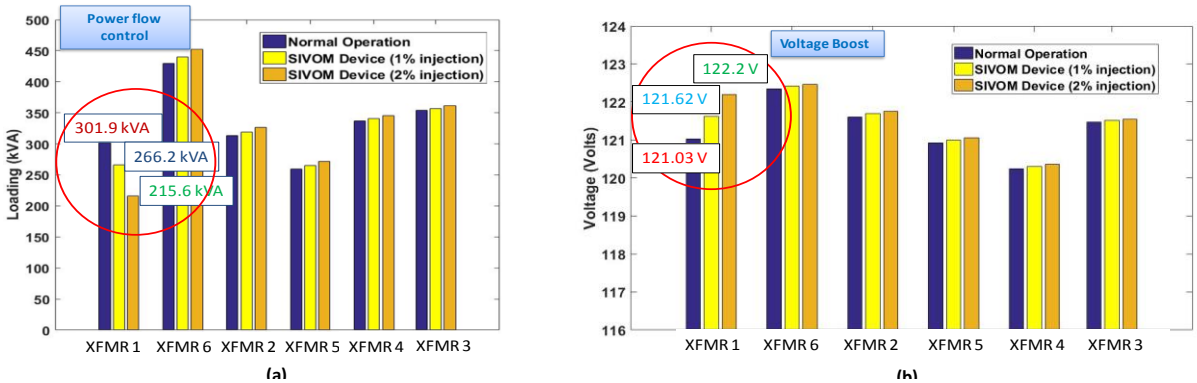

A. 8 (a) Power flow variation and (b) Voltage variation with 1% and 2% injection.

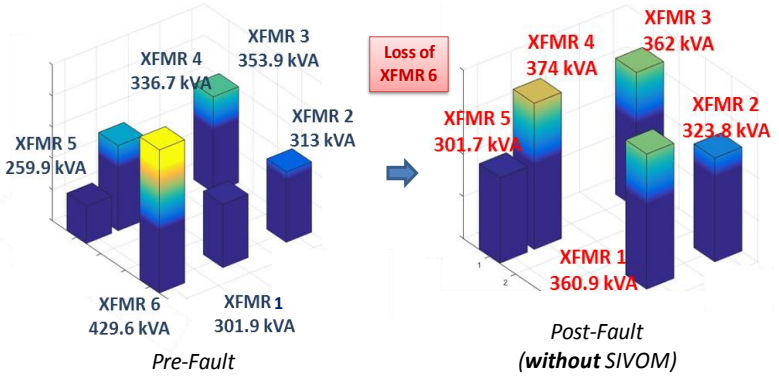

A. 9 Transformer loading levels (post contingency)

adjacent transformer units, the loading levels on operating units could drastically change. The most optimal solution would be to redistribute the loading proportionately across the under loaded units. In order to verify this, an (N-1) condition was simulated. Transformer 6 was taken out of service to investigate the effect of lost system capacity. The change in transformer loading patterns is shown in Fig. A.9.

The load is largely distributed unevenly across the sub-grid. Further, another contingency on this system would overload at least one of these transformers. The distribution of the load in this case would depend on a variety of network parameters making it entirely unpredictable. This scenario serves to show that centralized controls over

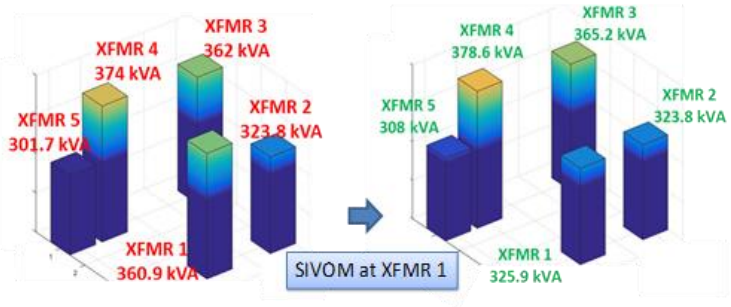

A. 10 Improved transformer loading under (N-1) contingencies

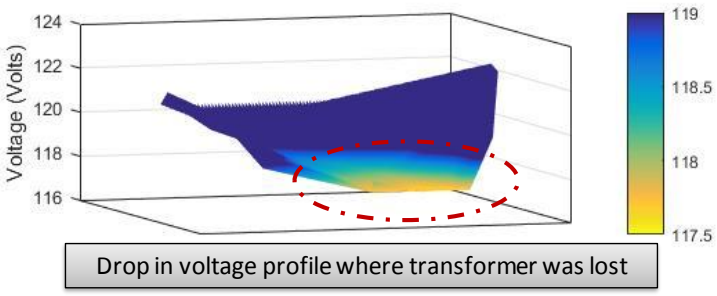

A. 11 Area voltage profile (post contingency)

power flows through the medium voltage feeder network wouldn't help rectify this issue. Moreover, a high degree of observability on the entire network would have to be maintained to exercise centralized controls. Although, the case shown here doesn't showcase overloads it is apparent that the result of any contingency is unpredictable and can alter transformer loading patterns in drastic fashions. By introducing SIVOM into the system, it is possible to control power flows to alter transformer loading under such contingencies. This can drive the system to a more optimal loading state. By introducing SIVOM at Transformer 1 an even loading pattern can be achieved through a 1% quadrature injection. Fig. A.10 presents the distribution of load with added control in the form of SIVOM modules.

Another (N-1) contingency was simulated to understand its effect on the area's voltage profile. Transformer 5 was taken out of service. The area voltage profile is shown in Fig. A.11. A pronounced voltage drop is observed in the area where the transformer was lost. SIVOM modules are installed at transformers 1, 2, 3, 4 and 6 for this simulation study. The control logic implemented in each module only observes the local voltage and

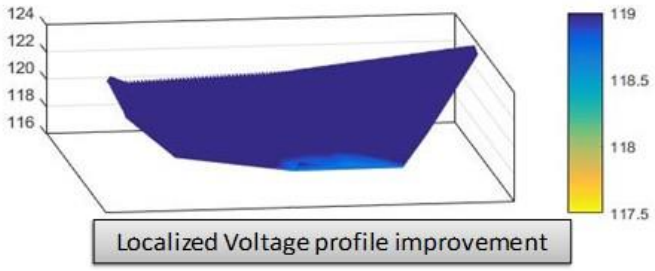

A. 12 Improved voltage profile under (N-1) contingencies

performs an in-phase injection to correct the local voltage profile based on set points. It is seen that when each module injects a 1% in-phase voltage, the net voltage profile in the area significantly improves as seen in Fig. A.12.

Thus, SIVOM modules demonstrate the ability to optimize voltage profiles and transformer loading patterns across the system. Moreover, by introducing controllability even under the face of contingencies, a more resilient and optimum operation state can be achieved. By utilizing the same concept as the hybrid transformer, an implementation is achieved that can provide control over numerous grid parameters at bulk power, medium voltage and low voltage levels, while being retrofittable and low cost. All of this achieved while ensuring that harsh environmental and fault current requirements are met and managed.

APPENDIX B. LIMITATIONS OF HYBRID TRANSFORMERS UNDER EXTREME SCENARIOS

Hybrid transformers showed the ability to exercise control over line flows in the simulation test case presented in Section 6.2. However, there are extreme scenarios where the ability to affect control over power flows is limited by the physical impedances of the grid structure itself. An extreme scenario for the test system presented in Section 6.1 is shown in Fig. B.1. The PV injection at bus 4 has been raised to 3.26 MW for the purposes of this study. The system seen in Fig. B.1 shows several points of congestion, with line 2-3 loaded to 107% and line 4-5 loaded to 204% of their individual capacities.

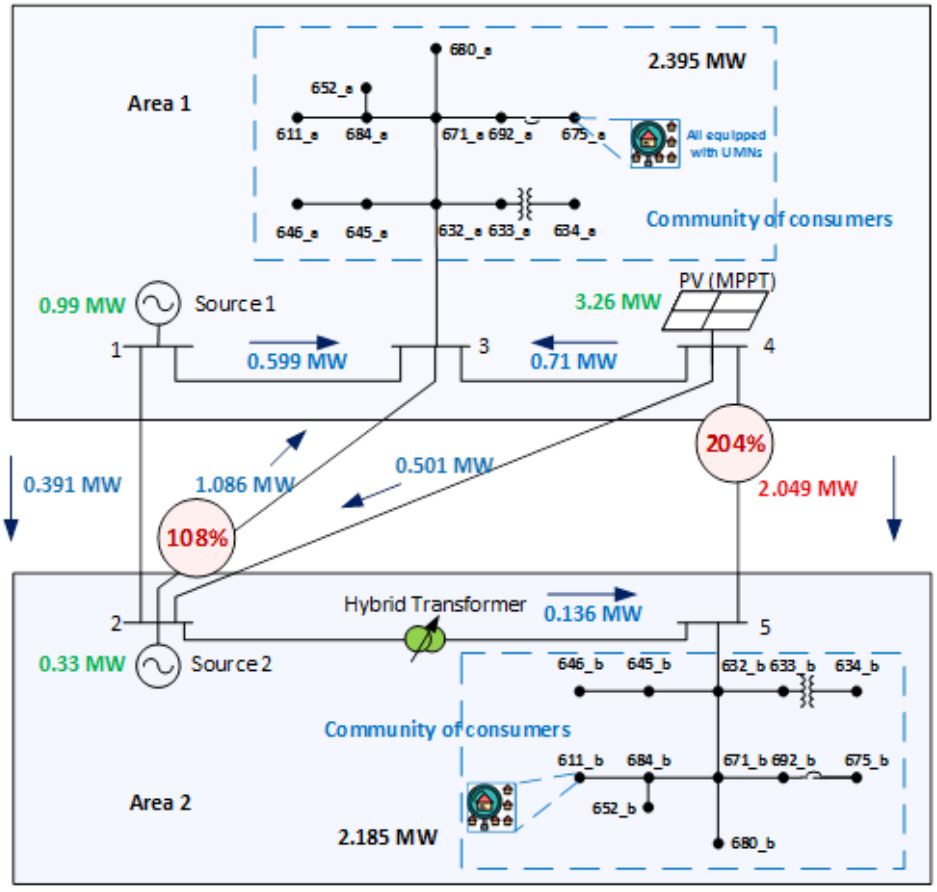

B. 1 Line flows under extreme scenarios with high PV penetration

The hybrid transformer could relieve the line loading on line 4-5 by attempting to maximize the ampacity of its own link. Fig. B.2 shows the line flows when the hybrid transformer utilizes its own link to reduce congestion patterns. However, this leads to a new violation on line 2-3. Moreover, the loading level for line 4-5 remains extremely high. Under such scenarios, the hybrid transformer would raise an urgent flag to signal the operator. Such extreme scenarios may only be addressed through centralized control. However, in most normal scenarios, hybrid transformers remain an effective grid management tool.

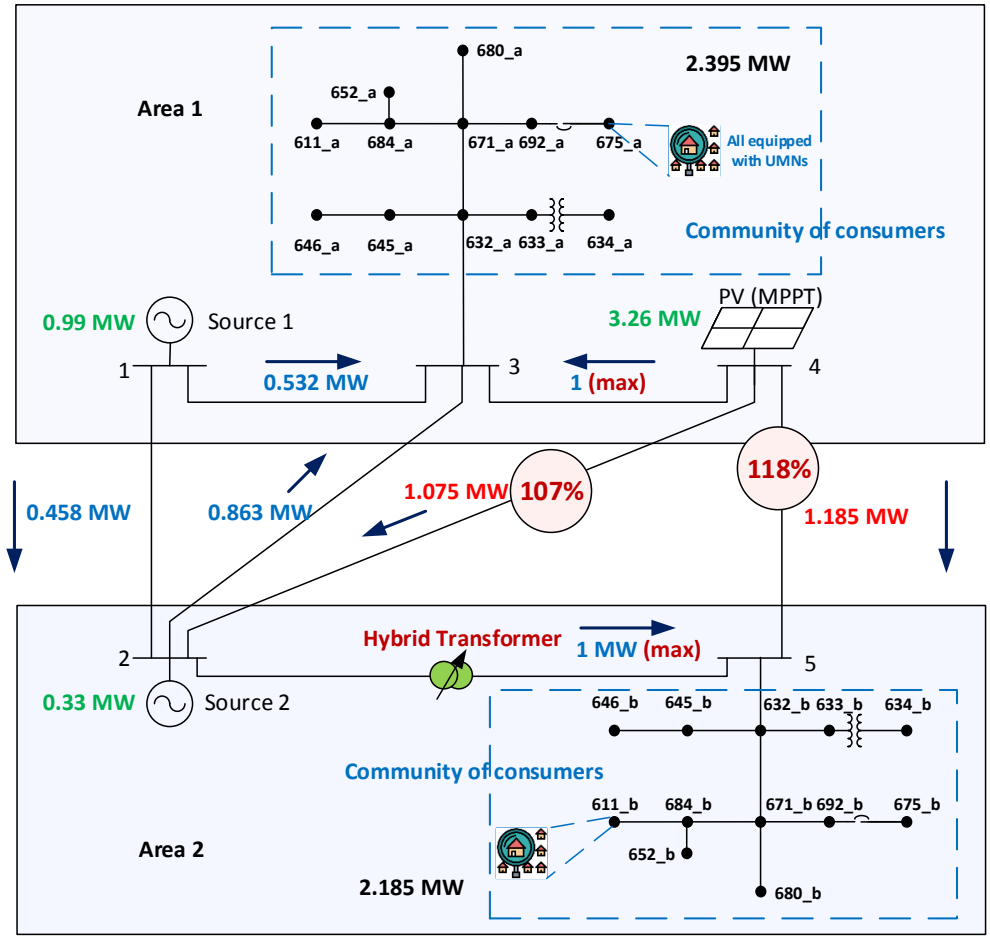

B. 2 Inability to resolve congestion issues using hybrid transformers

APPENDIX C. PUBLICATIONS

Conference Publication:

1. **Jinsiwale, R**., Jayaraman, S., Kandula, R. P., Lambert, F., Divan, D., Reid, A., & Day, P. (2018, October). Implementing Volt-Var Control in Meshed Low Voltage Grids. In *2018 IEEE PES Innovative Smart Grid Technologies Conference Europe (ISGT-Europe)* (pp. 1-6). IEEE.

2. **Jinsiwale, R.**, Mauger, M. J., Kandula, R. P., Divan, D., Jaroszewski, M., & Schatz, J. (2018, November). Cost-Effective Dynamic Control for Transmission Systems. In 2018 IEEE Electronic Power Grid (eGrid) (pp. 1-6). IEEE.

3. **Jinsiwale, R.,** & Divan, D. (2019, February). Energy Access in Community Microgrids based on Decentralized Real-time Pricing. In 2019 IEEE Decentralized Energy Access Solutions Workshop (DEAS) (pp. 206-212). IEEE.

4. **Jinsiwale, R**., Kulkarni, S., Divan, D. Low-cost smart Home energy Management System based on Decentralized Frequency-based Markets. 2020 IEEE Innovative Smart Grid Technologies Conference (ISGT –NA)

5. Liptak, S., Miranbeigi, M., Kulkarni, S., **Jinsiwale, R.,** & Divan, D. (2019, February). Self-Organizing NanoGrid (SONG). In 2019 IEEE Decentralized Energy Access Solutions Workshop (DEAS) (pp. 206-212). IEEE.

6. **R. Jinsiwale**, S. Paran and D. Divan, "Decentralized Operation of Resource Constrained Microgrids — Multi-agent Demand-based Approach," 2020 Clemson University Power Systems Conference (PSC)

Journal Publications

1. **R. Jinsiwale** and D. Divan, "Decentralized Real-Time Pricing to Achieve Integrated Transactive and Physical Grids," in IEEE Access, vol. 7, pp. 132525-132541, 2019. doi: 10.1109/ACCESS.2019.2941424

2. **R. Jinsiwale** and D. Divan, "Robust Edge Intelligence Framework to support a Decentralized Transactive Grid Architecture," in IEEE Trnasactions on Smart Grids ***(in review at the time when this document was written)***

Relevant Reports

1. Kandula, R. P., Divan, D., **Jinsiwale, R.,** & Mauger, M. (2018). ‘’Modular controllable transformers (MCT)’’ (No. DE-OE0000855). Georgia Institute of Technology, Atlanta, GA (Unites States).

REFERENCES

[1] "Levelized Cost and Levelized Avoided Cost of New Generation Resources in the Annual Energy Outlook 2019," p. 25.

[2] "Nevada's 2.3-Cent Bid Beats Arizona's Record-Low Solar PPA Price | Greentech Media." https://www.greentechmedia.com/articles/read/nevada-beat-arizona-record-low-solar-ppa-price#gs.62j56p (accessed Apr. 16, 2019).

[3] "Solar Market Insight Report 2019 Q2," *SEIA*. /research-resources/solar-market-insight-report-2019-q2 (accessed Oct. 23, 2019).

[4] Y. Cai, T. Huang, E. Bompard, Y. Cao, and Y. Li, "Self-Sustainable Community of Electricity Prosumers in the Emerging Distribution System," *IEEE Trans. Smart Grid*, vol. 8, no. 5, pp. 2207–2216, Sep. 2017, doi: 10.1109/TSG.2016.2518241.

[5] B. Jones-Albertus, "Confronting the Duck Curve: How to Address Over-Generation of Solar Energy," *Energy.gov*. https://www.energy.gov/eere/articles/confronting-duck-curve-how-address-over-generation-solar-energy (accessed Apr. 17, 2019).

[6] D. Divan, R. Moghe, and A. Prasai, "Power Electronics at the Grid Edge : The key to unlocking value from the smart grid," *IEEE Power Electron. Mag.*, vol. 1, no. 4, pp. 16–22, Dec. 2014, doi: 10.1109/MPEL.2014.2360811.

[7] E. Bompard, P. Correia, G. Gross, and M. Amelin, "Congestion-management schemes: a comparative analysis under a unified framework," *IEEE Trans. Power Syst.*, vol. 18, no. 1, pp. 346–352, Feb. 2003, doi: 10.1109/TPWRS.2002.807077.

[8] T. Orfanogianni and G. Gross, "A General Formulation for LMP Evaluation," *IEEE Trans. Power Syst.*, vol. 22, no. 3, pp. 1163–1173, Aug. 2007, doi: 10.1109/TPWRS.2007.901297.

[9] R. Francis and B. Bekera, "A metric and frameworks for resilience analysis of engineered and infrastructure systems," *Reliab. Eng. Syst. Saf.*, vol. 121, no. Supplement C, pp. 90–103, Jan. 2014, doi: 10.1016/j.ress.2013.07.004.

[10] "Gerry Cauley, and Mark Lauby. (2010) High-Impact, Low-Frequency Event Risk to the North American Bulk Power System. NERC. [Online]. Available: http://www.nerc.com/files/HILF-060210.pdf." Accessed: Apr. 16, 2019. [Online]. Available: https://www.energy.gov/sites/prod/files/High-Impact%20Low-Frequency%20Event%20Risk%20to%20the%20North%20American%20Bulk%20Power%20System%20-%202010.pdf.

[11] "The Role of Microgrids in Helping to Advance the Nation's Energy System," *Energy.gov*. https://www.energy.gov/oe/activities/technology-development/grid-modernization-and-smart-grid/role-microgrids-helping (accessed Oct. 17, 2020).

[12] O. P. Veloza and F. Santamaria, “Analysis of major blackouts from 2003 to 2015: Classification of incidents and review of main causes,” *Electr. J.*, vol. 29, no. 7, pp. 42–49, Sep. 2016, doi: 10.1016/j.tej.2016.08.006.

[13] F. H. Jufri, V. Widiputra, and J. Jung, “State-of-the-art review on power grid resilience to extreme weather events: Definitions, frameworks, quantitative assessment methodologies, and enhancement strategies,” *Appl. Energy*, vol. 239, pp. 1049–1065, Apr. 2019, doi: 10.1016/j.apenergy.2019.02.017.

[14] A. F. Campbell, “It took 11 months to restore power to Puerto Rico after Hurricane Maria. A similar crisis could happen again.,” *Vox*, Aug. 15, 2018. https://www.vox.com/identities/2018/8/15/17692414/puerto-rico-power-electricity-restored-hurricane-maria (accessed Apr. 16, 2019).

[15] “Large power transformers and the U.S. electric grid.” US DOE (2012).

[16] “U.S. Risks National Blackout From Small-Scale Attack - WSJ.” https://www.wsj.com/articles/u-s-risks-national-blackout-from-small-scale-attack-1394664965 (accessed Oct. 17, 2020).

[17] J. W. Climate The Daily, “U.S. Electrical Grid Undergoes Massive Transition to Connect to Renewables,” *Scientific American*. https://www.scientificamerican.com/article/what-is-the-smart-grid/ (accessed Oct. 17, 2020).

[18] “Smart Grid Technologies: Communication Technologies and Standards - IEEE Journals & Magazine.” https://ieeexplore.ieee.org/document/6011696 (accessed Oct. 17, 2020).

[19] “AMI Smart Meter Big Data Analytics for Time Series of Electricity Consumption - IEEE Conference Publication.” https://ieeexplore.ieee.org/document/8456135 (accessed Oct. 17, 2020).

[20] J. Peppanen, M. J. Reno, R. J. Broderick, and S. Grijalva, “Distribution System Model Calibration With Big Data From AMI and PV Inverters,” *IEEE Trans. Smart Grid*, vol. 7, no. 5, pp. 2497–2506, Sep. 2016, doi: 10.1109/TSG.2016.2531994.

[21] K. Ashok, D. Divan, and F. Lambert, “Grid edge analytics platform with AMI data,” in *2018 IEEE Power Energy Society Innovative Smart Grid Technologies Conference (ISGT)*, Feb. 2018, pp. 1–5, doi: 10.1109/ISGT.2018.8403364.

[22] S.-H. Choi, S.-J. Kang, N.-J. Jung, and I.-K. Yang, “The design of outage management system utilizing meter information based on AMI (Advanced Metering Infrastructure) system,” in *8th International Conference on Power Electronics - ECCE Asia*, May 2011, pp. 2955–2961, doi: 10.1109/ICPE.2011.5944797.

[23] R. E. Wilson, “PMUs [phasor measurement unit],” *IEEE Potentials*, vol. 13, no. 2, pp. 26–28, Apr. 1994, doi: 10.1109/45.283885.

[24] A. Rendon Salgado, C. R. Fuerte Esquivel, and J. G. Calderon Guizar, "SCADA and PMU Measurements for Improving Power System State Estimation," *IEEE Lat. Am. Trans.*, vol. 13, no. 7, pp. 2245–2251, Jul. 2015, doi: 10.1109/TLA.2015.7273784.

[25] A. Monticelli, *State Estimation in Electric Power Systems: A Generalized Approach*. Springer US, 1999.

[26] J. Giri, M. Parashar, J. Trehern, and V. Madani, "The Situation Room: Control Center Analytics for Enhanced Situational Awareness," *IEEE Power Energy Mag.*, vol. 10, no. 5, pp. 24–39, Sep. 2012, doi: 10.1109/MPE.2012.2205316.

[27] D. Orihara and D. Iioka, "Sensitivity-based AGC Dispatching for Mitigation of Short-Term Power Flow Variation," in *2018 IEEE Electronic Power Grid (eGrid)*, Nov. 2018, pp. 1–6, doi: 10.1109/eGRID.2018.8598675.

[28] "Alternative Fuels Data Center: Key Federal Legislation." https://afdc.energy.gov/laws/key_legislation (accessed Oct. 17, 2020).

[29] E. J. Anderson and X. Hu, "Forward contracts and market power in an electricity market," *Int. J. Ind. Organ.*, vol. 26, no. 3, pp. 679–694, May 2008, doi: 10.1016/j.ijindorg.2007.05.002.

[30] "Renewable Energy Power Purchase Agreements (PPAs)," *Ameresco*. https://www.ameresco.com/solution/power-purchase-agreements/ (accessed Apr. 17, 2019).

[31] T. S. Chung, S. H. Zhang, C. W. Yu, and K. P. Wong, "Electricity market risk management using forward contracts with bilateral options," *Transm. Distrib. IEE Proc. - Gener.*, vol. 150, no. 5, pp. 588–594, Sep. 2003, doi: 10.1049/ip-gtd:20030532.

[32] F. Wang and X. Y. Zhou, "Power market risk management based on range forward contracts," in *2009 International Conference on Sustainable Power Generation and Supply*, Apr. 2009, pp. 1–7, doi: 10.1109/SUPERGEN.2009.5347889.

[33] B. H. Chowdhury and S. Rahman, "A review of recent advances in economic dispatch," *IEEE Trans. Power Syst.*, vol. 5, no. 4, pp. 1248–1259, Nov. 1990, doi: 10.1109/59.99376.

[34] J. Zhu, "Security-Constrained Economic Dispatch," in *Optimization of Power System Operation*, IEEE, 2015.

[35] J. Q. Xin, E. Bompard, and R. Napoli, "Security Coordinated Economic Dispatch for Joint Energy and Reserve Markets," in *2006 International Conference on Power System Technology*, Oct. 2006, pp. 1–5, doi: 10.1109/ICPST.2006.321848.

[36] "Optimal Power Flow," in *Electricity Markets: Theories and Applications*, IEEE, 2017, pp. 147–171.

[37] C. Konstantinou, M. Sazos, A. S. Musleh, A. Keliris, A. Al-Durra, and M. Maniatakos, "GPS spoofing effect on phase angle monitoring and control in a real-time digital simulator-based hardware-in-the-loop environment," *IET Cyber-Phys. Syst. Theory Appl.*, vol. 2, no. 4, pp. 180–187, 2017, doi: 10.1049/iet-cps.2017.0033.

[38] N. Kshetri and J. Voas, "Hacking Power Grids: A Current Problem," *Computer*, vol. 50, no. 12, pp. 91–95, Dec. 2017, doi: 10.1109/MC.2017.4451203.

[39] W. Yao *et al.*, "GPS signal loss in the wide area monitoring system: Prevalence, impact, and solution," *Electr. Power Syst. Res.*, vol. 147, pp. 254–262, Jun. 2017, doi: 10.1016/j.epsr.2017.03.004.

[40] M. Yagami, T. Hasegawa, and J. Tamura, "Transient stability assessment of synchronous generator in power system with high-penetration photovoltaics," in *2012 15th International Conference on Electrical Machines and Systems (ICEMS)*, Oct. 2012, pp. 1–6.

[41] A. Vaccaro, V. Loia, G. Formato, P. Wall, and V. Terzija, "A Self-Organizing Architecture for Decentralized Smart Microgrids Synchronization, Control, and Monitoring," *IEEE Trans. Ind. Inform.*, vol. 11, no. 1, pp. 289–298, Feb. 2015, doi: 10.1109/TII.2014.2342876.

[42] Z. Zhang, X. Ying, and M.-Y. Chow, "Decentralizing the economic dispatch problem using a two-level incremental cost consensus algorithm in a smart grid environment," Sep. 2011, pp. 1–7, doi: 10.1109/NAPS.2011.6025103.

[43] V. Loia and A. Vaccaro, "A decentralized architecture for voltage regulation in Smart Grids," in *2011 IEEE International Symposium on Industrial Electronics*, Jun. 2011, pp. 1679–1684, doi: 10.1109/ISIE.2011.5984414.

[44] E. Mashhour and S. M. Moghaddas-Tafreshi, "Bidding Strategy of Virtual Power Plant for Participating in Energy and Spinning Reserve Markets—Part I: Problem Formulation," *IEEE Trans. Power Syst.*, vol. 26, no. 2, pp. 949–956, May 2011, doi: 10.1109/TPWRS.2010.2070884.

[45] S. Hijgenaar, Z. Erkin, T. Keviczky, J. Siemons, R. Bisschops, and A. Verbraeck, "A decentralised energy trading architecture for future smart grid load balancing," in *2017 IEEE International Conference on Smart Grid Communications (SmartGridComm)*, Oct. 2017, pp. 77–82, doi: 10.1109/SmartGridComm.2017.8340707.

[46] K. Gai, Y. Wu, L. Zhu, M. Qiu, and M. Shen, "Privacy-Preserving Energy Trading Using Consortium Blockchain in Smart Grid," *IEEE Trans. Ind. Inform.*, vol. 15, no. 6, pp. 3548–3558, Jun. 2019, doi: 10.1109/TII.2019.2893433.

[47] D. Livingston, V. Sivaram, M. Freeman, and M. Fiege, "Applying Blockchain Technology to Electric Power Systems," p. 37.

[48] J. Kang, R. Yu, X. Huang, S. Maharjan, Y. Zhang, and E. Hossain, "Enabling Localized Peer-to-Peer Electricity Trading Among Plug-in Hybrid Electric Vehicles Using Consortium Blockchains," *IEEE Trans. Ind. Inform.*, vol. 13, no. 6, pp. 3154–3164, Dec. 2017, doi: 10.1109/TII.2017.2709784.

[49] N. R. Asr, Z. Zhang, and M. Y. Chow, "Consensus-based distributed energy management with real-time pricing," in *2013 IEEE Power Energy Society General Meeting*, Jul. 2013, pp. 1–5, doi: 10.1109/PESMG.2013.6672511.

[50] P. Bajpai, S. Chanda, and A. K. Srivastava, "A Novel Metric to Quantify and Enable Resilient Distribution System using Graph Theory and Choquet Integral," *IEEE Trans. Smart Grid*, vol. PP, no. 99, pp. 1–1, 2017, doi: 10.1109/TSG.2016.2623818.

[51] S. Yang, S. Tan, and J. Xu, "Consensus Based Approach for Economic Dispatch Problem in a Smart Grid," *IEEE Trans. Power Syst.*, vol. 28, no. 4, pp. 4416–4426, Nov. 2013, doi: 10.1109/TPWRS.2013.2271640.

[52] Y. Liu, L. Xiao, G. Yao, and S. Bu, "Pricing-Based Demand Response for a Smart Home With Various Types of Household Appliances Considering Customer Satisfaction," *IEEE Access*, vol. 7, pp. 86463–86472, 2019, doi: 10.1109/ACCESS.2019.2924110.

[53] M. Pipattanasomporn, M. Kuzlu, and S. Rahman, "An Algorithm for Intelligent Home Energy Management and Demand Response Analysis," *IEEE Trans. Smart Grid*, vol. 3, no. 4, pp. 2166–2173, Dec. 2012, doi: 10.1109/TSG.2012.2201182.

[54] H. Shareef, M. S. Ahmed, A. Mohamed, and E. A. Hassan, "Review on Home Energy Management System Considering Demand Responses, Smart Technologies, and Intelligent Controllers," *IEEE Access*, vol. 6, pp. 24498–24509, 2018, doi: 10.1109/ACCESS.2018.2831917.

[55] "Agile Fractal Systems: Reenvisioning Power System Architecture," *NAE Website*. https://nae.edu/177000/Agile-Fractal-Systems-Reenvisioning-Power-System-Architecture (accessed Sep. 10, 2019).

[56] M.-C. Alvarez-Herault, N. N'Doye, C. Gandioli, N. Hadjsaid, and P. Tixador, "Meshed distribution network vs reinforcement to increase the distributed generation connection," *Sustain. Energy Grids Netw.*, vol. 1, no. Supplement C, pp. 20–27, Mar. 2015, doi: 10.1016/j.segan.2014.11.001.

[57] I. Totonchi, H. A. Akash, A. A. Akash, and A. Faza, "Sensitivity analysis for the IEEE 30 bus system using load-flow studies," in *2013 3rd International Conference on Electric Power and Energy Conversion Systems*, Oct. 2013, pp. 1–6, doi: 10.1109/EPECS.2013.6713060.

[58] M. Behnke *et al.*, "Secondary Network Distribution Systems Background and Issues Related to the Interconnection of Distributed Resources," NREL/TP-560-38079, 15016566, Jul. 2005. doi: 10.2172/15016566.

[59] H. Mahala and Y. Kumar, "Optimal re-dispatch of generator for congestion management using PSO," in *2014 International Conference on Green Computing Communication and Electrical Engineering (ICGCCEE)*, Mar. 2014, pp. 1–4, doi: 10.1109/ICGCCEE.2014.6922307.

[60] Xu Cheng and T. J. Overbye, "PTDF-based power system equivalents," *IEEE Trans. Power Syst.*, vol. 20, no. 4, pp. 1868–1876, Nov. 2005, doi: 10.1109/TPWRS.2005.857013.

[61] R. A. Jabr, "Radial Distribution Load Flow Using Conic Programming," *Power Syst. IEEE Trans. On*, vol. 21, pp. 1458–1459, Sep. 2006, doi: 10.1109/TPWRS.2006.879234.

[62] X. Bai, H. Wei, K. Fujisawa, and Y. Wang, "Semidefinite programming for optimal power flow problems," *Int. J. Electr. Power Energy Syst.*, vol. 30, no. 6, pp. 383–392, Jul. 2008, doi: 10.1016/j.ijepes.2007.12.003.

[63] Chee Wei Tan, D. W. H. Cai, and Xin Lou, "DC optimal power flow: Uniqueness and algorithms," in *2012 IEEE Third International Conference on Smart Grid Communications (SmartGridComm)*, Nov. 2012, pp. 641–646, doi: 10.1109/SmartGridComm.2012.6486058.

[64] B. Stott and O. Alsac, "Fast Decoupled Load Flow," *IEEE Trans. Power Appar. Syst.*, vol. PAS-93, no. 3, pp. 859–869, May 1974, doi: 10.1109/TPAS.1974.293985.

[65] E. A. Goldis, X. Li, M. C. Caramanis, A. M. Rudkevich, and P. A. Ruiz, "AC-Based Topology Control Algorithms (TCA) – A PJM Historical Data Case Study," in *2015 48th Hawaii International Conference on System Sciences*, Jan. 2015, pp. 2516–2519, doi: 10.1109/HICSS.2015.302.

[66] B. Venkatesh, R. Ranjan, and H. B. Gooi, "Optimal reconfiguration of radial distribution systems to maximize loadability," *IEEE Trans. Power Syst.*, vol. 19, no. 1, pp. 260–266, Feb. 2004, doi: 10.1109/TPWRS.2003.818739.

[67] Xiaoling Jin, Jianguo Zhao, Ying Sun, Kejun Li, and Boqin Zhang, "Distribution network reconfiguration for load balancing using binary particle swarm optimization," in *2004 International Conference on Power System Technology, 2004. PowerCon 2004.*, Nov. 2004, vol. 1, pp. 507-510 Vol.1, doi: 10.1109/ICPST.2004.1460047.

[68] T. Ding, R. Bo, Z. Bie, and X. Wang, "Optimal Selection of Phase Shifting Transformer Adjustment in Optimal Power Flow," *IEEE Trans. Power Syst.*, vol. 32, no. 3, pp. 2464–2465, May 2017, doi: 10.1109/TPWRS.2016.2600098.

[69] W. J. Lyman, "Controlling Power Flow with Phase Shifting Equipment," *Trans. Am. Inst. Electr. Eng.*, vol. 49, no. 3, pp. 825–829, Jul. 1930, doi: 10.1109/T-AIEE.1930.5055584.

[70] R. Rezvanfar, M. E. Mosayebian, H. Monsef, and H. Ghasemi, “Impact of optimally located thyristor controlled phase angle regulator on system security and reliability,” in *2011 10th International Conference on Environment and Electrical Engineering*, May 2011, pp. 1–4, doi: 10.1109/EEEIC.2011.5874829.

[71] S. Nyati, M. Eitzmann, J. Kappenman, D. VanHouse, N. Mohan, and A. Edris, “Design issues for a single core transformer thyristor controlled phase-angle regulator,” *IEEE Trans. Power Deliv.*, vol. 10, no. 4, pp. 2013–2019, Oct. 1995, doi: 10.1109/61.473349.

[72] A. Perilla, J. L. R. Torres, M. A. M. M. van der Meijden, A. Alefragkis, and A. M. Lindefelt, “Analysis of a power factor regulation strategy for an embedded point-to-point MMC-HVDC system,” in *2018 IEEE International Energy Conference (ENERGYCON)*, Jun. 2018, pp. 1–6, doi: 10.1109/ENERGYCON.2018.8398845.

[73] Lihua Hu and R. E. Morrison, “The use of modulation theory to calculate the harmonic distortion in HVDC systems operating on an unbalanced supply,” *IEEE Trans. Power Syst.*, vol. 12, no. 2, pp. 973–980, May 1997, doi: 10.1109/59.589796.

[74] A. Bodin, “HVDC Light® - a preferable power transmission system for renewable energies,” in *Proceedings of the 2011 3rd International Youth Conference on Energetics (IYCE)*, Jul. 2011, pp. 1–4.

[75] “Evolution of HVDC Light®.” https://new.abb.com/news/detail/4224/evolution-of-hvdc-lightr (accessed Oct. 17, 2020).

[76] L. Gyugyi, C. D. Schauder, S. L. Williams, T. R. Rietman, D. R. Torgerson, and A. Edris, “The unified power flow controller: a new approach to power transmission control,” *IEEE Trans. Power Deliv.*, vol. 10, no. 2, pp. 1085–1097, Apr. 1995, doi: 10.1109/61.400878.

[77] C. Schauder *et al.*, “AEP UPFC project: installation, commissioning and operation of the /spl plusmn/160 MVA STATCOM (phase I),” *IEEE Trans. Power Deliv.*, vol. 13, no. 4, pp. 1530–1535, Oct. 1998, doi: 10.1109/61.714855.

[78] H. Cao, H. Liu, Z. Zhou, X. Wang, and D. Du, “A novel protection principle for turn to turn fault of valve side winding of series transformer of UPFC project,” in *2018 International Conference on Power System Technology (POWERCON)*, Nov. 2018, pp. 3827–3833, doi: 10.1109/POWERCON.2018.8601680.

[79] D. M. Divan *et al.*, “A Distributed Static Series Compensator System for Realizing Active Power Flow Control on Existing Power Lines,” *IEEE Trans. Power Deliv.*, vol. 22, no. 1, pp. 642–649, Jan. 2007, doi: 10.1109/TPWRD.2006.887103.

[80] “Evaluation of SmartValveTM Devices Installation at Central Hudson.” https://www.epri.com/research/products/000000003002019771 (accessed Oct. 17, 2020).

[81] A. Nour, A. Hatata, A. Helal, and M. El-Saadawi, “A Review on Voltage Violation Mitigation Techniques of Distribution Networks with Distributed Rooftop Photovoltaic Systems,” *IET Gener. Transm. Distrib.*, vol. 14, Nov. 2019, doi: 10.1049/iet-gtd.2019.0851.

[82] J. Dong *et al.*, “Operational impacts of high penetration solar power on a real-world distribution feeder,” in *2018 IEEE Power Energy Society Innovative Smart Grid Technologies Conference (ISGT)*, Feb. 2018, pp. 1–5, doi: 10.1109/ISGT.2018.8403344.

[83] E.-E. E. Portal, “4 Essential Features of Transformer On-Load Tap Changer,” *EEP - Electrical Engineering Portal*, Jan. 28, 2015. https://electrical-engineering-portal.com/4-essential-features-of-transformer-on-load-tap-changer-oltc (accessed Oct. 18, 2020).

[84] J. Mössinger, “OILTAP® G - OILTAP® G.” https://www.reinhausen.com/desktopdefault.aspx/tabid-235/82_read-34/ (accessed Oct. 18, 2020).

[85] D. Martin *et al.*, *Effect of Rooftop-PV on power transformer insulation and on-load tap changer operation*. 2015.

[86] “Pole-mounted capacitor banks,” *Eaton*. https://www.eaton.com/us/en-us/catalog/medium-voltage-power-distribution-control-systems/pole-mounted-capacitor-banks.html (accessed Oct. 18, 2020).

[87] R. Bose, K. Samanta, K. Ghosh, R. Bandyopadhyay, and S. Chatterjee, “Transient analysis of mechanically switched capacitors with and without damping network connected to A.C grid,” in *2016 2nd International Conference on Control, Instrumentation, Energy Communication (CIEC)*, Jan. 2016, pp. 274–278, doi: 10.1109/CIEC.2016.7513789.

[88] S. Rahmani, A. Hamadi, K. Al-Haddad, and L. A. Dessaint, “A Combination of Shunt Hybrid Power Filter and Thyristor-Controlled Reactor for Power Quality,” *IEEE Trans. Ind. Electron.*, vol. 61, no. 5, pp. 2152–2164, May 2014, doi: 10.1109/TIE.2013.2272271.

[89] “IEEE Guide for Application of Power Electronics for Power Quality Improvement on Distribution Systems Rated 1 kV Through 38 kV,” *IEEE Std 1409-2012*, pp. 1–90, Apr. 2012, doi: 10.1109/IEEESTD.2012.6190701.

[90] M. Kaplan, “Optimization of Number, Location, Size, Control Type, and Control Setting of Shunt Capacitors on Radial Distribution Feeders,” *IEEE Trans. Power Appar. Syst.*, vol. PAS-103, no. 9, pp. 2659–2665, Sep. 1984, doi: 10.1109/TPAS.1984.318238.

[91] D. Thukaram and G. Yesuratnam, “Optimal reactive power dispatch in a large power system with AC-DC and FACTS controllers,” *Transm. Distrib. IET Gener.*, vol. 2, no. 1, pp. 71–81, Jan. 2008, doi: 10.1049/iet-gtd:20070163.

[92] G. Sheble, “Demand Is Very Elastic!,” *IEEE Power Energy Mag.*, vol. 9, no. 2, pp. 14–20, Mar. 2011, doi: 10.1109/MPE.2011.940264.

[93] “Impacts of Demand-Side Management on T and D???Now and Tomorrow - IEEE Journals & Magazine.” https://ieeexplore.ieee.org/document/5527063 (accessed Jun. 18, 2020).

[94] “Reports on Demand Response and Advanced Metering | Federal Energy Regulatory Commission.” https://www.ferc.gov/industries-data/electric/power-sales-and-markets/demand-response/reports-demand-response-and (accessed Oct. 18, 2020).

[95] F. Farzan, F. Farzan, M. A. Jafari, and J. Gong, “Integration of Demand Dynamics and Investment Decisions on Distributed Energy Resources,” *IEEE Trans. Smart Grid*, vol. 7, no. 4, pp. 1886–1895, Jul. 2016, doi: 10.1109/TSG.2015.2426151.

[96] B. Zeng, J. Zhang, X. Yang, J. Wang, J. Dong, and Y. Zhang, “Integrated Planning for Transition to Low-Carbon Distribution System With Renewable Energy Generation and Demand Response,” *IEEE Trans. Power Syst.*, vol. 29, no. 3, pp. 1153–1165, May 2014, doi: 10.1109/TPWRS.2013.2291553.

[97] C. D. Jonghe, B. F. Hobbs, and R. Belmans, “Optimal Generation Mix With Short-Term Demand Response and Wind Penetration,” *IEEE Trans. Power Syst.*, vol. 27, no. 2, pp. 830–839, May 2012, doi: 10.1109/TPWRS.2011.2174257.

[98] C. Li, Z. Dong, G. Chen, F. Luo, and J. Liu, “Flexible transmission expansion planning associated with large-scale wind farms integration considering demand response,” *Transm. Distrib. IET Gener.*, vol. 9, no. 15, pp. 2276–2283, 2015, doi: 10.1049/iet-gtd.2015.0579.

[99] F. K. Tuffner, N. Radhakrishnan, Y. Tang, and K. P. Schneider, “Grid Friendly Appliance Controllers to Increase the Dynamic Stability of Networked Resiliency-based Microgrids,” in *2018 IEEE/PES Transmission and Distribution Conference and Exposition (T D)*, Apr. 2018, pp. 1–5, doi: 10.1109/TDC.2018.8440136.

[100] P. Khajavi, H. Abniki, and A. B. Arani, “The role of incentive based Demand Response programs in smart grid,” in *2011 10th International Conference on Environment and Electrical Engineering*, May 2011, pp. 1–4, doi: 10.1109/EEEIC.2011.5874702.

[101] L. Zhao, Z. Yang, and W. Lee, “The Impact of Time-of-Use (TOU) Rate Structure on Consumption Patterns of the Residential Customers,” *IEEE Trans. Ind. Appl.*, vol. 53, no. 6, pp. 5130–5138, Nov. 2017, doi: 10.1109/TIA.2017.2734039.

[102] "Time-Of-Use Residential Rate Plans | Rates | Your Home | Home - SCE." https://www.sce.com/residential/rates/Time-Of-Use-Residential-Rate-Plans (accessed Apr. 18, 2019).

[103] M. Kii, K. Sakamoto, Y. Hangai, and K. Doi, "The effects of critical peak pricing for electricity demand management on home-based trip generation," *IATSS Res.*, vol. 37, no. 2, pp. 89–97, Mar. 2014, doi: 10.1016/j.iatssr.2013.12.001.

[104] "Critical Peak Pricing | Xcel Energy." https://www.xcelenergy.com/programs_and_rebates/business_programs_and_rebates/rates/critical_peak_pricing (accessed Apr. 18, 2019).

[105] J. Vuelvas and F. Ruiz, "Demand response: Understanding the rational behavior of consumers in a Peak Time Rebate Program," in *2015 IEEE 2nd Colombian Conference on Automatic Control (CCAC)*, Oct. 2015, pp. 1–6, doi: 10.1109/CCAC.2015.7345196.

[106] S. Mohajeryami, M. Doostan, and A. Asadinejad, "An investigation of the relationship between accuracy of customer baseline calculation and efficiency of Peak Time Rebate program," in *2016 IEEE Power and Energy Conference at Illinois (PECI)*, Feb. 2016, pp. 1–8, doi: 10.1109/PECI.2016.7459237.

[107] A. S. M. A. Mahmud and P. Sant, "Real-time price savings through price suggestions for the smart grid demand response model," in *2017 5th International Istanbul Smart Grid and Cities Congress and Fair (ICSG)*, Apr. 2017, pp. 65–69, doi: 10.1109/SGCF.2017.7947603.

[108] F. C. Schweppe, M. C. Caramanis, R. D. Tabors, and R. E. Bohn, *Spot Pricing of Electricity*. Springer US, 1988.

[109] K. Singh, N. P. Padhy, and J. Sharma, "Influence of Price Responsive Demand Shifting Bidding on Congestion and LMP in Pool-Based Day-Ahead Electricity Markets," *IEEE Trans. Power Syst.*, vol. 26, no. 2, pp. 886–896, May 2011, doi: 10.1109/TPWRS.2010.2070813.

[110] R. Korab and G. Tomasik, "AC or DC OPF based LMP's in a competitive electricity market?," in *International Symposium CIGRE/IEEE PES, 2005.*, Oct. 2005, pp. 61–68, doi: 10.1109/CIGRE.2005.1532727.

[111] "PJM - 5-Minute Settlements." https://www.pjm.com/markets-and-operations/billing-settlements-and-credit/5-minute-settlements.aspx (accessed Apr. 22, 2019).

[112] USPTO.report, "Hybrid Transformer Systems and Methods Patent Application," *USPTO.report*. https://uspto.report/patent/app/20200013546 (accessed Nov. 07, 2020).

[113] M. J. Mauger, R. P. Kandula, F. Lambert, and D. Divan, “Grounded Controllable Network Transformer for Cost-Effective Grid Control.”

[114] R. P. Kandula *et al.*, “Field test results for a 3-phase 12.47 kV 1 MVA power router,” in *2016 IEEE Energy Conversion Congress and Exposition (ECCE)*, Sep. 2016, pp. 1–8, doi: 10.1109/ECCE.2016.7855115.

[115] “IEEE PC57.12.00 - Standard for General Requirements for Liquid-Immersed Distribution, Power, and Regulating Transformers.” https://standards.ieee.org/project/C57_12_00.html (accessed Oct. 12, 2018).

[116] “‘Benefits of Using Mobile Transformers and Mobile Substations for Rapidly Restoring Electrical Service,’ a report to the United States Congress pursuant to Section 1816 of the Energy Policy Act of 2005, U.S. Department of Energy, August 2006. [Online]. Available: http://energy.gov/sites/prod/files/oeprod/DocumentsandMedia/MTS_Report_to_Congress_FINAL_73106.pdf.” .

[117] “Assessment of Large Power Transformer Risk Mitigation Strategies.- A report prepared for the Office of Energy Policy and System Analysis, U.S. Department of Energy. [Online]. Available: https://energy.gov/sites/prod/files/2017/01/f34/Assessment%20of%20Large%20Power%20Transformer%20Risk%20Mitigation%20Strategies.pdf.” Accessed: Oct. 25, 2017. [Online]. Available: https://energy.gov/sites/prod/files/2017/01/f34/Assessment%20of%20Large%20Power%20Transformer%20Risk%20Mitigation%20Strategies.pdf.

[118] S. Grijalva, L. Xiong, and S. Vejdan, “Resilience analysis of modular controllable transformers,” in *2018 IEEE Texas Power and Energy Conference (TPEC)*, Feb. 2018, pp. 1–6, doi: 10.1109/TPEC.2018.8312067.

[119] J. J. Thomas, J. Hernandez, and S. Grijalva, “Power flow router sensititvities for post-contingency corrective control,” in *2013 IEEE Energy Conversion Congress and Exposition*, Sep. 2013, pp. 2590–2596, doi: 10.1109/ECCE.2013.6647035.

[120] R. Jinsiwale *et al.*, “Implementing Volt-Var Control in Meshed Low Voltage Grids,” in *2018 IEEE PES Innovative Smart Grid Technologies Conference Europe (ISGT-Europe)*, Oct. 2018, pp. 1–6, doi: 10.1109/ISGTEurope.2018.8571495.

[121] N. Jaleeli, L. S. VanSlyck, D. N. Ewart, L. H. Fink, and A. G. Hoffmann, “Understanding automatic generation control,” *IEEE Trans. Power Syst.*, vol. 7, no. 3, pp. 1106–1122, Aug. 1992, doi: 10.1109/59.207324.

[122] O. I. Elgerd and C. E. Fosha, “Optimum Megawatt-Frequency Control of Multiarea Electric Energy Systems,” *IEEE Trans. Power Appar. Syst.*, vol. PAS-89, no. 4, pp. 556–563, Apr. 1970, doi: 10.1109/TPAS.1970.292602.

[123] B. Venkatesh, T. Geetha, and V. Jayashankar, “Frequency sensitive unit commitment with availability-based tariff: an Indian example,” *Transm. Distrib. IET Gener.*, vol. 5, no. 8, pp. 798–805, Aug. 2011, doi: 10.1049/iet-gtd.2010.0760.

[124] P. Gupta and Y. P. Verma, “Optimisation of deviation settlement charges using residential demand response under frequency-linked pricing environment,” *Transm. Distrib. IET Gener.*, vol. 13, no. 12, pp. 2362–2371, 2019, doi: 10.1049/iet-gtd.2018.7116.

[125] D. J. Shiltz, M. Cvetković, and A. M. Annaswamy, “An Integrated Dynamic Market Mechanism for Real-Time Markets and Frequency Regulation,” *IEEE Trans. Sustain. Energy*, vol. 7, no. 2, pp. 875–885, Apr. 2016, doi: 10.1109/TSTE.2015.2498545.

[126] A. W. Berger and F. C. Schweppe, “Real time pricing to assist in load frequency control,” *IEEE Trans. Power Syst.*, vol. 4, no. 3, pp. 920–926, Aug. 1989, doi: 10.1109/59.32580.

[127] B. B. Alagoz, A. Kaygusuz, M. Akcin, and S. Alagoz, “A closed-loop energy price controlling method for real-time energy balancing in a smart grid energy market,” *Energy*, vol. 59, pp. 95–104, Sep. 2013, doi: 10.1016/j.energy.2013.06.074.

[128] S. Kulkarni *et al.*, “Enabling a Decentralized Smart Grid Using Autonomous Edge Control Devices,” *IEEE Internet Things J.*, vol. 6, no. 5, pp. 7406–7419, Oct. 2019, doi: 10.1109/JIOT.2019.2898837.

[129] “PJM - Daily Energy Market Offer Data.” https://www.pjm.com/markets-and-operations/energy/real-time/historical-bid-data/unit-bid.aspx (accessed Oct. 21, 2020).

[130] F. Chen *et al.*, “Cost-Based Droop Schemes for Economic Dispatch in Islanded Microgrids,” *IEEE Trans. Smart Grid*, vol. 8, no. 1, pp. 63–74, Jan. 2017, doi: 10.1109/TSG.2016.2581488.

[131] K. Zhang *et al.*, “Incentive-Driven Energy Trading in the Smart Grid,” *IEEE Access*, vol. 4, pp. 1243–1257, 2016, doi: 10.1109/ACCESS.2016.2543841.

[132] P. R. Thimmapuram and J. Kim, “Consumers’ Price Elasticity of Demand Modeling With Economic Effects on Electricity Markets Using an Agent-Based Model,” *IEEE Trans. Smart Grid*, vol. 4, no. 1, pp. 390–397, Mar. 2013, doi: 10.1109/TSG.2012.2234487.

[133] S. N. A. U. Nambi, R. V. Prasad, and A. R. Lua, “Decentralized Energy Demand Regulation in Smart Homes,” *IEEE Trans. Green Commun. Netw.*, vol. 1, no. 3, pp. 372–380, Sep. 2017, doi: 10.1109/TGCN.2017.2721818.

[134] M. Muratori and G. Rizzoni, "Residential Demand Response: Dynamic Energy Management and Time-Varying Electricity Pricing," *IEEE Trans. Power Syst.*, vol. 31, no. 2, pp. 1108–1117, Mar. 2016, doi: 10.1109/TPWRS.2015.2414880.

[135] M. Daneshvar, B. Mohammadi-ivatloo, S. Asadi, K. Zare, and A. Anvari-Moghaddam, "Optimal Day-Ahead Scheduling of the Renewable Based Energy Hubs Considering Demand Side Energy Management," in *2019 International Conference on Smart Energy Systems and Technologies (SEST)*, Sep. 2019, pp. 1–6, doi: 10.1109/SEST.2019.8849131.

[136] N. Li, L. Chen, and S. H. Low, "Optimal demand response based on utility maximization in power networks," in *2011 IEEE Power and Energy Society General Meeting*, Jul. 2011, pp. 1–8, doi: 10.1109/PES.2011.6039082.

[137] P. Yang, G. Tang, and A. Nehorai, "A game-theoretic approach for optimal time-of-use electricity pricing," *IEEE Trans. Power Syst.*, vol. 28, no. 2, pp. 884–892, May 2013, doi: 10.1109/TPWRS.2012.2207134.

[138] D. Bertsimas and M. Sim, "Robust discrete optimization and network flows," *Math. Program.*, vol. 98, no. 1, pp. 49–71, Sep. 2003, doi: 10.1007/s10107-003-0396-4.

[139] X. Wang and H. Chiang, "Analytical Studies of Quasi Steady-State Model in Power System Long-Term Stability Analysis," *IEEE Trans. Circuits Syst. Regul. Pap.*, vol. 61, no. 3, pp. 943–956, Mar. 2014, doi: 10.1109/TCSI.2013.2284171.

[140] T. Van Cutsem, M.-E. Grenier, and D. Lefebvre, "Combined detailed and quasi steady-state time simulations for large-disturbance analysis," *Int. J. Electr. Power Energy Syst.*, vol. 28, no. 9, pp. 634–642, Nov. 2006, doi: 10.1016/j.ijepes.2006.03.005.

[141] W. H. Kersting, "Radial distribution test feeders," in *2001 IEEE Power Engineering Society Winter Meeting. Conference Proceedings (Cat. No.01CH37194)*, Jan. 2001, vol. 2, pp. 908–912 vol.2, doi: 10.1109/PESW.2001.916993.

[142] "UKERC Energy Data Centre." http://ukerc.rl.ac.uk/DC/cgi-bin/edc_search.pl?GoButton=Detail&WantComp=42&WantResult=&WantText=EDC0000041 (accessed Jan. 08, 2019).

[143] M. S. Rauls, D. W. Novotny, D. M. Divan, R. R. Bacon, and R. W. Gascoigne, "Multiturn High-Frequency Coaxial Winding Power Transformers," *IEEE Trans. Ind. Appl.*, vol. 31, no. 1, pp. 112–118, Jan. 1995, doi: 10.1109/28.363042.

[144] M. S. Rauls, D. W. Novotny, and D. M. Divan, "Design considerations for high-frequency coaxial winding power transformers," *IEEE Trans. Ind. Appl.*, vol. 29, no. 2, pp. 375–381, Mar. 1993, doi: 10.1109/28.216547.

VITA

ROHIT JINSIWALE was born in Mumbai, India. He received the bachelor's degree in Electrical Engineering from Sardar Patel College of Engineering, Mumbai, India, in 2013, and the M.S. degree in Electrical and Computer engineering from the Georgia Institute of Technology, Atlanta, GA, USA, in 2015, where he is currently pursuing the Ph.D. degree with the Center for Distributed Energy. His research interests include designing decentralized market structures for smart grids as well as designing decentralized control architectures for power systems.